Thermal Plumes in Ventilated Rooms

Kofoed, Peter

Publication date:
1991

Document Version
Early version, also known as pre-print

INSTITUTTET FOR BYGNINGSTEKNIK
DEPT. OF BUILDING TECHNOLOGY AND STRUCTURAL ENGINEERING
AALBORG UNIVERSITETSCENTER • AUC • AALBORG • DANMARK

THERMAL PLUMES IN VENTILATED ROOMS

PETER KOFOED
THERMAL PLUMES IN VENTILATED ROOMS
PH.D. THESIS
JANUARY 1991

INSTITUTTET FOR BYGNINGSTEKNIK
DEPT. OF BUILDING TECHNOLOGY AND STRUCTURAL ENGINEERING
AALBORG UNIVERSITETSCENTER • AUC • AALBORG • DANMARK

Peter V. Nielsen

THERMAL PLUMES IN VENTILATED ROOMS

PETER KOFOED
THERMAL PLUMES IN VENTILATED ROOMS
PH.D. THESIS

JANUARY 1991

ABSTRACT

Axisymmetric circular buoyant jets are treated both theoretically and experimentally. From a literature study the author concludes that the state of experimental knowledge is less satisfactory. Further three different measuring methods have been established to investigate the thermal plumes from pure sources of heat in ventilated rooms.

According to the analyses carried out the pure plume flow or the model of a plume above a point heat source has been verified in terms of showing the power rules expounded in the similarity analysis. The velocity and temperature excess profiles are found to be more narrow than the one observed by previous authors and therefore the entrainment factor is smaller. However, the complete similarity in terms of constant velocity and temperature distribution factors cannot be said to occur.

The plume axis wandering cannot be eliminated and it has to be treated as a phenomena of large scale instability and not as a normal turbulence phenomena. The influence of even very small vertical temperature gradients is reported to be significant. This makes the description of the flow by a simple pure plume model impossible and flow downwards it leads to disintegration tendencies or horizontal spread out. Further the flow is influenced by many other factors where co-flow phenomena from ventilating the room and room drafts are some of them.

The tests carried out show a significant reduction of the vertical volume flux when the buoyant flow takes place near to enclosing walls. Symmetry considerations are verified as regards buoyant wall jets, i.e. the volume flow rate makes out 63 % of the one in the corresponding free buoyant jet. When the flow takes place in a corner between two walls the percentage is even less.

It is the author's hope that the presented experimental mean data from the extrapolation method may form a basis for some future numerical work. Finally, in the conclusion the application of displacement ventilation systems is discussed as the stipulation of the necessary ventilating air.

PREFACE

This thesis represents the termination of my Ph.D. study at the Institute of Building Technology and Structural Engineering at the University of Aalborg, with Professor Peter V. Nielsen as supervisor.

The Ph.D. study was started in February 1988. From August 1990 to January 1991 I stayed for a period of six months at Sulzer Brothers Limited in Winterthur, Switzerland, with extra support from the Danish Research Academy and "Sulzer".

I am under great obligation to my supervisor Peter V. Nielsen. He has been an invaluable support as a source of inspiration and as a sparring partner during the execution of the Ph.D. project. I want to thank both Carl Erik Hyldgaard for his engagement in the laboratory in connection with measuring problems and Torben Christensen whose practical assistance and good ideas made the carrying out of a comprehensive experimental program possible. Beat Kegel (Sulzer) I also want to thank for his support, commitment and inspiration.

Further I want to thank Ingrid Christensen, Inge Nielsen and Mariann Bai Hansen for the working out figures and Bente Kjaergaard for her help with the english translation. They have all been working with great patience, competence and care.

Winterthur, Switzerland, January 1991.

Peter Kofoed

LIST OF SYMBOLS

AR	Archimedes' number
c_p	specific heat at constant pressure
d_0	diameter of source
E	kinetic energy flux
F_0	buoyancy flux
Fr	Froude's number
g	gravitational acceleration taken as a positive value
G	air volume flow supplied
Gr	Grashof's number
h	height of source
H	enthalpy flux
l	length of line source
m	velocity distribution factor
M	vertical momentum flux
n	air change rate in room
p	temperature distribution factor
P	pressure
Pr	Prandtl's number
Q	heat supplied to source
Q_0	convective heat
r	radial distance from plume axis
r_v, r_T	profile width where 1/e of the maximum value is obtained
Re	Reynold's number
S	stratification factor
T	mean temperature
ΔT	mean temperature excess, $\Delta T = T - T_\infty$
x	vertical height above top of source
x_0	position of virtual origin
y	first horizontal coordinate
z	second horizontal coordinate
u	vertical mean velocity
v	radial mean velocity
w	angular mean velocity
V	vertical volume flux

dT_∞/dx vertical temperature gradient

$-g\Delta\rho/\rho_\infty$ buoyancy in plume, $\Delta\rho = \rho - \rho_\infty$

Greek symbols:

α	entrainment factor
β	thermal expansion coefficient
δ	angle of spread
λ	ratio between profile widths, $\lambda = r_T/r_V$
ν	kinematic viscosity
π	pi
ρ	density

Subscripts:

F	floor
M	maximum value
R	return
S	supply
ST	stratification
T	temperature
V	velocity
0	source condition
∞	ambient condition

CONTENTS

1. INTRODUCTION

1. INTRODUCTION

1.1 Introductory Remarks

The mechanics of thermal flows, their propagation, entrainment and mixing are of general interest. With the appearance of a new ventilation principle, called displacement ventilation, the demand for a physical understanding of the processes in the thermal flows has been accelerated.

Apart from this particular problem the mechanics of thermal flows is important to a large range of engineering problems: From problems of reducing the pollution of our water and atmosphere, cooling of power plants, to exhaust above hot processes in industrial premises. From a more fundamental point of view the investigation of axisymmetical buoyant jets will contribute to the understanding of convection flows and free turbulence phenomena.

1.2 Displacement Ventilation

Ventilation of a room can be done in many ways. The task is to find a solution which satisfies the demands for both thermal and atmospheric comfort, and which has an efficient use of energy. The demands for comfort are characterized by low mean velocities and turbulence levels, low temperature gradients and low contaminant concentrations in the entire occupied zone. The efficient use of energy is mainly a question of optimum use of the supply air. The keywords are in this connection low air volume flow and little air treatment.

Within comfort ventilation the distinction can be made between to main principles: mixing ventilation and displacement ventilation. Which one is the best varies from one locality to another. The main idea in mixing ventilation is that the polluted air is diluted by supply air until it reaches an acceptable low

concentration. By utilizing displacement ventilation the contaminated air is displaced from the occupied zone by supplying fresh air to this part of the room.

Now and then a two zone model is used to describe the principle of displacement ventilation, see ref. /91/: The room is divided in an upper contaminant zone and a lower occupied zone with fresh air. This is experimentally verified by Heiselberg & Sandberg /31/. The principle is shown in fig.1.1.

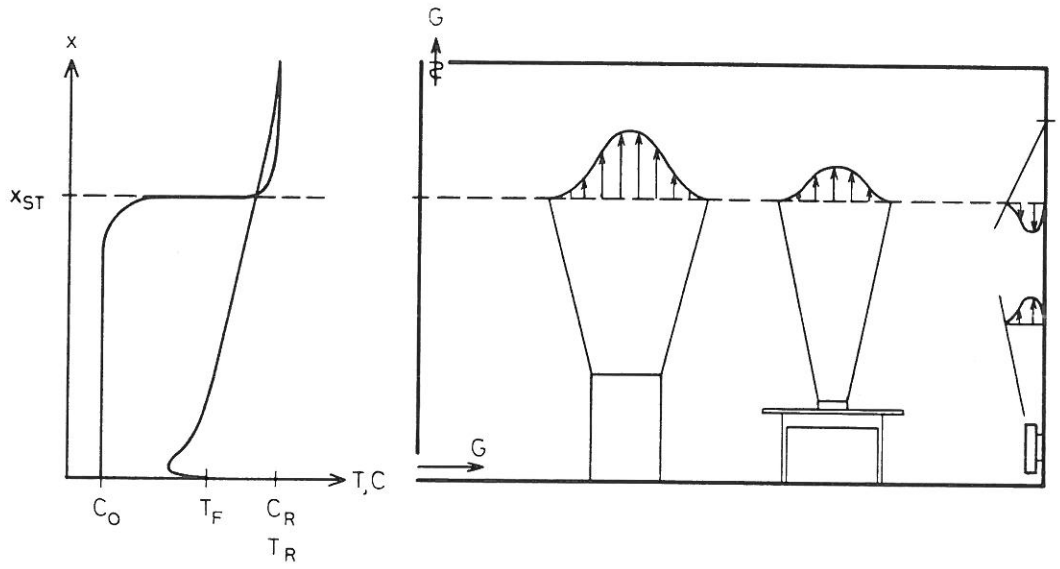

Fig.1.1. Two zone model of vertical displacement flow in an office room. The primary air is supplied in the occupied zone and is entrained in the warm plumes from heat sources (and in the cold down-draught). Dependent on the air flow supplied G and the vertical air flow in the room there must be a height x_{ST} where the upward moving air is equal to the supplied air flow. Above this height a recirculation flow appears. The grafs to the left show: I. the vertical temperature gradient created by interaction between the different plumes and by radiation between the surfaces in the room, and II. the contaminant distribution created only by the plumes, see ref. /31/.

The introduction of information technology has given a trend towards a higher heat load in the rooms, making increased demands on the air conditioning. Therefore, during the last few years much work has been done on developing efficient ventilation systems in the Scandinavian countries and in West Germany: see e.g., Mathisen & Skåret in Norway /51,90-92/, Malmström & Sandberg in Sweden /31,48-50,83-85/, Nielsen in Denmark /30,42,43,61-66/, Fitzner among others in Germany /3,16,21-24/, and later, Seppänen and Tapula in Finland /88,98/, Kegel in Switzerland /7,40,78/. In this work displacement ventilation systems have proved to have two major advantages compared with traditional mixing systems:

An efficient use of energy. It is possible to remove exhaust air from the room where the temperature is several degrees higher than the temperature in the occupied zone which allows a higher air inlet temperature at the same load.

A better air quality for the same airflow rate. The vertical contaminant distribution implies that fresh air and polluted air are separated. The most contaminant air can be found above the occupied zone.

As a result during the last ten years vertical displacement ventilation systems have grown popular as comfort ventilation in rooms with heat loads, e.g. office rooms. In the design process many questions still remain unanswered: questions about possibilities and limitations of displacement ventilation, including the shape of the temperature and contamination profiles, cooling ability, draught risk and general thermal comfort.

It is not the purpose of this work to discuss all aspects of displacement ventilation. A lot of work remains to be done before a complete and reliable design method can be described. One of the problems in the design process is to determine the necessary supply of ventilating air. Fig.1.2 provides two examples.

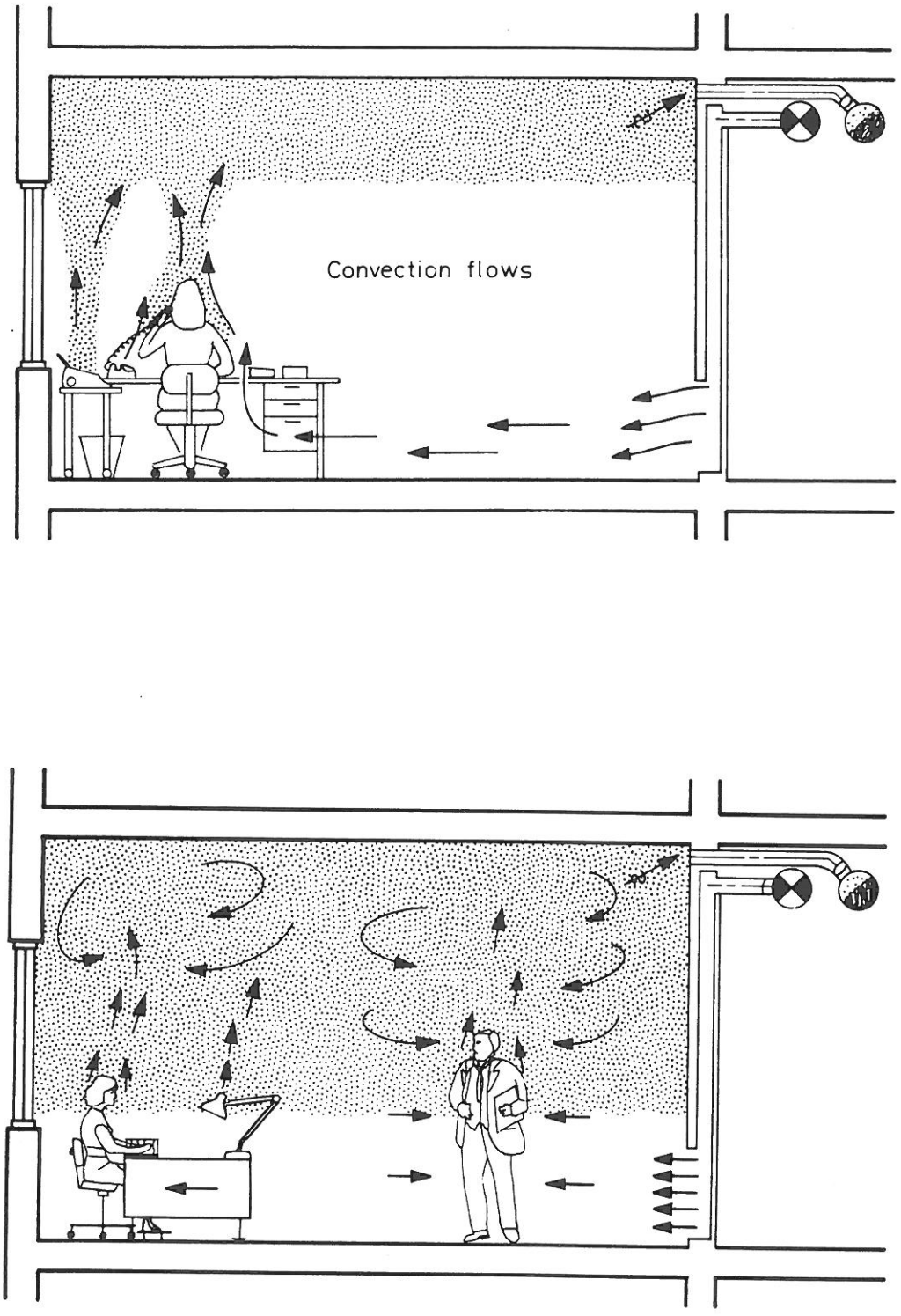

Fig.1.2 The air volume flow in the thermal flow together with the ventilating air determine the stratification height. In the upper case the correct amount of air is supplied to the occupied zone. In the lower case it is too small.

The two zone model can be used to explain the influence of the thermal flows, see e.g., Skåret /91/, Skistad /89/, or Mathisen /51/. Calculation of the airflow rates in the thermal flows is the basis for the stipulation of the necessary supply air, because they entrain (or use) the ventilating air supplied to the occupied zone. If the airflow rate supplied is too small the height of the occupied zone is too low as shown in the lower picture of fig.1.2.

1.3 Thermal Flows

A schematic representation of the thermal flows is given in fig.1.3.

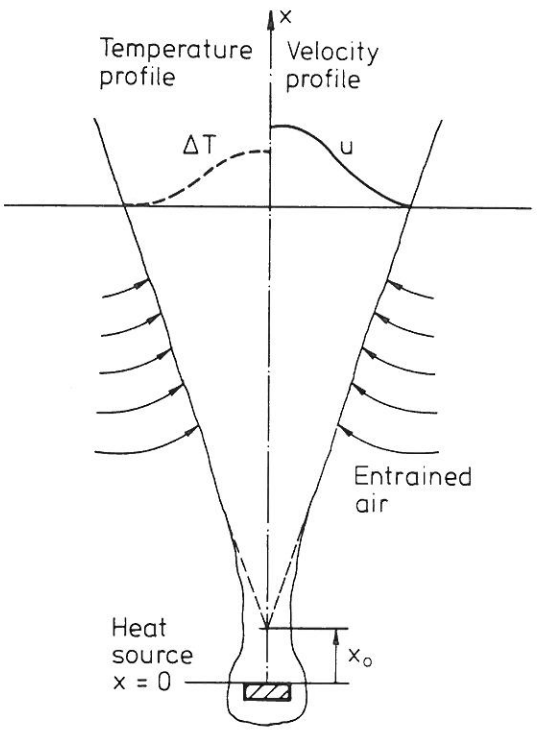

Fig.1.3 Thermal Flow.

From a fundamental point of view the thermal flow is a free convection flow. In practice simple formula systems based on plume models above a point heat source or a line heat source have been used to calculate the flow rate in the thermal flows, see e.g. Baturin /5pp125-127/ or Skåret /91p837/.

In both cases it is clear that the entrained air volume flow increases with the distance from the source, and the evaluation of the position of the virtual origin is essential. Often the necessary knowledge is not present.

Point heat source:

$$u = 0.13\ Q_0^{1/3}\ (x+x_0)^{-1/3} \tag{1.1}$$

$$\Delta T = 0.45\ Q_0^{2/3}\ (x+x_0)^{-5/3} \tag{1.2}$$

$$V = 0.0050\ Q_0^{1/3}\ (x+x_0)^{5/3} \tag{1.3}$$

Line heat source:

$$u = 0.0067 \left(\frac{Q_0}{l} \right)^{1/3} \tag{1.4}$$

$$\Delta T = 0.24 \left(\frac{Q_0}{l} \right)^{2/3} (x+x_0)^{-1} \tag{1.5}$$

$$\frac{V}{l} = 0.0014 \left(\frac{Q_0}{l} \right)^{5/3} (x+x_0) \tag{1.6}$$

where	u	maximum velocity	(m/s)
	ΔT	maximum temperature difference	(K)
	V	air volume flow	(m^3/s)
	x	vertical distance to source	(m)
	x_0	distance to the virtual origin, if negative below the source	(m)
	Q_0	convective heat emission	(W)
and	$\frac{V}{l}$	air volume flow per source length	$\left(\frac{m^3}{s\ m}\right)$
	$\frac{Q_0}{l}$	conv. heat emission per source length	(W/m)

However, the flow is much more complex and influenced by many factors which are not considered. Literature study and experiments show this, see ref. /11,42,43,53,54,71,89/. In displacement ventilated rooms the temperature increases with the height and a vertical temperature gradient influences the flow. Another problem is the heat source geometry which is important to the generation of the convective flow. Heat sources are seldom pure point sources or pure line sources from a flow mechanical point of view. In addition it is interesting to realize that exchange of heat from a room by means of conduction is connected with surface temperatures, different from that of the surrounding air. This may cause convective currents along the cold or warm surface influencing the flow pattern in the room. Skåret /91p837/ presents a set of equations to describe the flow from heated or cooled vertical surfaces.

1.4 Scope of This Work

From the discussion in the previous section it is obvious that knowledge about the mechanics of thermal flows is of great interest. One should consequently search for more.

This work is delimited to the study of axisymmetic buoyant jets arising from steadily maintained circular (or semi-circular) sources of heat, and it is the purpose:

Through literature study systematically to describe the fluid mechanical theories, dimensional analysis and integral methods,

through literature study systematically to describe the previous experiments, and if possible to classify in groups, for the deeper understanding of the problem.

Through experimentally carrying out to produce reliable experimental data which can form a basis for numerical simulation of the flow.

To carry out a wide range of experiments to improve the understanding of the buoyant jet mechanics including: importance of heat source geometry, influence of the vertical temperature gradient, influence by the already present ventilation flow in the room, influence on entrained air volume flow by enclosing walls.

The practical outcome of these investigations is to provide an input for the design of displacement ventilation systems, especially the choice of ventilating air supplied to the room.

2. THERMAL FLOWS AND PARAMETERS

2. THERMAL FLOWS AND PARAMETERS

A classification of the flows considered takes place in /chapter 2.1/, while /chapter 2.2/ describes similarity parameters.

2.1 Flow Classification

The thermal flows considered are low velocity flows, whose axis is aligned with the gravity vector and whose density (or temperature) is different from that of the surroundings, so that they are subject to buoyancy forces. The flow is generated from a single steadily maintained circular source. Axisymmetric thermal flows remote from walls and rising in stagnant, uniform surroundings form the main part of the theoretical work, but also the influence by stratification, by enclosing walls and by ventilating the room is taken into consideration.

2.1.1 Buoyant Jet Rise In Non Stratified Surroundings

When the buoyancy force acts in the direction of the thermal flow, it is called buoyant jet. Further classification leads to distinction between four types of buoyant jets, ref. /11/:

buoyant jet

negative buoyant jet

pure jet

pure plume

If the buoyancy force acts in the opposite direction, the thermal flow is labeled negative buoyant jet. A pure jet is defined as a source of kinematic momentum flux or when the effect of buoyancy

is negligible. The other limiting case is a source of kinematic buoyancy only or when the buoyancy force dominates the flow completely, this is termed a pure plume, or simply plume. It deserves notice that all buoyant jets change to plumes far away from the origin if non-stratified calm surroundings are present. Therefore, the four cases especially the pure plume should be delimited. In fig.2.1 the various examples of buoyant jets in calm uniform surroundings including their limiting cases are illustrated.

The pure jet is characterized by absent buoyancy forces, because the jet has the same density (or temperature) as the surroundings. Pure jets are known from isothermal ventilation inlets. The pure plume has no initial momentum and only the buoyancy force acts on the flow. It can be generated with a heat source such as a heated plate, a burning cigarette or a sitting person. The buoyant jet is the general case which can be considered as a plume with initial momentum. It is created by discharging lower density fluid and the examples are a chimney, a cooling tower or a burner. Often a buoyant jet can be divided in tree zones: A non-buoyant region where momentum forces dominate the flow, and it behaves like a pure jet. An intermediate region where the influence of the momentum becomes smaller and smaller. A buoyant region where the buoyancy forces dominate the flow, and it behaves like a pure plume.

The negative buoyant jet appears if higher density fluid is discharged upwards. When the negative buoyancy forces become dominant the flow will change direction and create a down flow.

When the buoyant jet rises in non stagnant surroundings a co-flow sometimes takes place. Such buoyant jets with the surrounding fluid also in motion in the direction of the jet are called compound buoyant jets. It appears when the ventilation of a room creates co-flow like situations. The compound jet problem is well known from other engineering areas such as spraying from moving aircraft and discharge of effluent into the atmosphere.

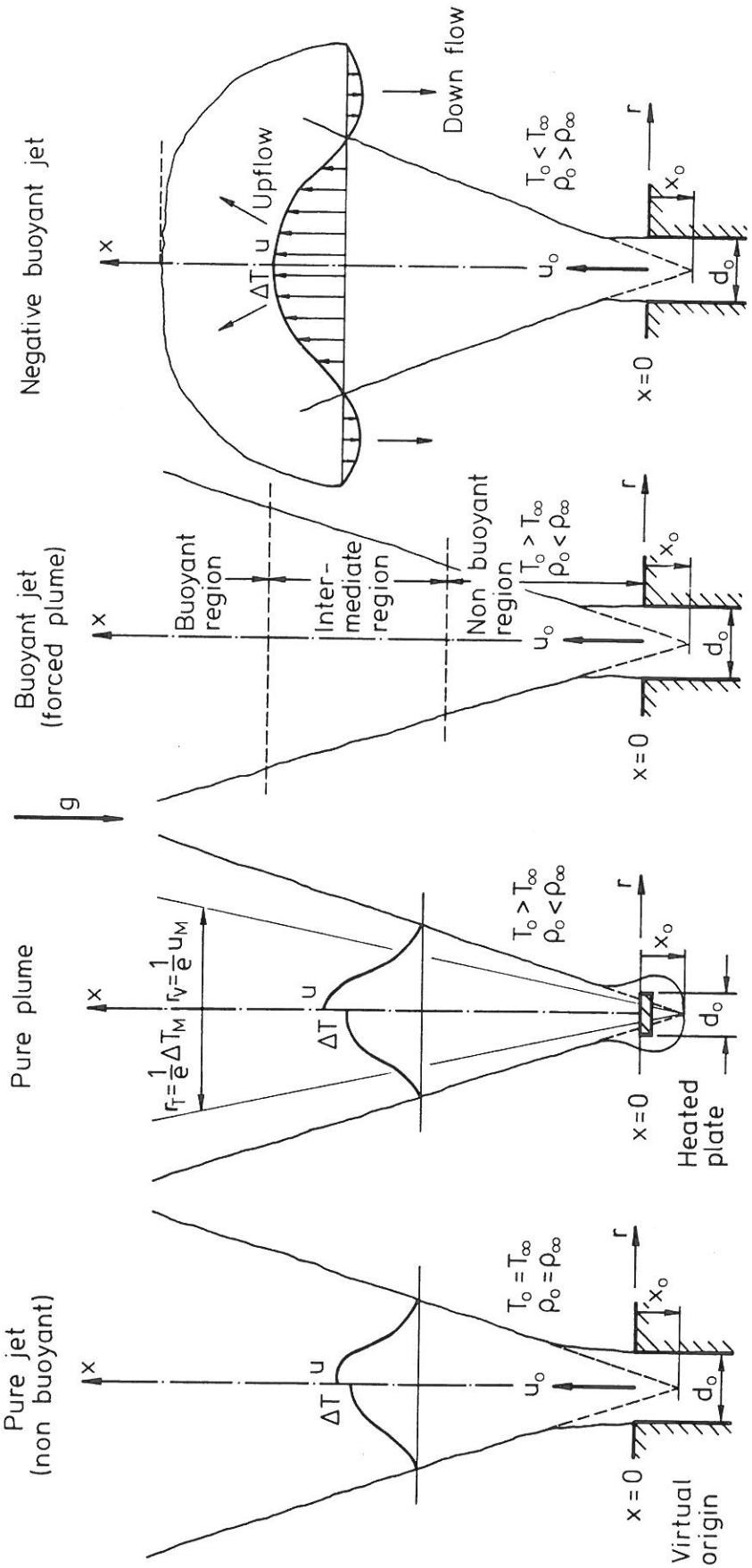

Fig. 2.1 Buoyant jets in non-stratified surroundings.

2.1.2 Buoyant Jet Rise In Stratified Surroundings

When the density of the surroundings decreases with the elevation (or the temperature increases), a case quite similar to the negative buoyant jet in fig 2.1 appears. It is called buoyant jet rise in stratified surroundings. Fig.2.2 shows a schematic representation of the flow.

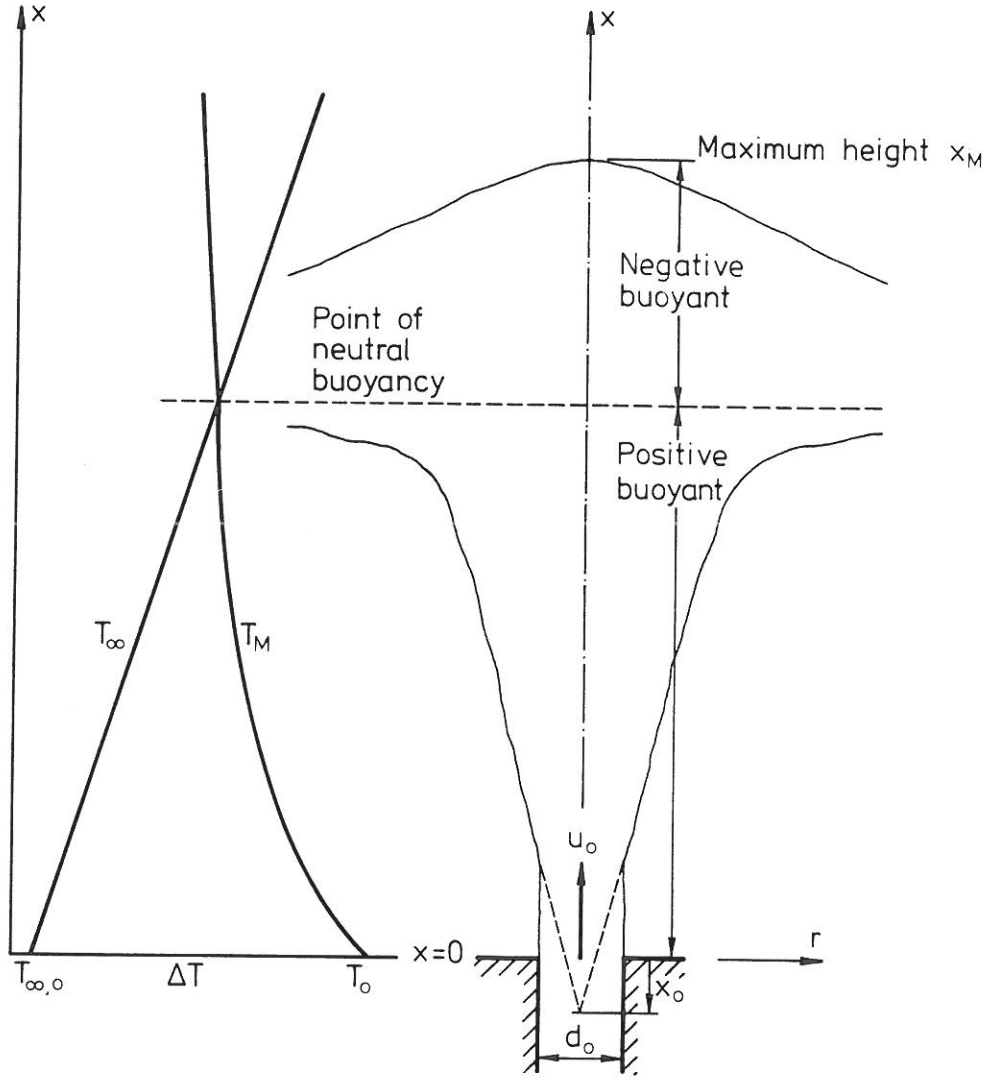

Fig.2.2. Buoyant jet in stratified surroundings.

In the beginning the jet behaves like the buoyant jet of fig.2.1. However, its density deficit (or positive buoyancy) reduces continuously due to the stratification of the environment. At a certain height, point of neutral buoyancy, the density deficit

becomes zero. From here the jet behaves similar to the negative buoyant jet of fig.2.1. Sometimes the flow simply disintegrates, or it reaches a maximum height of rise and it turns downward and spreads out horizontally. As a rule the surroundings are non-uniformly stratified. This makes the description complicated.

2.1.3 Buoyant Jet Rise Influenced By Enclosing Walls

Sometimes the buoyant flow takes place near to enclosing walls, in this case when the wall is close enough Coanda effects may appear. If the flow is influence by a single wall, it is termed buoyant wall jet. If the flow takes place in a corner, it is called buoyant jet in a corner.

2.2. Parameters

Inertial, buoyant and viscous forces influence the flow in buoyant jets. One can distinguish between a local or a global point of view. Considered from a local point of view the fluid motion is determined by the relative magnitude of the tree forces at each point. The global character is determined by the strength of the forces at the jet source and by the ambient conditions. According to the rules expounded in the theory of similarity, ref. /5, 11/, the equations of motion of a viscous fluid yield the following characterizing parameters (or criteria of similarity). The symbols are given in the nomenclature list. The right hand side of the equations (2.1-4) is characteristic global values corresponding to fig.2.1.

The Reynold's number, Re, gives the relation between inertial and viscous forces:

$$Re = \frac{u_0 \, d_0}{\nu} \qquad (2.1)$$

Grashof's criterion is a measure of the ratio of the gravitational (buoyancy) forces to the viscous forces. The Grashof's number, Gr, can be written as:

$$Gr = \frac{g\ (\rho_\infty - \rho_0)\ d_0^3}{\rho_0\ \nu^2} = \frac{g\ d_0^3\ \beta\ \Delta T}{\nu^2} \qquad (2.2)$$

The relation between the forces of inertia and buoyancy is called the Archimedes' number, Ar:

$$Ar = \frac{g\ d_0 (\rho_\infty - \rho_0)}{u_0^2\ \rho_0} = \frac{\beta\ g\ d_0\ \Delta T}{u_0^2} \qquad (2.3)$$

Prandtl's number, Pr, characterizes the physical properties of the fluid and may be defined as:

$$Pr = \frac{\nu}{\alpha} \qquad (2.4)$$

In pure jets only the Reynold's Number, Re, is of influence due to non-buoyancy, and in pure plumes only the Grashof's number, Gr, due to the lack of initial momentum. If the pure jet, pure plume and buoyant jet are assumed to be turbulent, the viscosity is negligible. Generally buoyant jets have high Reynold's and Grashof's numbers. When the numbers are high enough, Re >> 2320 and GrPr >> 2 10^7 for jets and plumes, respectively, auto similarity exists, ref. /5/. This implies that the phenomenon is independent of the individual criteria of similarity. However, these numbers are important to indicate whether the flow is turbulent or laminar, or, at what height above the source transition from laminar to turbulence can be expected to occur.

The parameters characterizing the inertial and buoyancy forces have been described. However, it is not their absolute magnitude but their relation that determines the fluid motion. This ration of the forces of inertia and buoyancy is termed the Archimedes' number, Ar, and it is the Reynold's number squared divided by the Grashof's number, $Ar = Re^2/Gr$. Now and then the square root of the Archimedes' number is defined as a Froude's number, Fr, giving a relation between gravitational and inertial forces, $Fr = \sqrt{Ar}$. But this definition is not convenient since it does not allow the Froude's number, Fr, to change sign.

Normally the Prandtl's number, Pr, is considered constant, for air $Pr \simeq 0.73$.

When the environment is stratified, the vertical temperature gradient

$$dT_\infty/dx \tag{2.5}$$

or sometimes the parameter, S, called the stratification factor, is used to describe the stratification:

$$S = -\frac{g}{\rho_{\infty,0}}\frac{d\rho_\infty}{dx} \cong g\beta\frac{dT_\infty}{dx} \tag{2.6}$$

where $\rho_{\infty,0}$ is the ambient density at the source

When S = 0 the surroundings are uniform or neutrally stratified, stably stratified for S > 0, and unstably stratified for S < 0.

3. THE MECHANICS OF THERMAL FLOWS

3 THE MECHANICS OF THERMAL FLOWS

Here the axisymmetric two-dimensional turbulent pure jets, pure plumes and buoyant jets rise vertically are studied, employing turbulence notation. Some basic definitions and assumptions are given in /chapter 3.1/, the governing equations of motion in /chapter 3.2/ so as in /Appendix B/.

3.1 Definitions and Basic Assumptions

The flow configuration and geometry are shown in fig 3.1.

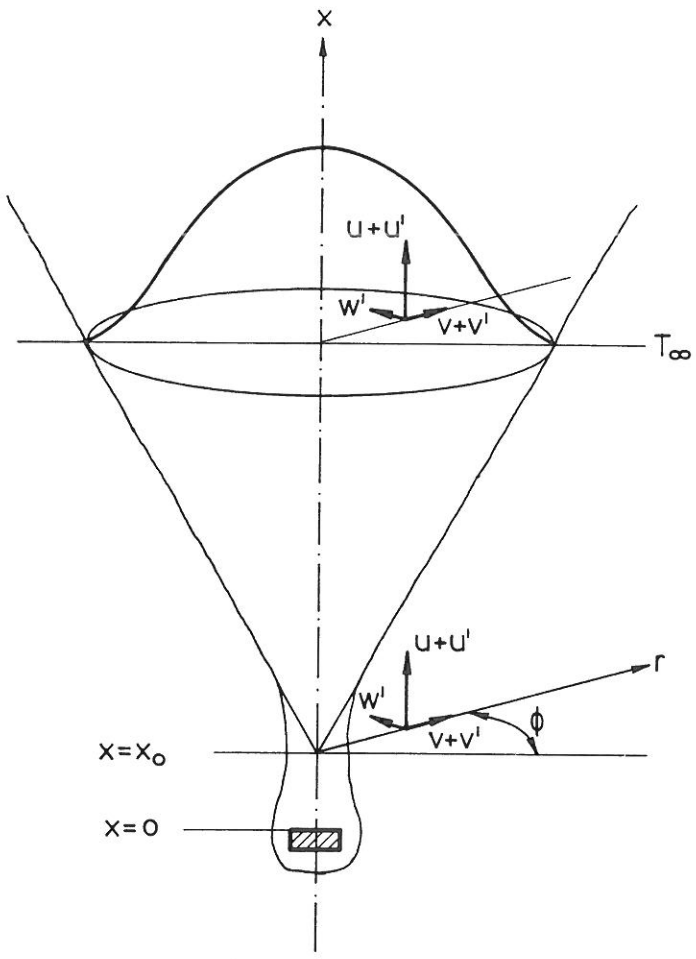

Fig.3.1. Axisymmetric buoyant jet, flow configuration and geometry.

The ambient fluid is assumed to be motionless, except for the flows induced by the jets. T_∞ is the local ambient temperature, and a neutrally or stable stratification $dT_\infty/dx >= 0$ is assumed. The source is a steadily maintained circular source of heat.

The flow is assumed axisymmetric and free of swirl. Relative to cylindrical polar coordinates (r,ϕ,x) with origin at the top of the source and Ox directed upward the velocity field has components $(v+v', w', u+u')$ where the primes signify fluctuations and unprimed symbols signify mean values. The excess temperature relative to the surroundings is $\Delta T(r,x)+\Delta T'(r,\phi,x)$ where ΔT is the mean and $\Delta T'$ the fluctuating excess temperature within the buoyant jet. Covariances are represented in the form $Cov\{v'u'\}$.

The fluid is taken to satisfy the Boussinesq approximation, but of being otherwise incompressible: The time averaged density variations are assumed to be small

$$- \frac{\rho - \rho_\infty}{\rho_\infty} << 1 \qquad (3.1)$$

so that there will be little error in using the ambient density ρ_∞ to replace the local density ρ in the description of inertia forces. However, the density difference $\rho-\rho_\infty$ is important in the description of the gravitational body forces. In addition the relation between the density and temperature is assumed to have a linear form

$$- \frac{\rho - \rho_\infty}{\rho_\infty} = \frac{T - T_\infty}{T_\infty} = \beta\Delta T \qquad (3.2)$$

The flow is further assumed fully turbulent and therefore viscosity and molecular diffusivity can be neglected relative to the turbulent transport.

3.2 Governing Equations Of Motion

Finally, under these conditions the time averaged equations of motion for the axisymmetric buoyant jet may be expressed in the following forms.

Conservation of mass, continuity:

$$\frac{\partial(rv)}{\partial r} + \frac{\partial(ru)}{\partial x} = 0 \qquad (3.3)$$

Conservation of vertical momentum:

$$\frac{\partial(rvu)}{\partial r} + \frac{\partial(ru^2)}{\partial x} + \frac{r}{\rho}\frac{\partial p}{\partial x} + \frac{\partial}{\partial r}(r\,\mathrm{Cov}\{v'u'\}) + \frac{\partial}{\partial x}(r\,\mathrm{Cov}\{u'^2\}) - \beta g r \Delta T = 0 \qquad (3.4)$$

Conservation of heat:

$$\frac{\partial(rv\Delta T)}{\partial r} + \frac{\partial(ru\Delta T)}{\partial x} + ru\frac{dT_\infty}{dx} + \frac{\partial}{\partial r}(r\,\mathrm{Cov}\{v'\Delta T'\}) + \frac{\partial}{\partial x}(r\,\mathrm{Cov}\{u'\Delta T'\}) = 0 \qquad (3.5)$$

Here the conservation of radial momentum, $p + \rho\,\mathrm{Cov}\{w'\} = 0$ and conservation of azimuthal momentum are lead out of the consideration.

The previous system of equations has more unknowns than equations, and therefore it cannot be solved even if the appropriate boundary conditions were provided. This is the fundamental problem of turbulent fluid mechanics.

It must be emphasized that the system of equations (3.3-5) only apply at each point inside the buoyant jet and quite different equations represent the flow induced in the surroundings.

Several authors introduce a further equation for conservation of the kinematic energy of axial mean motion. It can be produced by the multiplying of equation (3.4) with u, and using the "boundary layer approximations", see e.g. Morton /56/.

Conservation of axial motion kinetic energy:

$$\frac{\partial(\frac{1}{2}rvu^2)}{\partial r} + \frac{\partial(\frac{1}{2}ru^3)}{\partial x} + u\frac{\partial}{\partial r}(r\ \mathrm{Cov}\{v'u'\}) - \beta g r u \Delta T = 0 \qquad (3.6)$$

The system of equations (3.3-6) can be solved for turbulent pure plumes or pure jets in various ways, as it will presented in /chapter 4/.

When the so-called "boundary layer approximations" are used, and neutrally stratified surroundings $dT_\infty/dx = 0$ is assumed, the governing time averaged equations of motion, according to ref. /56,71/, can be reduced to:

Conservation of mass, continuity:

$$\frac{\partial(rv)}{\partial r} + \frac{\partial(ru)}{\partial x} = 0 \qquad (3.7)$$

Conservation of vertical momentum:

$$\frac{\partial(rvu)}{\partial r} + \frac{\partial(ru^2)}{\partial x} + \frac{\partial}{\partial r}(r\ \mathrm{Cov}\{v'u'\}) - \beta g r \Delta T = 0 \qquad (3.8)$$

Conservation of heat:

$$\frac{\partial(rv\Delta T)}{\partial r} + \frac{\partial(ru\Delta T)}{\partial x} + \frac{\partial}{\partial r}(r\ \mathrm{Cov}\{v'\Delta T'\}) = 0 \qquad (3.9)$$

The above simplified systems of equations also represents the fundamental problem of turbulent fluid dynamics, since it has more unknowns than equations. But it is convenient when one deals with dimensional analysis assuming strict self similarity, this fact will appear in /chapter 4.2/.

4. THEORIES

4 THEORIES

When dealing with turbulent fluid mechanics, the problem has been exposed to a large number of methods. The work on axisymmetric buoyant jets can be classified in one of two schools of thought: The differential methods which are touched in /chapter 4.1/, and the integral methods which are described in /chapter 4.2/, including the entrainment hypothesis in /chapter 4.3/. Plumes influenced by enclosing walls are treated in /chapter 4.4/.

4.1 Differential Methods

The first group of investigators tries to derive constitutive equations, e.g. a relation between the stress components and the time averaged components in the fluid. Prandtl /76,77/ succeeded in doing that, by introducing the mixing length conception.

The early workers of this school assumed in addition self preservation for the mean and fluctuating quantities, see e.g., Schmidt /86/ or Taylor /99,100/. The axisymmetric turbulent buoyant plume in a uniform environment is treated, Schmidt makes basic assumptions about the flow from a point heat source extending Prandtl's mixing length theory. For the axial velocity and excess temperature and the width the results are:

$$u_M \approx x^{-1/3} \tag{4.1}$$

$$\Delta T_M \approx x^{-5/3} \tag{4.2}$$

$$r \approx x \tag{4.3}$$

The flow pattern spreads out linearly with the height above the source, the maximum velocity decreases continuously, and the maximum excess temperature decreases even more rapidly.

4.1.1 Numerical Solutions

More recent workers use more complex constitutive equations and solve numerically the appropriate system of equations. The complex formulations contain differential transport equations for the individual fluxes which are solved. Such models give of course much more information about the flow than the simple Prandtl mixing length conception. However, often the level of sofistication is high and the drawback of this approach lies in the increased complexity of the formulation and the consequently increased computer time used.

Launder & Spalding /45/ gives a review and from that one may conclude, that the complex formulations give more information, but they also need more imperical input. Here, one must remember that experimental data are vital as a basis for developing a model and for the understanding of turbulence and to guide the formulation. Further experimental data must form a basis for determining the empirical constants in the model.

A review of experimental data is given by Chen & Rodi /11/, and it is concluded that the stage of experimental knowledge is less satisfactory. The modeling of buoyant jets still presents uncertainties and additional work is necessary.

4.2 Integral Methods

The second school integrates the equations of motion across the jet and derives conservation integrals for the mass, momentum and buoyancy fluxes, see e.g., Batchelor /4/, Rouse /82/, Morton /55,56/, Fox /25/, Popiolek /71-73/.

Having integrated the equations of motion (3.7-9) with the limits $r = 0$ and $r = \infty$, and having divided by 2π, it leads to the equations of the form.

Conservation of mass flux:

$$[rv]_0^\infty + \frac{d}{dx}\int_0^\infty ru\, dr = 0 \qquad (4.4)$$

Conservation of vertical momentum flux:

$$[rvu]_0^\infty + \frac{d}{dx}\int_0^\infty ru^2\, dr + [r\, Cov\{v'u'\}]_0^\infty - \int_0^\infty \beta g r \Delta T\, dr = 0 \qquad (4.5)$$

Conservation of heat flux:

$$[rv\Delta T]_0^\infty + \frac{d}{dx}\int_0^\infty ru\Delta T\, dr + [r\, Cov\{v'\Delta T'\}]_0^\infty = 0 \qquad (4.6)$$

The boundary conditions yield

$$\lim_{r \to \infty} (rvu) = 0 \tag{4.7}$$

$$\lim_{r \to \infty} (r \, \mathrm{Cov}\{v'u'\}) = 0 \tag{4.8}$$

and

$$\lim_{r \to \infty} (rv\Delta T) = 0 \tag{4.9}$$

$$\lim_{r \to \infty} (r \, \mathrm{Cov}\{v'\Delta T'\}) = 0 \tag{4.10}$$

Therefore, the integrated equations of motion are the following.

Conservation of mass flux:

$$\frac{d}{dx} \int_0^\infty ru \, dr = - [rv]_0^\infty \tag{4.11}$$

Conservation of vertical momentum flux:

$$\frac{d}{dx} \int_0^\infty ru^2 \, dr = \int_0^\infty \beta g r \Delta T \, dr \tag{4.12}$$

Conservation of heat flux:

$$\frac{d}{dx}\int_0^\infty ru\Delta T\, dr = 0 \qquad (4.13)$$

The equations (4.11-13) form the basic framework for most of the previous work on jets, plumes and buoyant jets. Further the investigations can be divided in two groups.

4.2.1 Dimensional Analysis

Buoyant jets have a tendency to become self-similar in certain flow regions. Dimensional analysis can be used to find the basis of two distinct forms, i.e. pure jets and pure plumes. This information is very useful when dealing with experimental data.

4.2.2 Pure Jet Similarity

For a jet in uniform environment the kinematic momentum is conserved. Dimensional analysis where similarity relations are introduced into the continuity, momentum and heat equations gives, see e.g., Abramovich /1/, Chen & Rodi /11pp70-73/, Rajaratnam /79/, Popiolek /71pp68-76/:

$$u \approx x^{-1} \qquad (4.14)$$

$$\Delta T \approx x^{-1} \qquad (4.15)$$

$$r \approx x \qquad (4.16)$$

With the information given in equations (4.11-16) it is possible to reach the following expressions for the volume flux, V:

$$V = 2\pi \int_0^\infty ru \, dr \approx x \tag{4.17}$$

and the vertical momentum flux, M, is conserved:

$$M = 2\pi \int_0^\infty \rho r u^2 \, dr \approx x^0 \tag{4.18}$$

4.2.3 Pure Plume Similarity

For a plume, dimensional analysis leads to, see e.g., Batchelor /4/, Chen & Rodi /11pp70-73/,Rouse /82/, Popiolek /71pp68-76/:

$$u \approx x^{-1/3} \tag{4.19}$$

$$\Delta T \approx x^{-5/3} \tag{4.20}$$

$$r \approx x \tag{4.21}$$

The results of the similarity hypothesis in equations (4.19-20) are consistent with Schmidt's, equations (4.1-3). The flow pattern spreads out linearly with the height above the source, the velocity (for any constant value of r/x) decreases continuously,

and the excess temperature decreases even more rapidly.

With the information given in equations (4.11-13) and (4.19-21) it is possible to reach the following expressions for the

Volume flux, V:

$$V = 2\pi \int_0^\infty ru \, dr \qquad \approx x^{5/3} \tag{4.22}$$

Vertical momentum flux, M:

$$M = 2\pi \int_0^\infty \rho r u^2 \, dr \qquad \approx x^{4/3} \tag{4.23}$$

Kinetic energy flux, E:

$$E = 2\pi \int_0^\infty \frac{\rho u^3}{2} r \, dr \qquad \approx x \tag{4.24}$$

Enthalpy flux, H, which is conserved:

$$H = 2\pi \int_0^\infty \frac{\rho c_p u \Delta T}{2} r \, dr \approx x^0 \tag{4.25}$$

In the plume the velocity and temperature excess can be expressed by means of the convective heat output of the source. The dimensional hypothesis leads to:

$$u \approx Q_0^{1/3} \tag{4.26}$$

$$\Delta T \approx Q_0^{2/3} \tag{4.27}$$

Traditionally the profile shapes are approximated by Gaussian curves. Popiolek /71/ in his analysis assumes the following dimensionless velocity and temperature excess distributions, f_1 and f_2, respectively:

$$f_1\left(\frac{r}{x}\right) = \exp\left(-m\left(\frac{r}{x}\right)^2\right) \tag{4.28}$$

$$f_2\left(\frac{r}{x}\right) = \exp\left(-p\left(\frac{r}{x}\right)^2\right) \tag{4.29}$$

The parameter m is termed the velocity distribution factor and it describes the width of the velocity profile, high values giving narrow profiles. It also characterizes the angle of spread. The parameter p is called the temperature distribution factor, having the same function.

Further the similarity hypothesis gives functions for the velocity and buoyancy:

$$u = \left(\frac{3}{2\pi} \right)^{1/3} \left(\frac{m^2}{p} + m \right)^{1/3} F_0^{1/3} x^{-1/3} \exp\left(-m \left(\frac{r}{x} \right)^2 \right) \tag{4.30}$$

$$-g \frac{\rho - \rho_\infty}{\rho_\infty} = \left(\frac{3}{2\pi^2} \right)^{1/3} \left(\frac{p\,(p+m)^2}{m} \right)^{1/3} F_0^{2/3} x^{-5/3} \exp\left(-p \left(\frac{r}{x} \right)^2 \right) \tag{4.31}$$

Since the flow in plumes is generated by buoyancy forces the buoyancy flux F_0 is used instead of the convective heat output Q_0 to get a more general solution. They are connected in this way:

$$F_0 = \frac{\beta g}{c_p \rho} Q_0 \tag{4.32}$$

If equation (4.32) and the values c_p = 1005 J/kgK and ρ = 1.205 Kg/m^3 are introduced, the result is:

$$u = 0.023 \left(\frac{m^2}{p} + m \right)^{1/3} Q_0^{1/3} x^{-1/3} \exp\left(-m \left(\frac{r}{x} \right)^2 \right) \tag{4.33}$$

$$\Delta T = 0.011 \left(\frac{p\,(p+m)^2}{m} \right)^{1/3} Q_0^{2/3}\, x^{-5/3}$$

$$\exp\left(-p \left(\frac{r}{x} \right)^2 \right) \qquad (4.34)$$

The problem is now to find the appropriate velocity and temperature excess distribution factors, m and p, respectively. Baturin /5/ recommends, m = 81 to 90, and , p = 100 to 105, giving the set of equations usually taken into consideration, see the equations (1.1-3) presented in the /Introduction/.

4.3 Entrainment Factor

The system of equations (3.3-6) can be closed by introducing an assumption about the entrainment of ambient fluid into the buoyant jet. The entrainment coefficient approach is based on the hypothesis of Taylor /55/: that the entrainment should be proportional to some characteristic velocity in the jet. In this way the right hand side of the integrated continuity equation (4.11) can be described by the following formula:

$$- [rv]_0^{\infty} = \alpha u_M r_v \qquad (4.35)$$

where α is the entrainment coefficient (or factor)

In addition the ratio, λ, between the Gaussian velocity and temperature excess profiles has been introduced:

$$\lambda = \frac{r_T}{r_v} \qquad (4.36)$$

where r_T and r_V are the temperature excess and velocity in the buoyant jet, respectively, where the value is e-times lower than the axial value:

$$u(x,\mp r_V) = \frac{1}{e}\, u(x,0) = \frac{1}{e}\, u_M(x) \qquad (4.37)$$

$$\Delta T(x,\mp r_T) = \frac{1}{e}\, \Delta T(x,0) = \frac{1}{e}\, \Delta T_M(x) \qquad (4.38)$$

4.3.1 Integral Method Of Plume Calculation

If the Gaussian shaped profiles of equations (4.28-29) are substituted into the equations of motion (3.3-6), integration leads to the following integrated equations of motion, see e.g., Morton /56/ or Popiolek /71pp61-62,72pp12-13/:

Conservation of mass flux:

$$\frac{d}{dx}\,(u_M r_V^2) = -\,2[rv]_\infty = 2\alpha u_M r_V \qquad (4.39)$$

Conservation of vertical momentum flux:

$$\frac{d}{dx}\,(u_M^2 r_V^2) = 2\beta g \Delta T_M r_V^2 \lambda \qquad (4.40)$$

Conservation of heat flux:

$$\frac{d}{dx}\left(\frac{\lambda^2}{2(1+\lambda^2)}\,\Delta T_M u_M r_V^2\right) + \frac{d}{dx}\int_0^\infty \mathrm{Cov}\{u'\Delta T'\} r\,dr$$

$$= -\frac{dt_\infty}{dx}\,\frac{u_M r_V^2}{2} \qquad (4.41)$$

When considering the closure equations (4.35-36) the next problem that arises is: firstly to describe the entrainment coefficient α characterizing the entrainment of surrounding air by the buoyant jet and secondly the eventual change of the profiles ratio λ.

In the beginning Morton et al. /55/ have assumed the entrainment coefficient to be a universal constant with the same value for jets, plumes and buoyant jets. Later Fox /25/ and Morton /56/ find that the entrainment coefficient α could not be a universal constant due to further analysis and disagreement with experimental results, and the ration λ between the profiles even-so: The entrainment is a function of the local character of the flow and it also depends on the ambient conditions. This leads Fox /25/ to make the entrainment a function of the local Archimedes number, Ar, the Reynold's stresses "α_1" and the form of the similarity profiles "α_2". It is accomplished, using the axial kinetic energy conservation equation (3.6), and assuming that the Reynold's stress can be represented by a similarity variable.

$$\alpha = \alpha_1 + \alpha_2 \mathrm{Ar} \qquad (4.42)$$

$$\text{where } \alpha_2 = \left(2\lambda^2 - \frac{3\lambda^2}{1+\lambda^2}\right) \qquad (4.43)$$

Sometimes a constant λ value, e.g. $\lambda = 1$, is recommended in the whole pure plume region. This approach gives a constant α_2 value.

However, Seban & Behnia /87/ give an analysis which allows the variation of λ. Their assumption is similar to Fox, but it refers to the heat diffusion and not to the momentum diffusion.

Further an analysis of the integral method of plume calculation is given by Popiolek /71/ and Popiolek & Knapek /72/. They show that the assumption of Seban an Behnia is not necessary. Later Popiolek & Mierzwinski /73/ present some results: Their calculation results have been experimentally verified in four cases, with and without stable stratification, confirming the compatibility of measurement results and the integral method results. It must be emphasized that the flow is strongly dependent on stratification, and the integral method is difficult to use when the stratification is a complex function of the height x, ref. /74/. In reality linear stratification is seldom found. Further the accuracy of the integral method strongly depends on the accuracy with which the boundary parameters, i.e. the local Archimedes number Ar and the ratio λ between the velocity and temperature excess profiles in the beginning section, are determined. An other problem arises when the buoyant jet becomes negative and the similarity of the profile shapes has disappeared.

4.3.2 Pure Plume

Popiolek & Knapek /72/ conclude in their analysis of the buoyant jet integral method that Fox's formula (4.42), for the entrainment coefficient α, owing to the assumption of similarity of the shear stress distribution, only is completely correct in two particular cases: namely for a pure jet and for a pure plume (from a point heat source), since strict self similarity, i.e. also of the shear stress distribution, occurs in both cases. This has been experimentally verified in the plume case by Popiolek, see ref. /71p49,72p7-8,74/.

In dimensional analysis for a pure plume the ratio λ, the entrainment factor α and the local Archimedes number Ar are constants, ref. /71,74/. The analysis leads to the following expressions where the parameters α, λ and the local Archimedes number Ar are expressed by means of the velocity and temperature excess distribution factors, m and p, respectively.

The entrainment factor in a pure plume:

$$\alpha = \frac{5}{6} m^{-1/2} \tag{4.44}$$

The ration between the temperature excess and velocity profiles in a pure plume:

$$\lambda = \left(\frac{m}{p} \right)^{1/2} \tag{4.45}$$

The local Archimedes number:

$$Ar = \frac{2}{3} \frac{p}{m^{2/3}} \tag{4.46}$$

The comparison of calculation results from the integral method of plume calculation and the model of a plume above a point heat source from the similarity hypothesis are connected with certain problems, because the velocity and temperature excess distribution factors reported in the literature significantly differ from each other. This problem is taken up in /chapter 5.1.2/.

4.4 Plumes Influenced By Enclosing Walls

When the thermal flow rises near to enclosing walls, the entrainment is affected, ref. /42/. This may also be the case if two or more convection flows influence each other.

4.4.1 Volume Flux Symmetry Considerations

Equation (4.22 & 4.26) lead to the following power law for the volume flux in a

Free plume:

$$V \approx Q_0^{1/3} \tag{4.47}$$

Coanda effects may be present in flows near to enclosing walls so that they are no more axisymmetrical. However, the following symmetry considerations may give some ideas of the vertical volume flux in such flows, ref. /67/.

Wall Plume:

$$2V \approx (2Q_0)^{1/3} \tag{4.48}$$

$$V \approx 0.63\ Q_0^{1/3} \tag{4.49}$$

Plume in a corner:

$$4V \approx (4Q_0)^{1/3} \tag{4.50}$$

$$V \approx 0.40\ Q_0^{1/3} \tag{4.51}$$

Two equal sources close together forming one thermal flow:

$$V \approx (2Q_0)^{1/3} \tag{4.52}$$

$$V \approx 1.26\ Q_0^{1/3} \tag{4.53}$$

The above mentioned symmetry considerations lead to the conclusion, that the flow in a buoyant wall plume amounts 63 % of the flow in the corresponding free plume, for a plume in a corner it is 40 %. Further two equal sources close to another form a flow where the volume flux amounts 126 % of that from a single free source.

5. PREVIOUS EXPERIMENTS

5 PREVIOUS EXPERIMENTS

The experimental knowledge of axisymmetric buoyant jets arising from steadily maintained sources of heat are characterized by the lack of reliable data. Chen & Rodi /11/ conclude in their review that the state of experimental knowledge is much less satisfactory for buoyant jets with buoyancy effects and/or density differences than for non-buoyant jets with nearly uniform density.

The investigation of round buoyant jets is connected with the overcoming of difficulties in the laboratory. The thermal flows are difficult to measure, especially the plumes, because the flow velocity and temperature excess in plumes are small. This fact presents demands for sofisticated calibration and measuring techniques. The flow is very sensitive to outside disturbances such as room stratifications and room drafts, and the entrainment may be restricted by the presence of enclosing walls. Instability and plume axis wandering phenomena are reported. Further the flow itself maybe will warm up the room and create differences in surface temperatures, giving radiant exchange of heat between the enclosing surfaces and giving other convection flows of influence. Normally the surface temperatures in test rooms cannot completely be controlled.

5.1 Three Flow Regions

The flow in a buoyant round jet can be divided in 3 distinct regions: non-buoyant or pure jet region, intermediate region, buoyant region or plume region. The decay laws indicated by the dimensional analysis for the pure jet equations (4.14-16), and the pure plume equations (4.19-20) have been verified. Further an intermediate region between these two regions appears where the following purely empirical decay laws seem to exist, see ref. /11/:

$$u_M \approx x^{-4/5} \tag{5.1}$$

$$\Delta T_M \approx x^{-5/4} \tag{5.2}$$

The drawing up boundaries between the three regions of a buoyant jet is not easy. Firstly, because the length of the non-buoyant region is short even at small Archimedes' numbers, and the length of the intermediate region is fairly long. Secondly, because there is no abrupt change from one region to the other. Therefore, the data of these two regions often are treated as one group. The plume region can be considered separately, and it is not delimited flow downwards. But it is difficult to make this region fall within the zone considered, due to demand for high initial Archimedes' numbers.

5.1.1 Transition To Turbulence

Next it must be mentioned that completely similarity between two flows cannot normally be achieved, e.g. between a model and large scale reality. The problem is that the Archimedes' number is kept at a constant level in the flows compared, while the Reynold's and the Grashof's numbers are allowed to change due to auto similarity and therefore they do not influence the turbulent flow. However, the Reynold's and Grashof's numbers determine the transition to turbulence and thereby the length of the laminar flow region. Normally the Grashof's and Reynold's numbers are allowed to be smaller in models, and the length of the laminar flow, herein, are considerably larger than in the real large scale plumes, giving the result: The virtual origin of the turbulent plume is shifted toward higher x/d_0 values.

The mechanism of transition from laminar to turbulent flow is a very little understood process. Jaluria & Gebhart have studied the flow forming near a flat vertical surface, see ref. /36/. Of principle interest are: the definitions of the boundaries of the transition regime and their determination at several values of the surface heat flux. The results show, that firstly the transition events are not correlated in terms of the Grashof's number and that secondly the definition from common practice, to take the first turbulent burst as the onset of transition, is not sharply defined.

Jaluria & Gebhart /37/ have also studied the influence of a stable ambient thermal stratification on the development of the buoyant flow. The stratification is found to cause initial stabilization of the flow but later destabilization downstream. Measurements of natural transition indicate that a stable ambient stratification delays the onset of transition.

The natural convection flow over heated hemispheres has been studied experimentally by Jaluria & Gebhart /38/, similar tests in the flow above a spheric surface are carried out by Powe et Al. /75/ and Pera & Gebhart /70/. From their experiments it may be concluded: that firstly the shapes of the velocity and temperature excess profiles in the initial stage of buoyant jet evolution depend on the amount of convective heat emitted by the source, and that secondly the surface geometry and orientation of the heat source are of significant influence. Later Mierzwinski & Popiolek /54/ investigated the transition process from various sources, i.e. a sphere 35 mm diameter and a tube 30 mm diameter with an inside bulb. Smoke visualization shows that the flow in the latter case is already destabilized in the inlet cross section.

Elimination of the laminar region or an early transition to turbulence can be produced, either by introducing artificial disturbances in the flow to promote the transition process or by using a special constructed thermal plume generator where the flow is already turbulent at the exit nozzle, ref. /74/.

5.1.2 Experiments On Pure Plumes

Experiments on pure plume regions with both the velocity and the temperature excess distributions measured are carried out by four authors: Schmidt /86/, Rouse et Al. /82/, George et Al. /26/, Nakagome & Hirata /59/. Their m and p parameters are listed in fig.5.1 and the various profiles are compared grafically in fig.5.2.

Several others tried to produce the pure plume flow but they did not succeed due to disturbances such as instability, plume axis wandering and stratifications: see e.g., Mierzwinski & Popiolek /54/, Popiolek /71/, Kofoed & Nielsen /42,43/.

Velocity & temperature distribution factors and instruments			
m	p	Author & year	Instrumentation
45	45	Schmidt 1945 /86/	1 HWA & 1 TC
55	65	George 1977 /26/	1 HWA & 1 RT
65	70	Nakagome 1976 /59/	1 HWA & 1 RT
96	71	Rouse 1952 /82/	1 VA & 1 TC

Abbreviatons:
HWA hot wire anemometer
VA vane anemometer
RT resistance thermometer
TC thermocouple

Fig.5.1 Velocity and temperature distribution factors and instrumentation

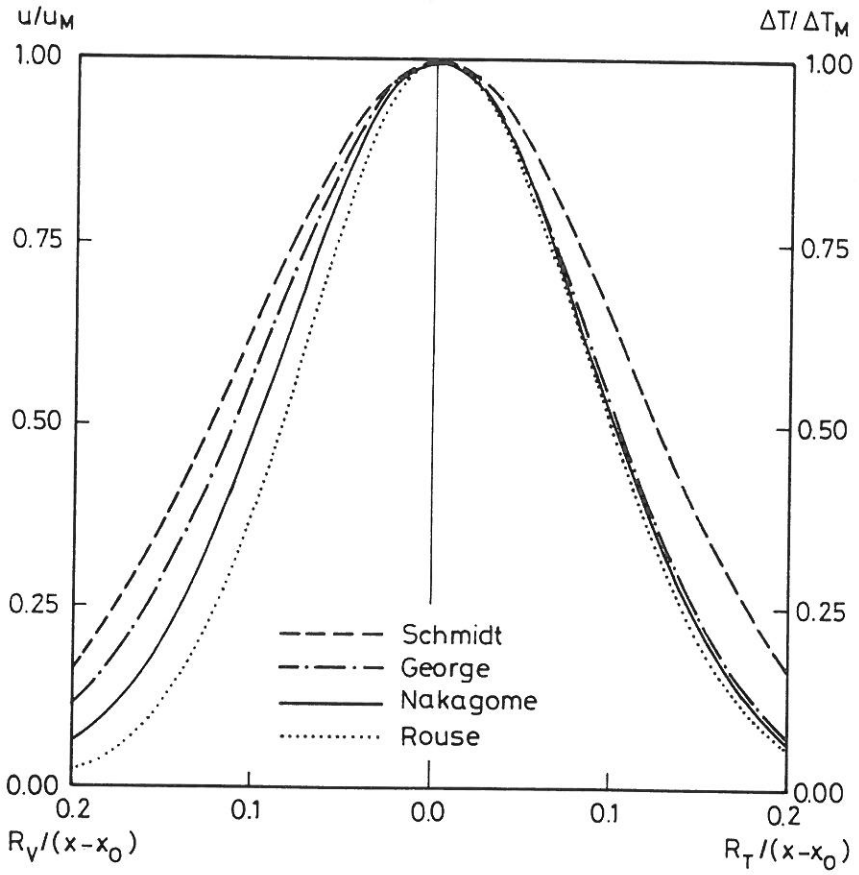

Fig.5.2 Distribution of dimensionless mean velocity u/u_M and mean temperature excess $\Delta T/\Delta T_M$ in the plume region.

The analysis is performed using local values of the velocity and temperature excess distribution factors, m and p, respectively. They are evaluated on the basis of u_M, ΔT_M, r_V and r_T values measured in the considered cross section of the plume. Such a local approximation can in no way predict the flow, but it is useful when analyzing the results of such experiments.

Schmidt /86/ uses a heat spiral in air to create the flow, and the velocity is measured with a hot wire anemometer, and the temperature with a thermocouple. The temperature measurements seem reliable but the velocity measurements are probably not very reliable using a hot wire of the beginning of the 1940's, ref. /86p362/. In their review Chen and Rodi /11/ reach the same conclusion. Problems of measuring in the border of the plume are

reported and maybe it could not be solved properly, and too high velocity values seem to appear here. No information is given about the stratification of the surroundings.

Rouse et. Al. /82/ establish the flow using a heat sourced of a recessed gas burner yielding low blue flames. The length of the laminar flow region is observed, and the measurements are carried out with a special constructed vane anemometer and a thermocouple. Since the vane anemometer has a diameter of 3 cm and a lower limit of 6 cm/s, the velocity measurements are not considered of very high quality. As the only author Rouse et. Al. indicate that the spread of buoyancy is greater than that of momentum, $p = 71 < m = 96$, and $\lambda = r_T/r_v = 1.16$. The temperature of the surrounding has not been reported.

George et Al. /26/ build a special thermal plume generator in air with a exit nozzle of 63.5 mm diameter and no laminar flow behavior is observed. The measurements are done using a two wire DISA P76 system, also giving the fluctuating quantities. Chen & Rodi /11/ consider these measurements to be the most reliable. However, it must be pointed out that the ambient air temperature changed within $\mp$ 1 K, so maybe the zero stratification has not been present. As the only author George et Al. observes no evidence of plume axis wandering either visually or in the reported data.

Nakagome & Hirata /59/ have a heated circular brass disk 70 mm diameter as heat source, and the measurements are taken with a hot wire anemometer and a resistance thermometer, and the fluctuating quantities are also measured. The flow can be divided in 2 regions, and in the fully turbulent region similarity between mean profiles and turbulent quantities is obtained. However, their plume is not symmetrical and, therefore, their measurements do not seem very reliable. Further the vertical temperature gradient is not reported and only about 25% of the heat supplied is found in the plume.

From the previous discussion concerning plumes it can be concluded, that the scatter in the reported m and p values is considerable. This could be caused by even very small stratification, which is of great influence, ref. /74/. But unfortunately the stratification has not been measured or regarded of influence. Further it seems more likely that the spread of momentum is at least equal or wider than that of thermal energy, i.e. $p >= m$ and $\lambda = r_T/r_V <= 1$.

5.2. Experiments On The Flow From Extensive Heat Sources

The air flow phenomena generated by human body represents an interesting case of a buoyant flow arising from an extensive heat source. The flow has been visualized by some authors employing smoke tests, and some information of both the convective flow pattern and the flow in the room as a total is obtained, see e.g. Daws /15/, Dittes & Mangelsdorf /16/, and Fitzner /21,22,24/. Homma's work is a wide study of the problem, presenting the actual knowledge, see ref. /33,34/.

Thermovision systems have also been used to visualize the temperature field in buoyant flows. A piece of paper is hung vertically in the flow, which warms up the paper, and a picture is taken. Fig.5.3 provides an example of the infrared camera technique, one can easily imagine the influence of the heat source geometry and orientation on the buoyant flow arising.

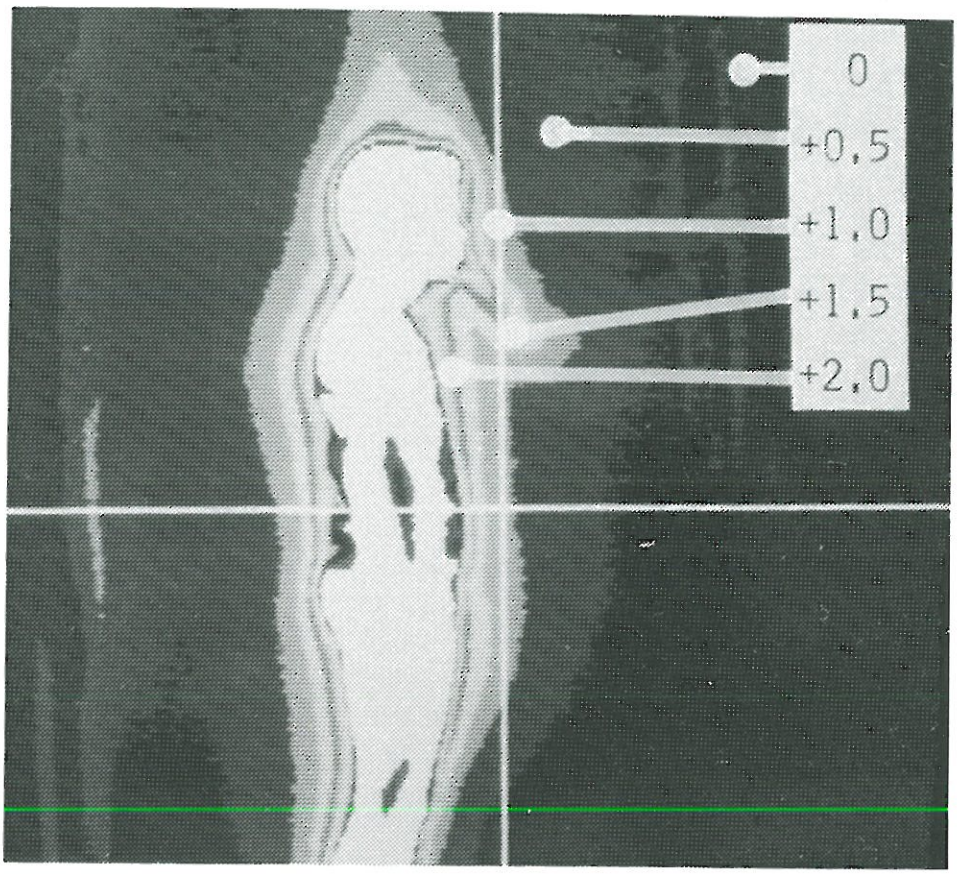

Fig.5.3 Thermografic picture of the boundary flow around a human being. The picture above is taken by aiming an infrared camera at a piece of paper which is hung beside the body. This picture indicates that the air around a body absorbs body heat, and the buoyant force causes the upward air stream, Homma */35/.*

Mierzwinski /53/ has carried out measurements in buoyant jets arising from standing or sitting people. The tests are performed in a calm undisturbed environment, and the room temperature as well as the stratification is referred particularly. Quantitative information regarding the evolution of the velocity and temperature excess fields in the convective flow has been provided. At the height of 0.75 m above the human head of a sitting or standing human being, in normal conditions of dwelling and offices at a temperature of 19 to 23 C, the following average properties are displayed:

Average properties in the flow 0.75 m above human head	
Temperature excess	ΔT_M = 0.5 to 0.8 K
Velocity	u_M = 0.17 to 0.23 m/s
Enthalpi flux	H = 30 to 80 % of Q_0
Volume flux	V = 0.030 to 0.060 m^3/s
Momentum flux	M = 0.003 to 0.005 m^2/s
Kinetic energy flux	E = 0.0003 to 0.0004 W
Angle of spread	δ = 17 to 24 ^{o}

Fig.5.4 Mierzwinski's measured average fluid dynamic properties in the buoyant flow 0.75 m above human head, ref. /53/.

The convective heat emission by human body is well know from Fanger's equation of heat losses from human beings and from Rapp's work, see ref. /18/ and /80/, respectively. There ought to be a direct correlation between the amount of convective heat emitted Q_0 and the heat enthalpy H in the buoyant jet. However, this is not observed in Mierzwinski's experiments and the presented 30 to 80 % relation has not been determined before.

Fig.5.5 shows a schematic representation of the flow. Up to the height 0.50 m above the head Mierzwinski /53/ observed transition flow, the profile shapes gradually change and the plume like flow evolves. The flow in this region is considered approximately to be axisymmetric. Beyond that height a mean flow self similarity occurs, the flow is axisymmetric, maybe considered turbulent, and the stream profiles of quasi Gaussian shape. But it can in no way be considered plume like.

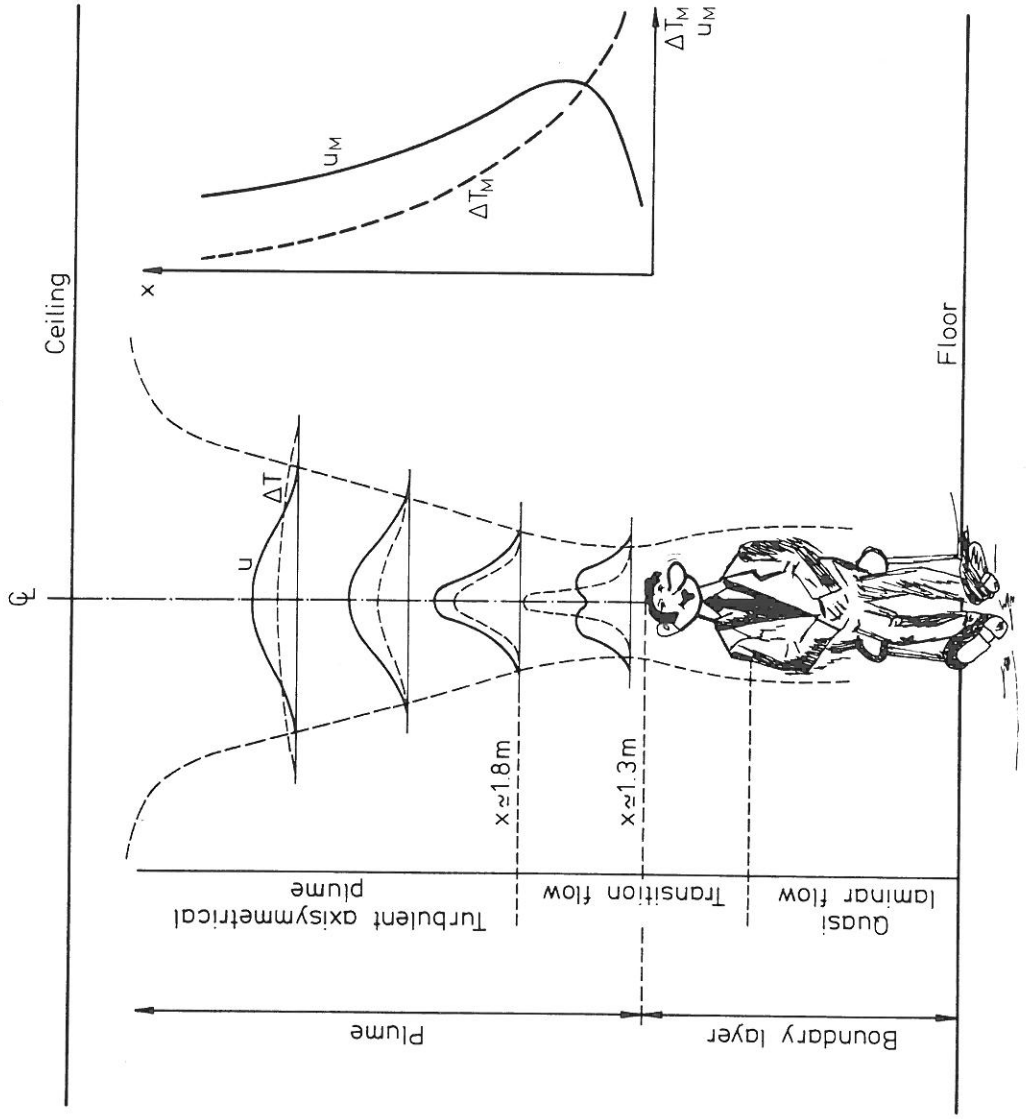

Fig.5.5 Schematic representation of the flow and of the mean temperature excess and velocity distribution in the buoyant jet above a human body, see Popiolek /71p13/.

5.2.1 Influence By Vertical Temperature Gradients

When designing a displacement ventilation system the question of influence by the vertical temperature gradient on the plume flow rates soon arises. However, the volume flux in the plumes and the vertical temperature gradient influence each other, and they may be influenced by many factors. Normally, the determination of the vertical temperature gradient is treated as the first part of the problem, then the flow rate in the buoyant jets is estimated.

Fitzner /22/ has carried out full scale measurements in ventilated rooms to examine the influence by the vertical temperature gradient on the flow rate in buoyant jets. Heated vertical cylinders are used as dummies to produce flow similar to that arising from a person, the source having a diameter and a height of 300 mm and 980 mm, respectively. The vertical temperature gradient is controlled by the ventilation of the room one may assume.

To measure the volume flux a so-called "Nullmethode" or Zero Method is employed. The principle is described in the following way, ref. /22/: That the air in different heights above the heat source is sucked out with a hood. In this way the air sucked out can be controlled by a helping ventilator and the volume flux is measured by a orifice. At the border of the hood it is tested if small horizontal air movements take place. If this is the case exactly the same amount of air is sucked out at this height as the heat source produces.

The measured volume flux from various measurements series with different temperature gradients in the room is shown in fig.5.6. The influence by the vertical temperature gradient appears clearly. The volume flux in the same height as the head of a sitting person is about 100 m^3/h and about twice as big in 2 m height at a temperature gradient of 0 K/m. At a gradient of 1 K/m it is about the half amount.

The results presented in fig.5.6, that the influence by the vertical temperature gradient is so great, is not consistent with the results of other authors. Kofoed & Nielsen /42p14/ find the same tendency, that the vertical volume flux from a heat source decreases when the gradient increases. But the effect is not reported so great. Maybe it is due to their source, which is a tube diameter 100mm with heating coils, such a source produces a much stronger flow with large temperature differences.

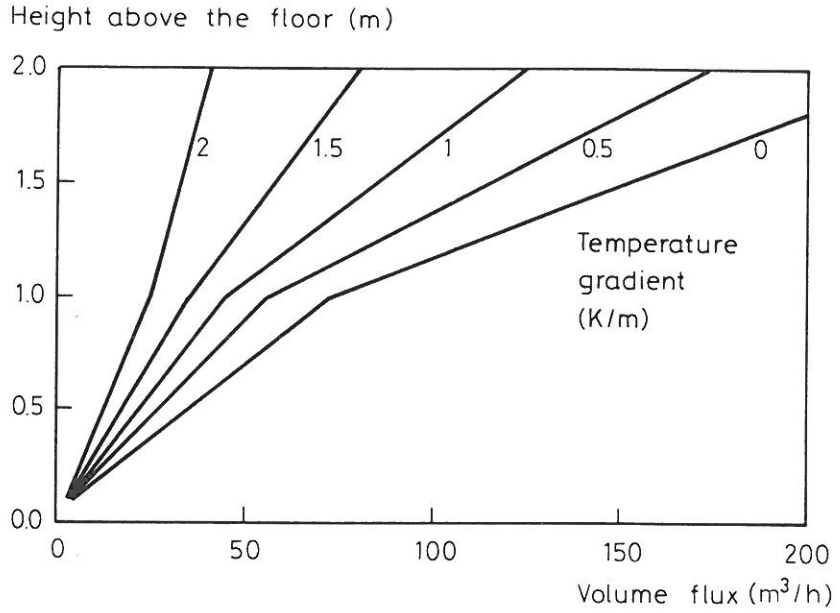

Fig.5.6 Volume flux from a person dummy at different temperature gradients in the room, Fitzner /22 Bild 23, 24p479/.

However, Mundt /57,58/ have carried out investigation of the same type as Fitzner's with a vertical cylinder, diameter 400 mm, height 1000 mm. These investigations do also not show this great influence of the vertical temperature gradient, ref. /57p7-9,58/.

When having Fitzner's investigation report /22p14/ it is possible to re-analyze and explain the results given in fig.5.6 in a slightly different way: In the case reported with a gradient of 2 K/m maybe the heat source has been cooled by forced convection,

because of ventilating the room. The vertical temperature distribution implies this , and the gradient between 1 m and 2.5 m height, where the free convection flow actually takes place, is only about 1 K/m.

5.2.2 Calculation Of Vertical Temperature Gradient

The gradient is a function of the temperature difference between the inlet and outlet air and sometimes the so-called 50%-rule is used, ref. /89/: That in office rooms half of the temperature gradient is evened out in the floor area, and the rest of the difference is linear from the floor to the ceiling. In fig.5.7 the principle is shown.

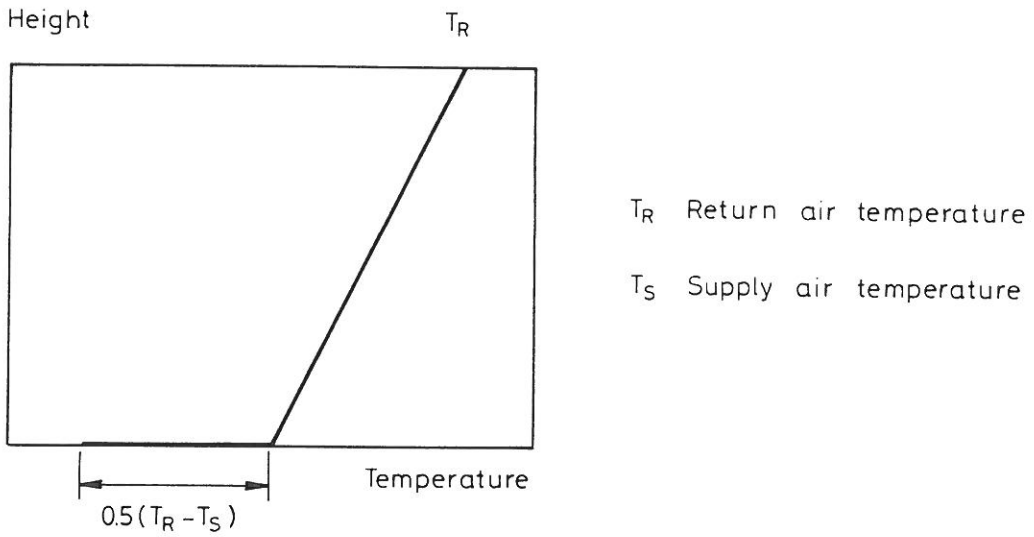

Fig.5.7 Calculation of the temperature gradient in offices by the 50%-rule, Skistad */89/*.

Mundt /57,58/ has carried out investigations to get more information about the vertical temperature distribution. Firstly, the temperature gradients are reported rather linear in the room and secondly, a simple but rather well fitting calculation model is presented: The radiation from the ceiling to the floor = the forced convection from the floor to the moving air steam above = the up warming of the air. This approach leads to the following equation:

$$\frac{T_{AF} - T_S}{T_E - T_S} = \frac{1}{\frac{G\rho c_P}{A}\left(\frac{1}{\alpha_R} + \frac{1}{\alpha_{CF}}\right)} \qquad (5.3)$$

where α_R radiative heat transfer coefficient $\left(\frac{W}{m^2K}\right)$

α_{EF} conv. heat tran. coef. at the floor $\left(\frac{W}{m^2K}\right)$

ρ air density $\left(\frac{kg}{m^3}\right)$

A floor area $\left(m^2\right)$

c_P specific heat of air $\left(\frac{J}{kgK}\right)$

G ventilation air flow rate $\left(\frac{m^3}{s}\right)$

T_{AF} air temperature at the floor (K)

T_E exhaust air temperature (K)

T_F floor temperature (K)

T_S Supply air temperature (K)

For the calculation of the left hand side of the equation (5.3) as a function of the air flow pr. floor area, $G\rho c_p/A$, the following values seem to be suitable: α_R = 5 W/m^2K and $\alpha_{EF} \in \{ 3 ; 5 \}$ W/m^2K, ref. /57p4-5/.

5.3 Flow Stability

When dealing with convective flows the problem of flow stability is incorporated. Rouse et al. /82/ have observed the smoke from cigarettes, presenting an example. The initial steadiness of the smoke indicates purely laminar motion for a considerable distance, then the flow becomes unstable and the filament breaks up into clouds. So even small sized sources with low thermal power produce unstable flows. Jaluria & Gebhart /38/ observe the flow generated by heated hemispheres of two sizes, 152 and 305 mm diameter. It can be concluded from their tests that the instability occurs sooner when the source size is bigger and the heat emission larger. Mierzwinski's investigation of the flow above human body proves that the buoyant jet, after it is formed, can be considered as turbulent, see ref. /53/. This is also indicated by the Gaussian shaped velocity and temperature excess profiles shown in fig.5.5.

5.3.1 Large Scale Flow Instability

In his report Popiolek presents an analysis of the methodic of buoyant flow investigation and measuring, see ref. /71/. The measurement results scattering of previous authors are observed, and the magnitude of the scatter is considered larger than one can expect from scale studies. Popiolek reaches the conclusion that the methodic has to be improved in order to reduce the measurement results scatter observed in previous experiments and to increase the measuring accuracy.

Large scale instability phenomena is often present when measuring buoyant jets, and the maximum values of mean velocity and temperature excess are reported to occur slightly deviated from the vertical symmetry axis to the source. This plume axis wandering George et Al. /26/ as the only author do not find in their investigations. The phenomenon is not completely understood yet, and one can not expect such ideal conditions as George et Al. Popiolek /71/ concludes that large scale flow instability in buoyant jets is the reason for the local unsteadiness of the flow. However, it does not exclude the steadiness of plume integral properties such as enthalpy flux, volume flux, momentum flux, or kinetic energy flux.

The above mentioned considerations leads Popiolek to accept the plume axis wandering and he has developed a measuring and data processing method where the phenomenon can be eliminated. In this report it is called the extrapolation method and the description is included in /chapter 6.2/.

6. EXPERIMENTAL PROBLEMS AND MEASURING TECHNIQUES

6. EXPERIMENTAL PROBLEMS AND MEASURING TECHNIQUES

The superior objective of the investigations is to improve the understanding of the mechanics in round buoyant jets. When measuring in the laboratory, difficulties which must be overcome arise. The buoyant jet flow is very sensitive to outside disturbances such as room stratifications, room drafts, enclosing walls, and the flow itself will maybe influence the conditions of the room. Further the flow is unstable and the velocities and temperature excesses are small presenting demands for calibration and measuring techniques.

These things necessitate thoughts about and work at experimental set up and procedures, which will be described in the following sections. /Chapter 6.1/ concerns some preliminary investigations, which have been carried out, concluding in the choice of three different measuring methods. The measuring methods have been established and optimization has taken place, this will be presented in /chapter 6.2-4/, where the advantages and disadvantages of each of them are taken into consideration. The way of measuring temperature and velocity with the related calibration technique will bee discussed in /chapter 6.5 and 6.6/, respectively. The choice of averaging time is treated in /chapter 6.7/. /Chapter 6.8/ touches the various heat sources which are axisymmetrical steadily maintained sources of heat. The investigations have taken place in two full-scale clima chambers. The description of these are in /chapter 6.9/.

6.1 Measuring Methods

Preliminary experiments have been carried out and smoke visualizations show, so as to leave no room for doubt, that any attempt to eliminate the large scale unstability of the flow does not give a positive result. /Appendix A/ provides some pictures of the flow. It may be concluded that the boundary flow near the source and the processes taking place are very little understood

and of unstable character them self. This fact alone produces unstable phenomena flow downwards. Thoughts about the cryolis force influence have arisen, but not inquired into. Further preliminary velocity and temperature excess measuring with nine velocity probes and nine temperature probes placed on a single horizontal strait line through the vertical symmetry axis to the source show considerable measurement result scatter and reasonable constant integral values for the volume flux could not be obtained, even at long time signal averaging, e.g. 5, 10, 15, 20 minutes. These observations are consistent with Popiolek's analysis of buoyant jet measuring methods and his analysis of the results from previous authors, see ref. /71/ and /chapter 5.3.1/. In /chapter 7.3/ some results are given to illustrate this problem.

Finally, the large scale oscillation, i.e. the buoyant jet axis wandering, have been accepted as a feature of the buoyant jet flow and as a single problem which has to be dealt with and which cannot be treated as a normal turbulence phenomena that can be averaged out. To overcome the large scale unstability problem and to produce non scattering integral value results for the various fluxes at fixed distances to the source, three different measuring and data processing methods have been established:

The extrapolation method

The zero method

The stratification method

The extrapolation method gives basic information about the mean temperature excess and mean velocity distributions of the flow. The zero method and the stratification method are two easy used methods, developed just to give information about the vertical volume flux in the buoyant jet, since this parameter is essential when designing displacement ventilation.

6.2 Extrapolation Method

As mentioned in /chapter 5.3.1/ similar large scale stability considerations lead Popiolek /71/ to develop a measuring and data processing method, here called the extrapolation method: The buoyant jet axis wandering is taken into account and little, but acceptable, measurement result scatter can be obtained as regards the maximum velocity and temperature excess and the plume integral parameter values.

It must be mentioned that the considerations about measurement technic, calibration and choice of averaging time /chapter 6.5-7/ apply for the extrapolation method.

6.2.1 Set Up And Placement Of Measuring Points

To measure the buoyant jet the probes are placed in a coordinate system - in this work nine velocity probes and nine thermocouples on each axis, the common probe or origin is located in the symmetry axis to the source. Additionally one velocity probe and one thermocouple are placed outside the buoyant jet flow in the same height to assure stable surroundings and to produce a reference temperature for the excess temperature calculation. Further around 40 thermocouples are situated in the surroundings to measure the vertical temperature distribution, the surface and the inlet and outlet temperatures.

Fig.6.1 provides a close up picture of some of the probes placed in the coordinate system in the flow, and fig.6.2 is a picture of the measuring stand.

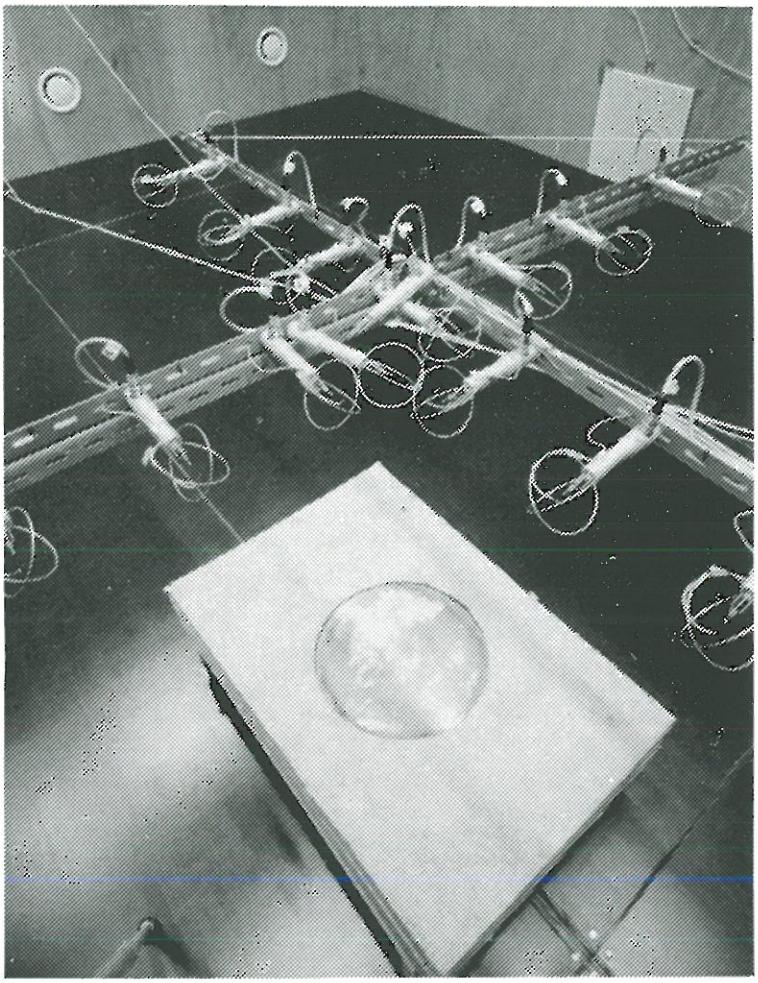

Fig.6.1 The picture illustrates the placement of the probes.

The vertical distance from the source to all the measuring points in the coordinate system has the same value. One single common velocity probe and one single common thermocouple or origin are located in the symmetry axis to the source. The distance between these two points is 1 cm and it is controlled that the warm sphere of the velocity probe does not influence the thermocouple. The rest of the probes are placed four velocity probes and four thermocouples on circle lines within a radius of 10, 30, 50 and 80 cm to the origin. The velocity probes are rotated ∓ 2 cm in relation to the thermocouples, so the eight measurement points have the same distance or radius to the symmetry axis to the source.

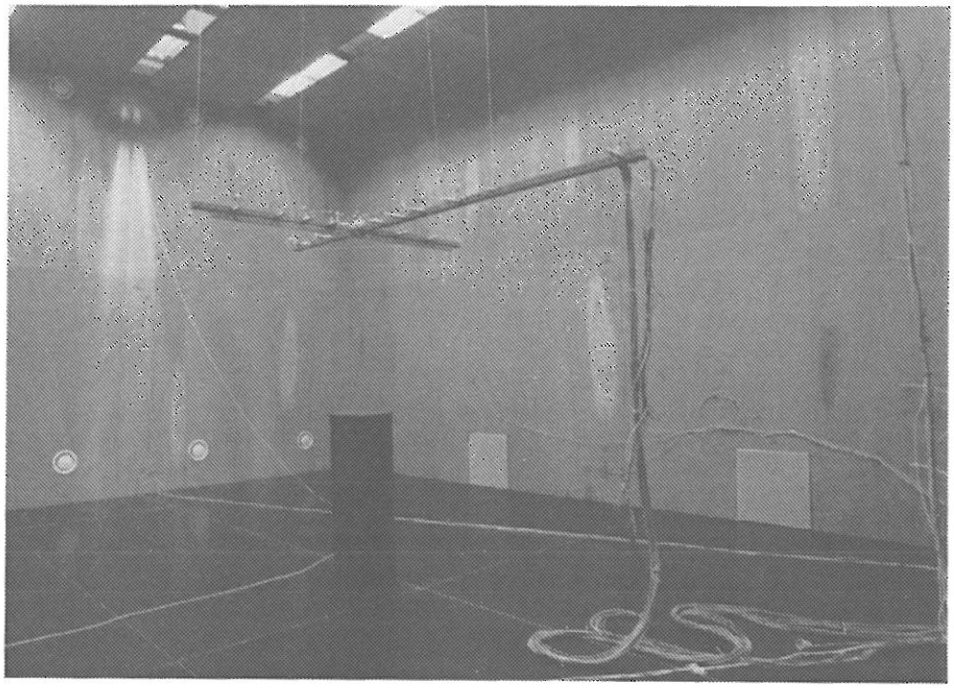

Fig.6.2 The extrapolation method measuring stand. The vertically traversable coordinate system above the heat source is shown, and in the front to the right some of the thermocouples measuring the vertical temperature distribution are seen.

6.2.2 Data Processing And Plume Parameters

The temperature measurements are chosen as the basis for the calculation of the buoyant jet axis position. Choosing these measurements rather than the velocity measurements is due to the fact that the principle of measuring is much more simple and of greater accuracy: There are no problems with self convection correction, with temperature compensation etc., see besides /chapter 6.5 & 6.6/.

From each measurement run the mean temperature excess is calculated: i.e. for each of the axes, y and z, the temperature excess distribution is approximated by a Gaussian curve, height "$\Delta T_{M,y}$", width "$r_{T,y}$" and location "y_0" or ($\Delta T_{M,z}$, $r_{T,z}$, z_0) preliminary estimated:

$$\Delta T(y) = \Delta T_{M,y} \exp\left(- \left(\frac{y - y_0}{r_{T,y}} \right)^2 \right) \qquad (6.1)$$

$$\Delta T(z) = \Delta T_{M,z} \exp\left(- \left(\frac{z - z_0}{r_{T,z}} \right)^2 \right) \qquad (6.2)$$

The calculations are performed on a Vax 8700 computer using the NAG E04JAF routine. E04JAF is an easy-to-use quasi-Newton algorithm for finding a minimum of a function subject to fixed upper and lower bounds of the independent variables using function values only. The position of the symmetry axes of these two distributions are characterized by the coordinates (y_0, z_0) and they also determine the real jet axis position. An example is plotted in fig.6.3.

Next the distances r from the real jet axis (y_0, z_0) to the measurement points (y,z) are calculated.

$$r = \left((y - y_0)^2 + (z - z_0)^2 \right)^{1/2} \qquad (6.3)$$

Then the mean temperature excess distribution in the buoyant jet is approximated by a Gaussian curve, the calculation is performed by the E04JAF routine on the base of the positions r of the measurement points. A total of 17 corresponding ΔT and r values is used.

$$\Delta T(r) = \Delta T_M \exp\left(- \left(\frac{r}{r_T} \right)^2 \right) \qquad (6.4)$$

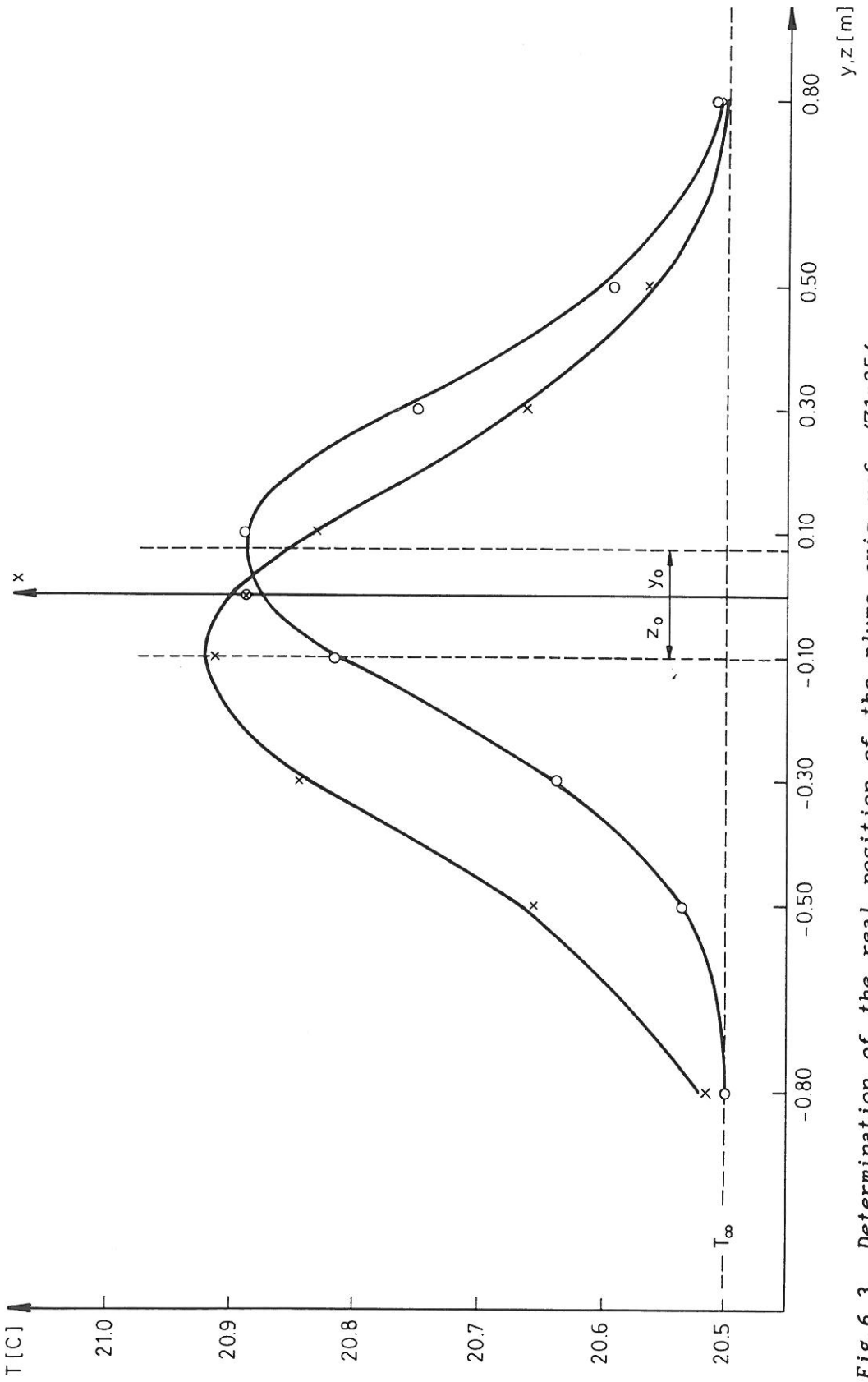

Fig. 6.3 Determination of the real position of the plume axis, ref. /71p35/.

Finally the mean velocity distribution is approximated by a Gaussian curve using the measurement point positions r. Again a total of 17 corresponding u and r values is used.

$$u(r) = u_M \exp\left(-\left(\frac{r}{r_V}\right)^2\right) \qquad (6.5)$$

By these step by step calculations which is called Gaussian fit the following parameters characterizing the plume are found:

Step	Plume parameters by Gaussian fit	
1	The jet axis position	y_0, z_0
2	The maximum mean temperature	ΔT_M
	The width of the temperature profile	r_T
3	The maximum mean velocity	u_M
	The width of the velocity profile	r_V

Fig.6.4 Gaussian fit gives characteristic plume paramter values. The height x above the source is known appriori.

6.2.3 Integral Plume Parameters

When approximating the results with Gaussian curves as described above it is possible to calculate the buoyant jet integral properties. If the equations (6.4-5) are substituted into the equations (4.22-25) the following expressions arise:

The volume flux, V:

$$V = \pi\, u_M\, r_V^2 \tag{6.6}$$

The vertical momentum flux, M:

$$M = \frac{\pi}{2}\, \rho\, u_M^2\, r_V^2 \tag{6.7}$$

The kinetic energy flux, E:

$$E = \frac{\pi}{3}\, \rho\, u_M^3\, r_V^2 \tag{6.8}$$

The enthalpy flux, H:

$$H = \pi\, \rho\, c_P\, u_M\, \Delta T_M\, \frac{r_V^2\, r_T^2}{r_V^2 + r_T^2} \tag{6.9}$$

Further the local Archimedes' number Ar defined on a local velocity radius scale and the ration between the temperature excess and velocity profile λ can be calculated as:

$$Ar = \frac{\beta g \Delta T_M r_V}{u_M^2} \qquad (6.10)$$

$$\lambda = \frac{r_T}{r_V} \qquad (6.11)$$

This is the two next steps in the extrapolation method.

Step	Additional plume parameter values	
4	The Local Archimedes number	Ar
	The ratio between temp. & vel. profile	λ
Step	Integral plume parameter values	
5	The enthalpy flux	H
	The volume flux	V
	The momentum flux	M

Fig.6.5 Additional characteristic parameter values and integral properties.

6.2.4 Local Approximation By A Model Of A Pure Plume

The pure plume similarity represents an interesting case and it is treated in connection with the dimensional analysis in /chapter 4.2.3/. Popiolek /71/ has analyzed the plume from a point heat source - a pure plume - assuming Gaussian shaped profiles, and he presents a local approximation by a model of a plume above a point heat source. Expressions for the local Archimedes' number and the ratio factor, by means of the temperature excess and velocity distribution factors in the equations (4.28-29) are given:

$$Ar = \frac{2}{3}\frac{p}{m^{3/2}} \tag{6.12}$$

$$\lambda = \left(\frac{m}{p}\right)^{1/2} \tag{6.13}$$

If the equations (6.10-11) are introduced, the temperature excess and velocity distribution factors, p and m, respectively, can be calculated explicitly:

$$p = \frac{4}{9} Ar^{-2} \lambda^{-6} \tag{6.14}$$

$$m = \frac{4}{9} Ar^{-2} \lambda^{-4} \tag{6.15}$$

Since, in the whole pure plume region, there is complete similarity the temperature excess and velocity distribution factors must display constant values, m = constant and p = constant. So the local approximation by means of the parameters m and p is a very useful way to analyze the flow and to check whether the pure plume similarity is present or not, simply due to the demand constant values.

Further the entrainment factor α can be calculated according to equation (4.44) as

$$\alpha = \frac{5}{6} m^{-1/2} \qquad (6.16)$$

Then the last two steps in the extrapolation method are given:

Step	Local approximation of a model of a pure plume	
6	The temperature distribution factor	p
	The velocity distribution factor	m
7	The entrainment factor	α

Fig.6.6 Local approxiamtion by a model of a pure plume.

6.3 Zero Method

To measure the vertical volume flux by means of the extrapolation method may be expected to give very precise values when the flow is axisymmetric and fully developed. But unfortunately it is a time consuming process, much measurement equipment is bound for a long period and the data processing is extensive.

In addition, the buoyant jets in ventilated rooms can not be expected to be axisymmetrical. Perhaps the heat source is a sitting person or another big source, which may produce an unstable flow with a strange form within a certain distance. The enclosing walls may also be of influence.

The above mentioned consideration makes the basis of the development of the easy to use:

Zero method

just giving information on the vertical volume flux in the buoyant jet.

6.3.1 Set Up

The method has previously been employed by several authors, e.g. Fitzner /22/ has used it for the same purpose as here, i.e. for measurements in air in ventilated rooms.

First smoke visualizations have taken place to assure the vertical direction of the flow. Next the air is exhausted above the heat source with a circular exhaust hood. The exhausted air volume can be controlled by a helping ventilator and the air flow rate is measured with a orifice Fig.6.7 shows a scheme of the set up, and fig.6.8 provides a picture of the measurement stand.

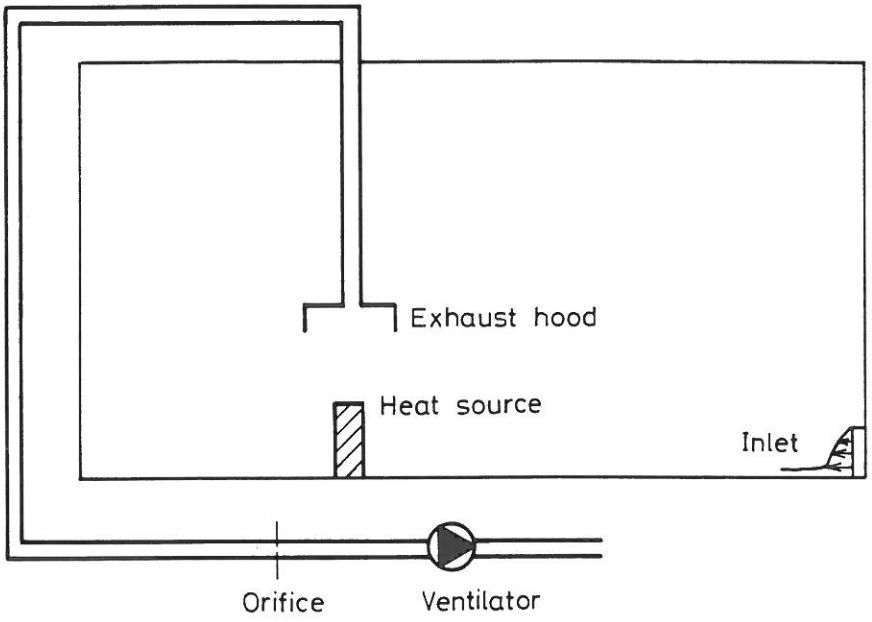

Fig.6.7 Scheme with the zero method set up: heat source, exhaust hood, helping ventilator, orifice etc. The vertical temperature gradient is measured outside the flow.

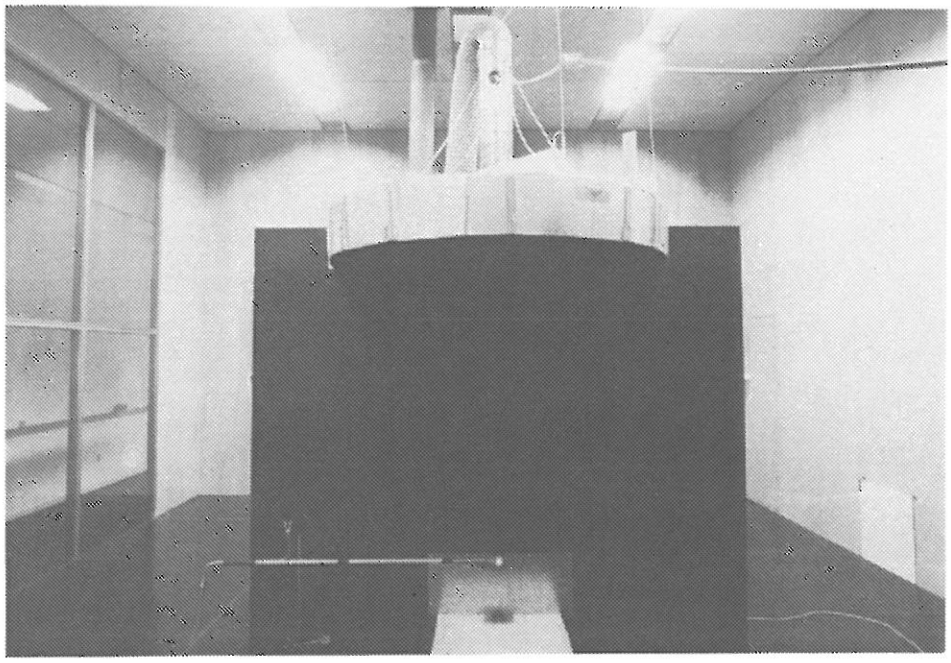

Fig.6.8 The measuring stand when investigating a wall jet.

At border of the exhaust hood from time to time small amounts of smoke are introduced, in this way it is controlled if no horizontal flow takes place. When this is the case one may assume that the same amount of air is exhausted through the hood as the vertical volume flux in the buoyant jet from the heat source at the same height. Fig.6.9 is a picture of one of the six smoke inlets, where the smoke is introduced as motionless as possible.

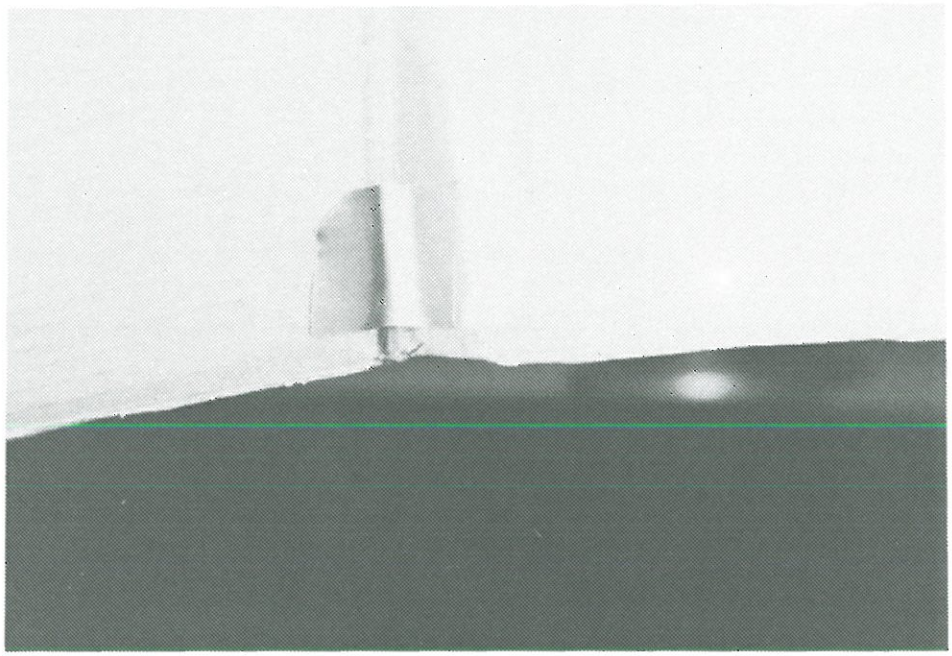

Fig.6.9 Smoke inlet at the border of the exhaust hood.

Hoods with different widths and side heights have been investigated to improve the method. One limit is reached when the effective width of the flow (including the axis wandering) is wider than the diameter of the hood. On the other hand, the hood may not bee to wide since, in this case, the horizontal velocities that determine the equilibrium between the exhaust and the air coming into the hood are very low. Practical carrying out of experiments and the results from the extrapolation method form the basis for the choice of hood diameter. A diameter 1.60 m is convenient for measurements in 2 m height above the floor when the heat sources are of the type described in /chapter 6.8/. The

necessary side height is dependent on the vertical velocity of the flow, high velocities giving high values. The maximum mean velocities in two m height above the floor from a heat source such as a sitting person are of the order 0.2 m/s, ref. /53p76/. A side height 0.20 m is found suitable, in this case the flow inside the hood remains stable. If considerable higher mean velocities were present the side height should have been higher to prevent fall outs due to pressure accumulation in the hood.

6.3.2 Smoke Observations

In reality the smoke picture changes a little all the time due to the structure of the buoyant flow. This fact necessitate measurements, i.e. smoke observation, during some minutes. These observations form the basis for the evaluation, whether the exhausted air volume rate is suitable, too big or too small to estimate the vertical volume flux. The operating person must have some experience with the zero method, since evaluation of the equilibrium depends on long time observations.

The figures 6.10-13 provide some typical pictures from the smoke observation at the border of the hood. Some relevant comments are also given. Fig.6.10 comprises a situation where the exhausted air flow rate is too small, in fig.6.13 it is too big. Fig.6.11 and 6.12 provide pictures of a situation with equilibrium where no horizontal flow as a total is present.

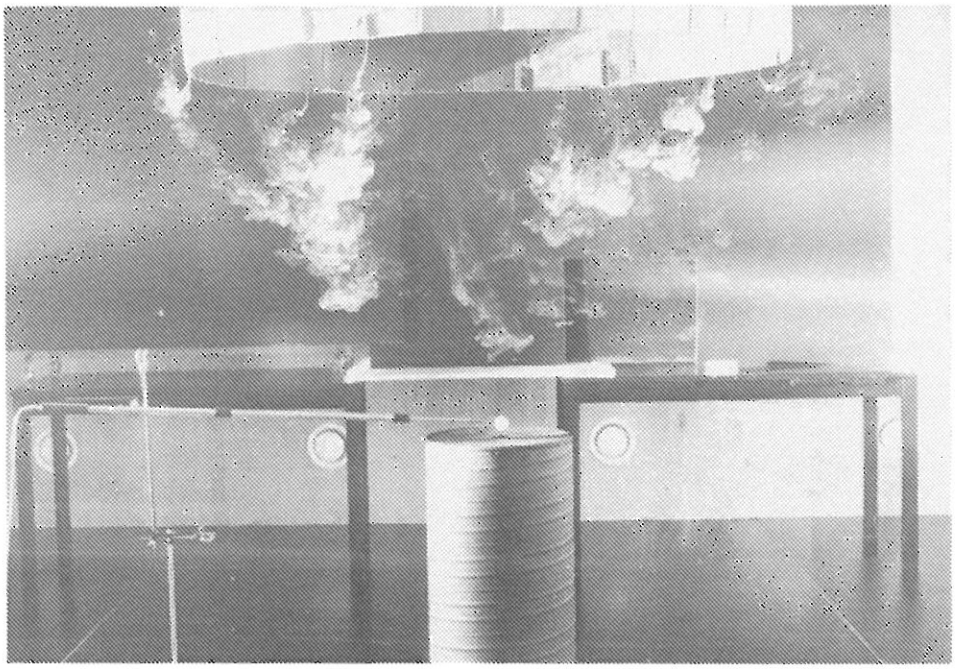

Fig.6.10 Smoke visualization at the border of the hood. Too little an amount of air is exhausted to estimate the volume flux in the buoyant jet.

In this case the filaments show a clear tendency to move outwards away from the hood. This indicates that the exhausted air volume rate is too little to estimate the vertical volume flux in the buoyant jet. The hood is continuously feeded with warm air from the buoyant jet flow. The hood is filled up and the surplus air drops out at the border of the hood creating a horizontal flow outwards.

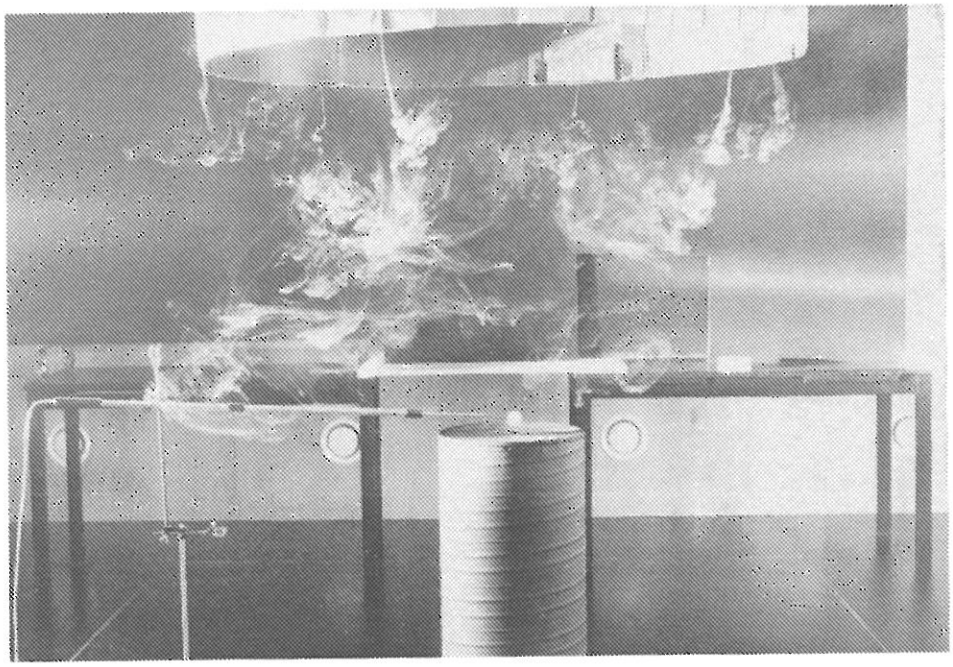

Fig.6.11 Smoke visualization at the border of the hood. A suitable amount of air is exhausted to estimate the volume flux in the buoyant jet.

When the equilibrium state is reached the filaments at the border of the hood become unstable. Several different smoke pictures can be observed. Here the filaments have moved vertically downwards for a limited period. This indicates that no horizontal flow takes place at the border at the hood. Therefore, one may assume that the the exhausted air volume rate estimates the volume flux in the buoyant jet.

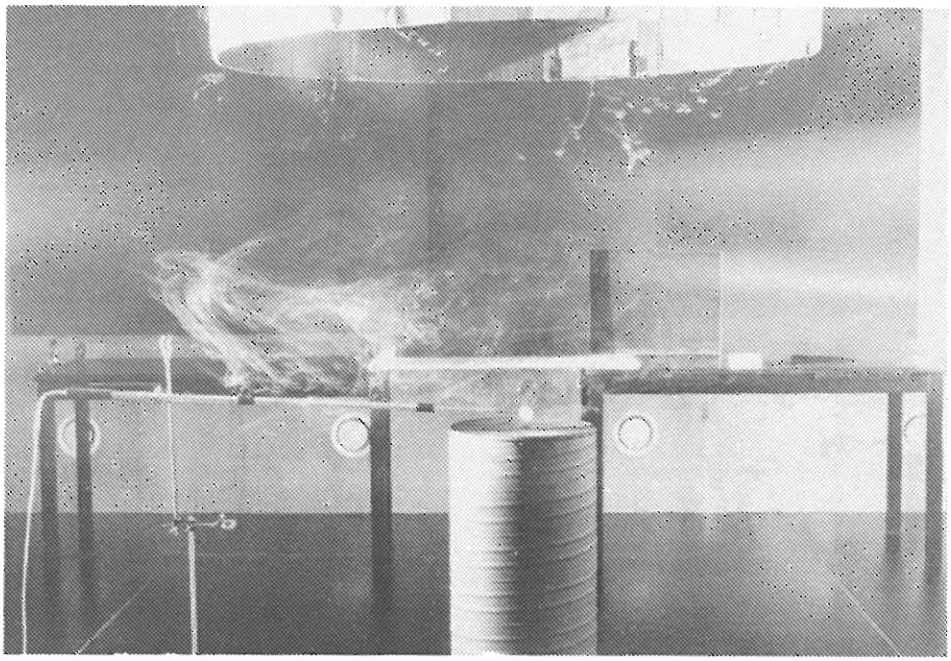

Fig.6.12 Smoke visualization at the border of the hood. A suitable amount of air is exhausted to estimate the volume flux in the buoyant jet.

This smoke picture also indicates the equilibrium state and it has been taken 3 minutes later than the one in fig.6.11. The flow at the border of the hood has now changed. At one side of the hood the filaments move outwards and at the other side they move inwards. Still, one may assume that the exhausted air volume rate estimates the volume flux in the buoyant jet.

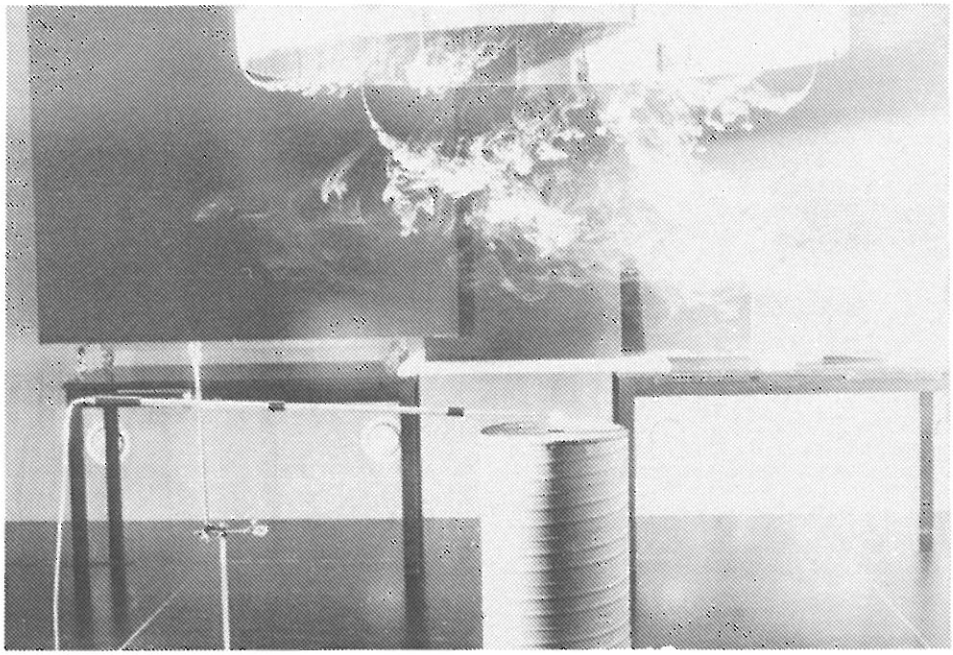

Fig.6.13 Smoke visualization at the border of the hood. A too large air volume rate is exhausted to estimate the volume flux in the buoyant jet.

In this case the filaments show a clear tendency to move into the hood. This indicates that the exhausted air volume rate is too big to estimate the vertical volume flux in the buoyant jet. The hood is continuously feeded with warm air from the buoyant jet flow. The volume flux in the buoyant jet is not big enough to fill up the hood and an extra amount of air is exhausted from the surroundings. This creates an inward moving horizontal flow at the border of the hood.

In the end of each measurement period smoke is introduced into the buoyant jet flow above the source and in the turbulent flow the smoke is soon dispersed. It follows the jet flow into the hood and at the border of the hood one can observe if the smoke drops out or not. Such experiments support the previously described smoke observations.

Two smoke pictures are given. Fig.6.14 corresponds to fig.6.10, i.e. the exhausted air volume rate is too little. This is also indicated by the fall outs at both sides of the hood. Fig.6.15 corresponds to fig.6.11 and 6.12, here the exhausted air volume rate estimates the volume flux in the buoyant jet. No smoke (or sometimes only a little amount) falls out of the hood.

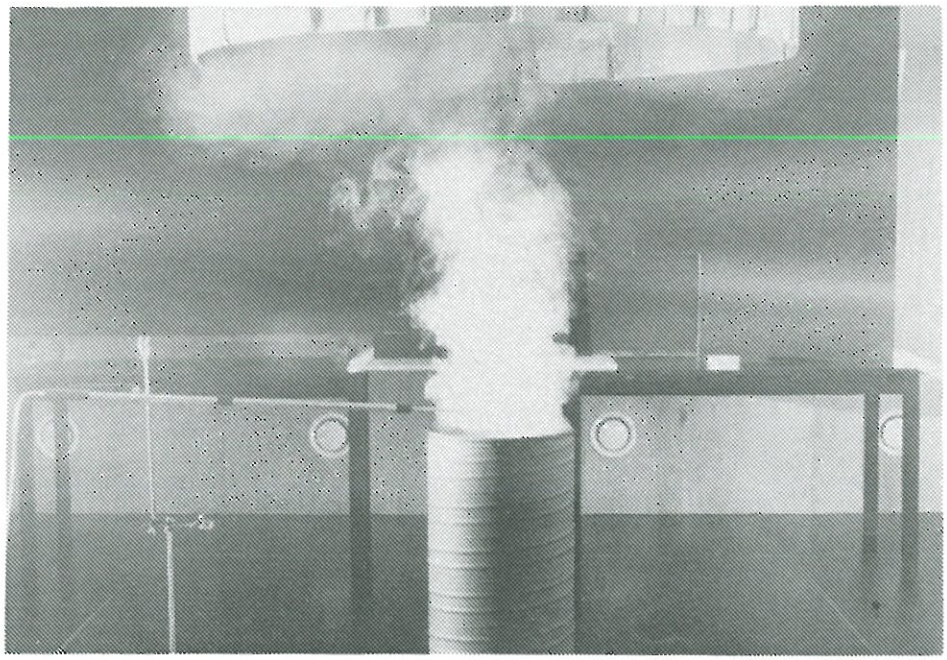

Fig.6.14 Smoke visualization of the total flow. Too little an air volume rate is exhausted since the smoke falls out of the hood.

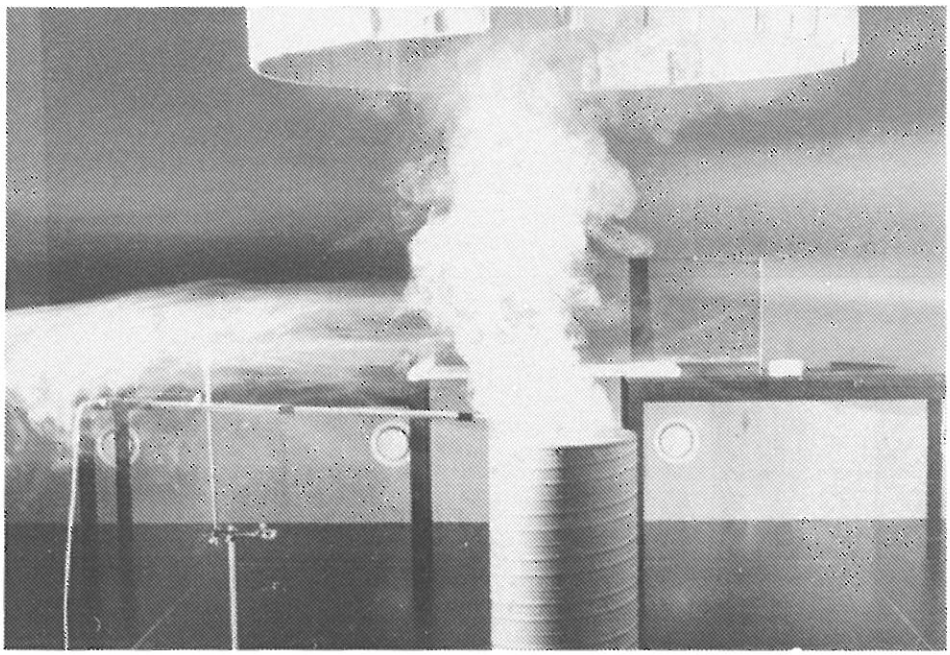

Fig.6.15 Smoke visualization of the total flow. A suitable amount of air is exhausted to estimate the volume flux in the buoyant jet since no smoke falls out of the hood.

6.3.3 The Accuracy Of The Zero Method

Since the zero method depends on individual observations by an operating person the question about accuracy soon arises. Therefore, the results from the zero method have been compared with reference results from the extrapolation method. Further, the same experiment has been carried out several times to find the spread of the results. On this basis it is concluded that the zero method gives the same result for the volume flux as the extrapolation method when investigating axisymmetrical buoyant jets. The volume flux can be estimated with an error about 10 % of the measured value. The zero method is easy to use and quickly it gives results. The investigated flow does not have to be axisymmetrical or fully developed. Further, flows influenced by enclosing walls, i.e. wall jets, comprise no problems since, in this case, the smoke observations just become more stable.

6.4 Stratification Method

The stratification method is an easy to use method like the zero method. It is just giving information about the vertical volume flux in the buoyant jet. Smoke observations form the main part of the work and no demand for a symmetric velocity profile ispresent. The method is applied for the investigation of buoyant round jets, wall jets and jets in a corner.

6.4.1 Set Up

The statification method is based on the principle of displacement ventilation. The two zone model, see /fig.1.1/, implies a recirculation flow above a certain height if the quantity of entrained air in the varm buoyant jets exceeds the air flow rate supplied. This have been verified by Heiselberg and Sandberg /31/ as regards the contaminant distribution in the room.

If no vertical air movement takes place near the walls one may assume that the air volume rate supplied estimates the vertical volume flux in the buoyant jets in the level of the stratification. This makes the basis of the stratification method.

In this work the convection flow from the heat source is visualized by continously introducing smoke into the source zone. The smoke reaches the ceiling where it is stabilized due to the recirculation flow. After a suitable periode of time the smoke picture does not change. Then the stratification level may be reported as a height above the floor. If more air is supplied to the room the stratification height will rise and vice versa. In this way the volume flux in the buoyant jet can be reported as a function of the height. Fig.6.16 comprises a scheme of the set up.

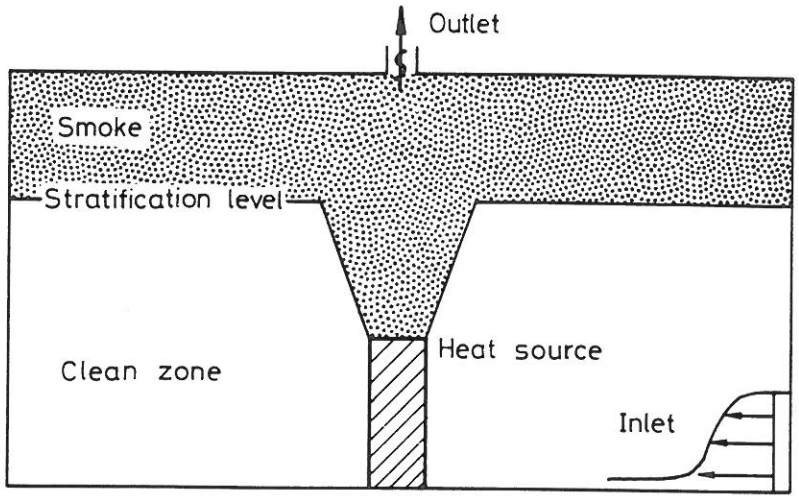

Fig.6.16 Scheme of the stratification method set up. The heat source is placed in center of the room. The air is supplied by a single wall mounted diffuser near the floor and it is exhausted in the ceiling. The vertical temperature gradient is measured outside the flow.

The heat source has been placed in various positions - free, close to single wall or in a corner between two walls - to determine the influence on the stratification height by the location of the heat source.

6.4.2 Smoke Observations

It has been possible to verify the two zone model by the smoke observations, because when measuring a stratification level is present. However, the height where the stratification takes place is not always so easy to determine due to the vertical air movements near the enclosing walls. In fig.6.17 a typical, problematic situation is drawn.

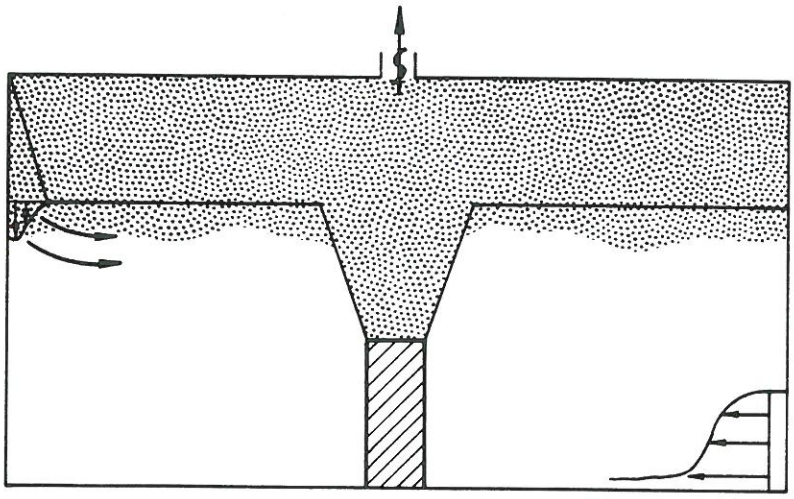

Fig.6.17 Typical smoke picture which illustrates the problem of determining the stratification height due to the vertical downdraught near the walls.

It has not been possible to control the temperature of the walls of the full-scale room. This comprises problems since the assumption about no vertical flow near the walls is not correct. Sometimes the recirculation flow under the ceiling has a temperature which is several degrees higher than the temperature of the walls. This causes cold downdraught near the wall in this height. The downdraught runs into the lower non contaminant zone bringing smoke from the upper contaminated recirculation zone. The downdraught spreads out in a certain height where the temperature has the same value as the temperature in the down flow? In this way a horizontal smoke cloud can be observed under the stratification level.

Sometimes it is difficult to distinguish the horizontal cloud from the stratification. However, this is the flow taking place in reality.

6.4.3 Accuracy Of The Stratification Method

The results by the stratification method depend on individual observations by an operating person. This principle is similar to the zero method. The results from the stratification method have not been compared with reference results from the extrapolation method for verification, and the same experiment has not been carried out several times to find the spread.

It is difficult to evaluate the accuracy of the stratification method. But there is a open demand for control of the wall temperatures to obtain a higher resolution. Like in the zero method the flow does not have to be axisymmetric and fully developed. In addition a wall jet and flow in a corner comprise no problems.

6.5 Temperature Measurements

Thermocouples are used for the temperature measurements. Usually when measuring the thermocouples are connected to a cold junction stabilization unit, and a millivolt meter is used for thermo electric force measurements. In such a set up the accuracy of the temperature measurement is limited:

by the accuracy of the cold junction temperature stabilization

by the sensitivity of the millivolt meter

by the accuracy of the temperature calibration

by the occurrence of electromotoric noise in the thermocouple circuit

A FLUKE Model 2240B Datalogger is employed for the thermoelectric force measurements and the resolution of the instrument is 1 μV. The constant cold junction temperature is maintained with a KAYE Icepoint Thermocouple Reference System which is capable of operating continuously with an error less than 0.02 K. It is a well known fact that it is difficult to obtain accuracies better than ∓ 0.2 K with such a system, even if the temperature area of measuring is limited. However, the temperature excess in plumes is normally very low, maybe even lower than 0.2 K. Since it is the purpose of this work to investigate such buoyant flows the described system of measuring is not considered appropriate.

6.5.1 Temperature Difference Measuring

Instead the temperature is measured as a difference between two points. Popiolek /71p16-20/ describe this method in his analysis of plume investigation methods, and it is concluded as an exemplary one for plume measurements. The method allows much more precise measurements since the measured difference between temperatures in two points does not acquire the same accuracy of the cold junction temperature stabilization as well as of the calibration accuracy. The accurate knowledge of the thermocouple sensitivity remains as important. The accuracy is limited by the non linearity of the thermocouple characteristic, because the sensitivity changes with the temperature. For the thermocouples copper-constantan type K used the following sensitivity is stated:

Thermocouple sentivity (mV/K)	Temperature (C)
0.0400	15
0.0400	20
0.0405	25
0.0410	30
0.0410	35

Fig.6.18 Thermocouple sensitivity in the temperature area measured.

Compensation for the non linearity of the thermocouple sensitivity has not taken place and the sensitivity 0.0400 mV/K is chosen as a proper value since most of the temperatures measured are near to or a little higher than the corresponding temperature value 20 C. If both temperatures were of the order 25 C this would produce a temperature measurement error which equals 0.012 K per temperature difference unit 1 K. One may conclude that the values of the temperature excess obtained systematically are only a little higher than those really occuring. This systematic error could have been corrected, but it is not done.

However, the accuracy of the temperature measured as a difference between to points is 10 times better than the normal set up.

6.6 Velocity Measurements

The velocity measurement results are produced by using a Dantec low velocity measurement system. It consists of the so-called DANTEC Multichannel Flow Analyser (Type 54N10), 18 probes (Type 54R10) and of the software package (Type 54G301). With this system one can present mean velocity, standard deviation (RMS), turbulence intensity, velocity histogram, air temperature measurement results. The data from the temperature part of this measurement system have not formed any basis for analysis, and therefore it is left out of further account.

The probes (Type 54R10) are omni directional, or at least they are called so, and therefore they do not tell anything about the direction of the flow. So before each measurement run smoke vizalization has taken place to assure vertical flow since measuring in horizontal flow or in flow showing disintegration tendensies would have no meaning.

The 54R10 probe or transducer consists of two sensor spheres, one flow sensor (the hot sphere) and one temperature compensation sensor (having the temperature of the surrounding air). When measuring turbulent non isothermal flows like buoyant jets, it is a problem that the temperature registration for the compensation do not take place at exactly the same point as the velocity measuring, here the distance between these two points is 3 cm. To reduce this systematical error the placement as well as orientation of the probes has received much attention: The two sensor spheres are situated having the same vertical distance to the source, and due to axisymmetric argumentation the two sensors are placed on one circle line having the same radius to the symmetry axis to the source. Fig.6.19 with some hand drawn circle lines illustrates the arrangement:

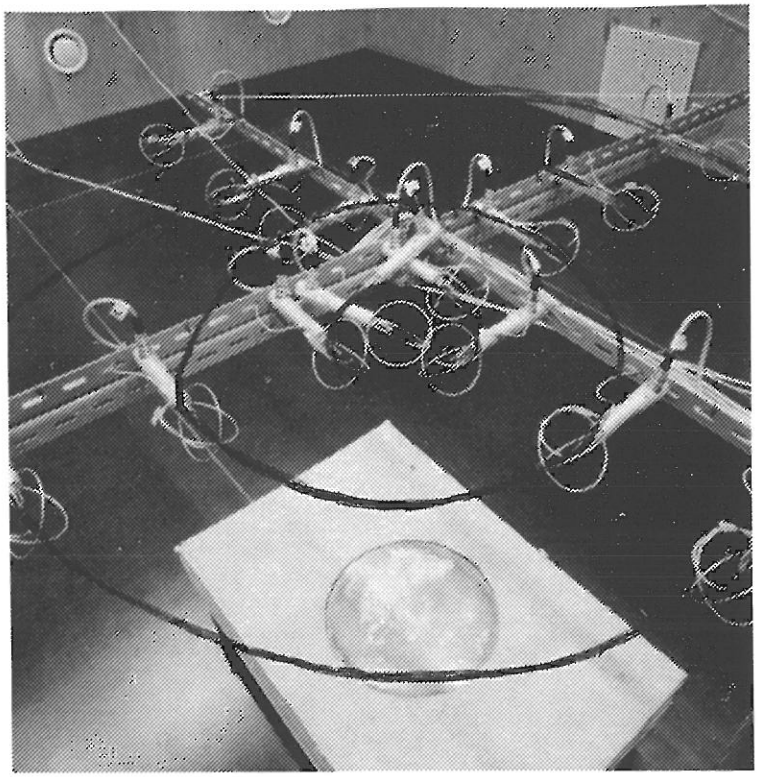

Fig.6.19 Placement of the velocity probes.

6.6.1 Velocity Calibration

The probe is adjusted and calibrated at the DANTEC factory. The calibration is carried out with the transducer oriented vertically and perpendicular to the horizontal flow, but it is a good habit always to calibrate before and after long periods of measuring to check the probe.

However, the buoyant flow from steadily maintained sources of heat rises vertically, therefore the probe is oriented horizontally. This placement necessitate calibration in vertical flow since the effect by the self convection of the hot sphere cannot be expected independent of the flow direction. Investigation has been carried out to get information about the self convection phenomenon. The same true velocity has been measured, firstly as a horizontal flow then as a vertical flow. Fig.6.20 shows increased showing in the latter case.

It may be concluded, so as to leave no room for doubt, that calibration in a flow with the same direction as the investigated flow is necessary to obtain accurate measurement values, fig.6. shows this. At a velocity of 0.05 m/s the increased velocity showing in vertical flow is close to 70 %, at 0.10 m/s it is 20 %, and at 0.50 it is 1 %, due to the effect of self convection. Of practical reasons all of the probes have been calibrated individually in horizontal flow, next compensation according to fig.6.20 has taken place.

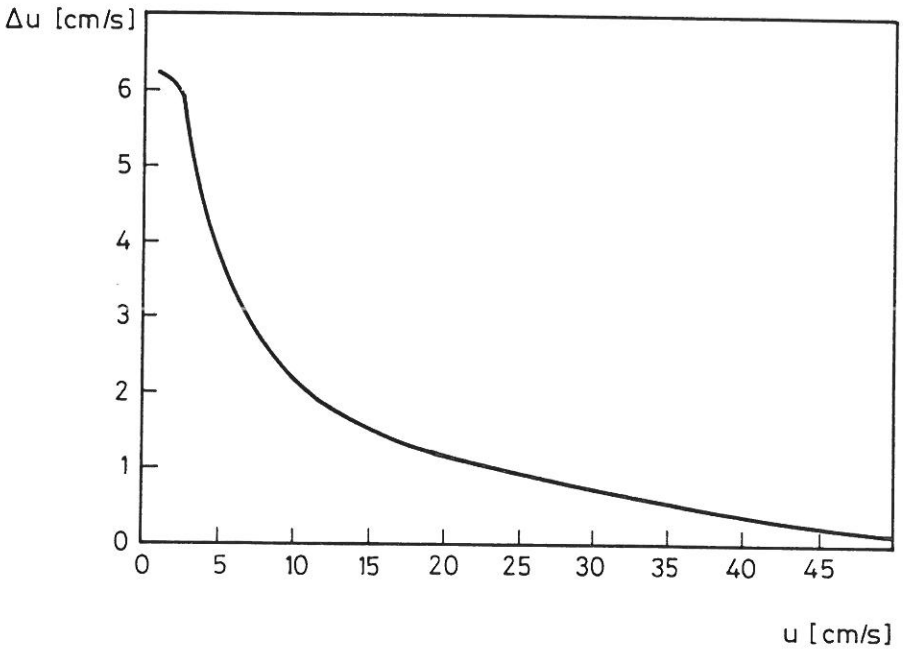

Fig.6.20 Effect of self convection - increased velocity showing in vertical flow versus horizontal velocity.

6.7 Statistical Errors And Averaging Time

Temperature and velocity measurement results show basic errors, due to the transducer construction and due to the calibration rutines. In addition statistical errors are present. The air velocity and temperature in turbulent flow change randomly and a averaging procedure is necessary to obtain mean values. The

statistical error of a mean measurement is dependent of the turbulence scale and of the averaging time: large turbulence scales giving large errors and the increase of averaging time giving smaller errors. Popiolek /71p20-25/ gives in his work an analysis, and for plume measurements an averaging time or time constant of the order 300 seconds is recommended.

In practice the averaging time must be chosen so that the mean estimators have the required accuracy. Leaving further discussion out of consideration an averaging time of 180 seconds is chosen. The temperatures are sampled once every 20 seconds, the velocity twice a second. The choise of 180 seconds may be confirmed by the fact, when employing the extrapolation method, that the plume integral fluxes do not differ much from their mean values, see /chapter 7.3/.

6.8 Heat Sources

Four different steadily maintained sources of heat have been used to produce the convection flows. In ventilated rooms the sources which produce the vertical convection flows are pure sources of heat. This states the reason for the choice. Further, the sources are round due to symmetry reasons. The four heat sources are individually described in /chapter 6.8.1-4/ and they consist of:

Tube, diameter 50 mm

Tube, diameter 100 mm

Horizontal plate, diameter 356.8 mm

Vertical cylinder, diameter 400 mm

According to the description in /chapter 2/ pure heat sources produce plume flows. However, the characteristics of the pure

plume, i.e. the pure plume similarity /chapter 4.2.3/, may fall far away from the source due to a long intermediate region. However, it is a part of this work to investigate this phenomenon.

6.8.1 Tube, diameter 50 mm

This source is constructed due to a demand for the highest amount of heat on the smalles place possible. The source consists of a steel tube, height 150 mm and diameter 50 mm, with hot wire inside. At the top of the source some artificial disturbances is introduced to speed up the transition to turbulence. During the measurements the source is vertically placed in mineral wool and the air is sucked through the source from below. The distance from the top of the source to the floor is 0.25 m. Fig.6.21 provides a picture of the measuring stand. It appears that the mineral woll is raised from the floor to allow a possible wall jet to pass without influencing the convective flow above the source.

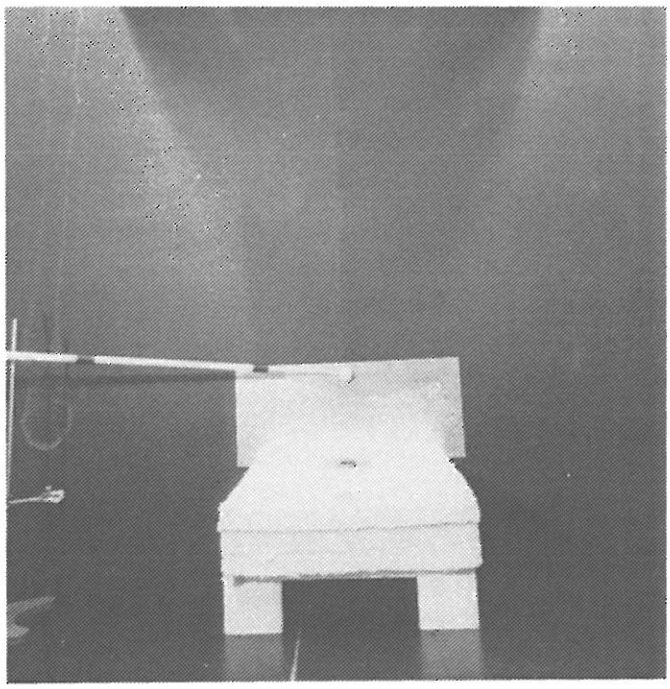

Fig.6.21 Measuring stand with tube diameter 50 mm. The heat source is placed in mineral wool and the air is sucked from below.

6.8.2 Tube, diameter 100 mm

A picture of the source is given in fig.6.22.

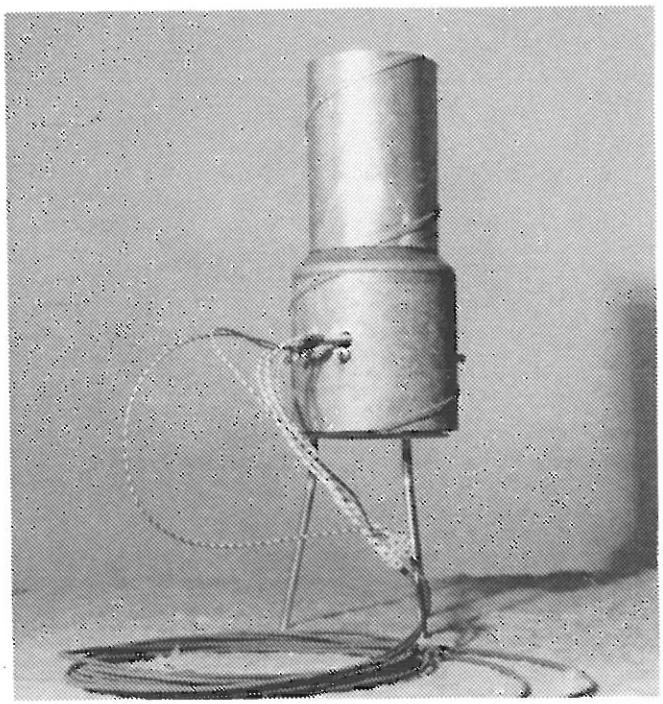

Fig.6.22 Tube diameter 100 mm.

The lower part of the heat source is a tube, 125 mm high and diameter 125 mm, with heating coils in. At the top of this tube a contraction tube is attached and then the flow runs in a tube, height 150mm and diameter 100 mm, before it leaves the source. The source extracts air from the horizontal surroundings and from below the source.

6.8.3 Plate, diameter 356.8 mm

An assembly drawing of the source is given in fig.6.23. It appears that the source is a silver-plated round plate. The power is induced by the hot wire which is screwed on the plate by means of a steel plate. The hot wire is thermal isolated from the steel plate. In this way a good transmission of heat by conduction is assured from the hot wire to the plate.

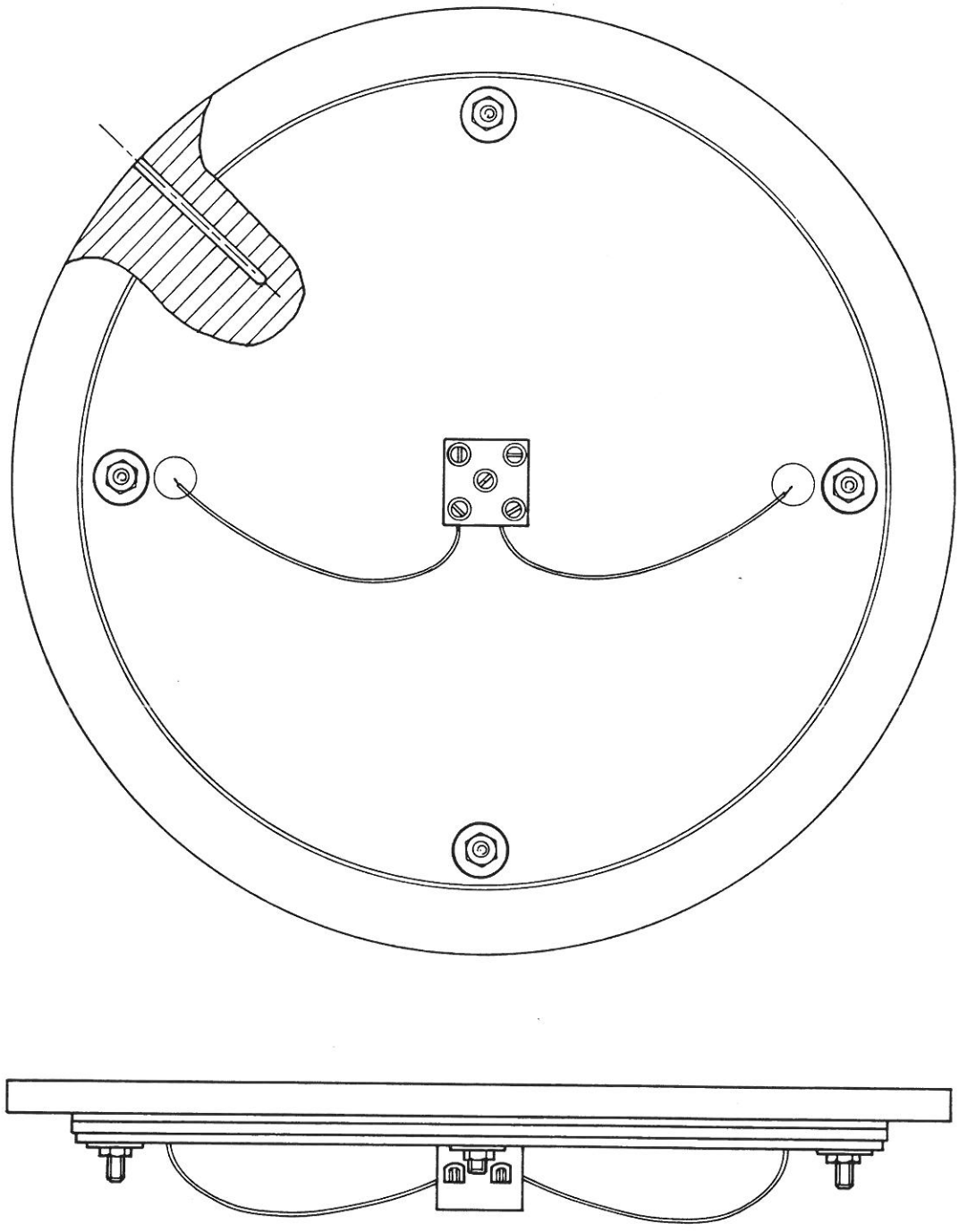

Fig.6.23 Plate diameter 356.8 mm. It consists of a 8 mm silver-plated copper plate, hot wire 1 mm arranged in a horizontal plane, isolation material 3 mm and a 2.5 mm steel plate. The partial view shows a hole for a thermocouple.

During the measurement series the plate has been placed horizontally in alu-covered mineral wool. The height from the floor to the top of the source is 0.25 m. The distance from the backside of the mineral wool to the floor is 0.10 m, so a possible wall jet does not influence the convection flow from the source.

6.8.4 Cylinder, Dia 400 mm

The cylinder is chosen to simulate the flow from a person. The construction is quite similar to the one Mundt uses, see ref. /57,58/. A picture of the source is shown in fig 6.24.

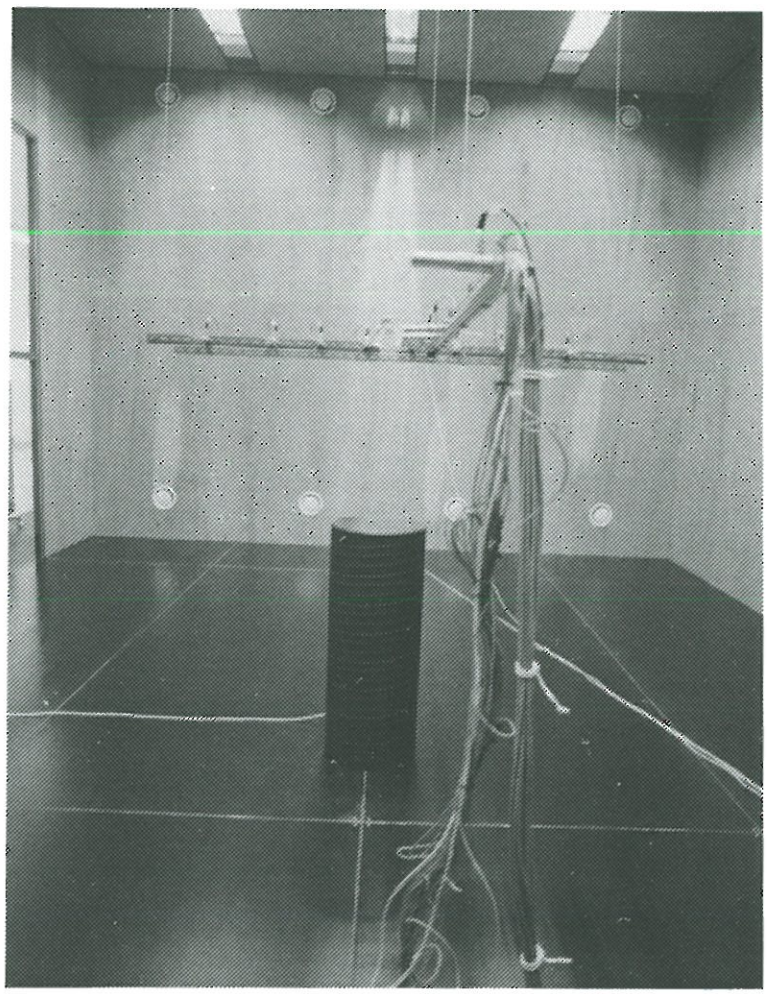

Fig.6.24 Vertical cylinder diameter 400 mm, height 1000 mm. The source is chosen to simulate the flow from a person.

The source is black painted and open in the bottom. It is 1000 mm high and has a 400mm diameter. Indside the source four electric bulbs are placed. The bulbs are spaced 0.25m apart in the centerline to the source. The first bulb is situated 0.125 m under the top of the source. The bulbs emit light and inside the cylinder reflection takes place. When a power of 100 W is induced, the source gives a surface temperature which is similar to the one of a person. During the measurements the source has been situated directly on the floor.

6.9 Full-Scale Clima Chambers

The experimental investigations are carried out in two full-scale clima chambers at The Institute of Building Technology, University of Aalborg. The measurements involving the extrapolation method are carried out in clima chamber L. This is the smallest of the two chambers and it has the height (and size) of a normal office room. Chamber F is considerably higher (and bigger), and in this room the investigations employing the extrapolation method and the zero method are completed. In the following two chapters the full-scale clima chambers will be described as regards size, construction and function.

6.9.1 Clima Chamber F

Clima chamber F is placed in a laboratory hall. The dimensions of the chamber are:

Height 4.60 m

Length 8.00 m

Width 6.00 m

These values give by computation a floorage of 48.0 m^2 and a cubic content of 221.0 m^2. The clima chamber is built up on a steel skeleton - walls, floor and ceiling are made of 19 mm Douglas plates. It is possible to light up the room making vertical, sectional views in two directions, i.e. in the longitudinal direction or perpendicular to this direction for visualization of introduced smoke. Through two of the walls it is possible to observe the air movements since double glased windows are installed. An view of the clima chamber appears in fig.6.25.

Fig.6.25 Clima chamber F. Two wall mounted diffusers are placed and in the ceiling exhaust openings, and three rows of double glas appear through which a sectional visualization of the flow by means of light is possible.

The room is ventilated by means of the displacement ventilation principle with two wall mounted diffusers near the floor situated on one side wall and with two exhaust openings in the ceiling. The air change rate, under the described conditions, may reach approximately 8 h^{-1} and the excess temperature of the inlet exceeds the value ∓ 5 K.

6.9.2 Clima Chamber L

Clima chamber L is also placed in a laboratory hall and it has the dimensions:

Height 2.40 m

Length 5.40 m

Width 3.60 m

These values give by computation a floorage of 19.4 m^2 and a cubic content of 46.7 m^2. The clima chamber is built up of a wooden skeleton - walls, floor and ceiling made of 19 mm Douglas plates. It is possible to light up the room making vertical, sectional views in the longitudinal direction for visualization of introduced smoke. Through two of the wall it is possible to observe the air movements, since double glased windows are installed. The chima chamber appears in fig.6.26.

It is possible to ventilate the room in various ways. The highest air change rate lies between 7 and 10 h^{-1} dependent on the form of the inlet and the inlet temperature excess may vary approximately ∓10 K. The displacement ventilation principle is employed: one wall mounted diffuser is situated near the floor at one of the end walls and one exhaust opening is placed in the center point of the ceiling.

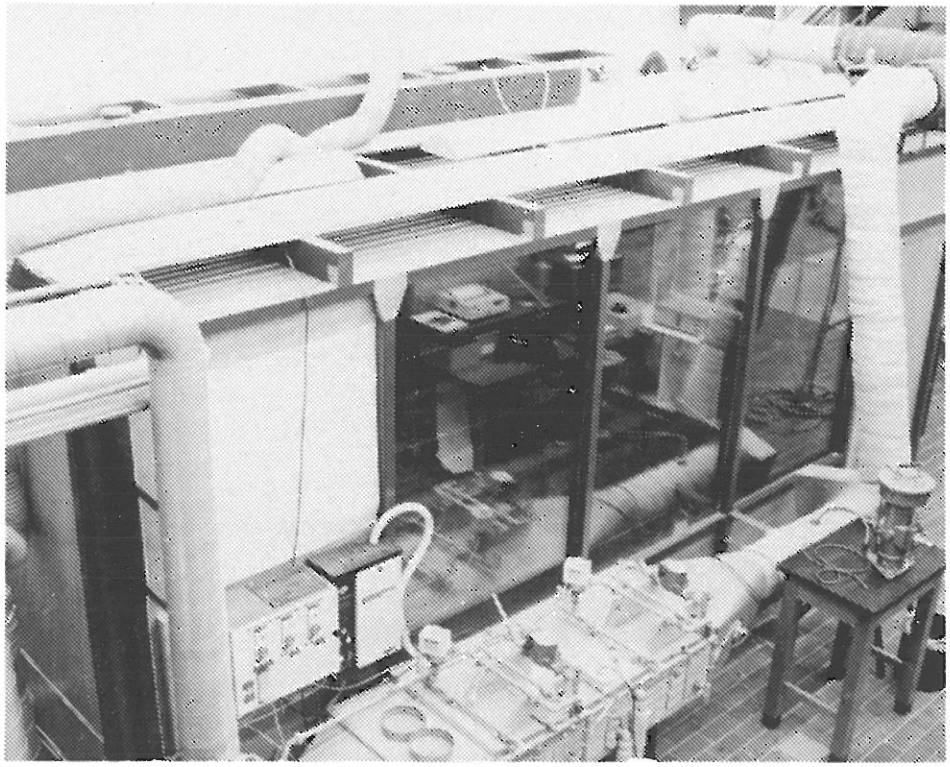

Fig.6.26 Clima chamber L. The ventilaton plant is seen in the front of the picture.

7. EXTRAPOLATION METHOD MEASUREMENTS

7 EXTRAPOLATION METHOD MEASUREMENTS

These investigations concern axisymmetric buoyant plumes arising from steadily maintained round sources of heat. Three different heat sources are used to produce the flow:

Tube, diameter 50 mm

Plate, diameter 356.8 mm

Cylinder, diameter 400 mm

The sources are individually described in /chapter 6.8.1, 6.8.3 & 6.8.4/, respectively. Different amounts of heat are supplied to each of the sources, except for the cylinder - a person dummy - where the heat supplied is 100 W.

Clima chamber F is the place where the measurements have taken place, see /chapter 6.9.1/. Sometimes the room is ventilated and sometimes it is not. Two different flow situations appear:

The room is ventilated by the displacement ventilation principle: The ventilating air is supplied via two wall mounted diffusers and forms a floor jet, that fills up the lower part of the room. Later it is entrained by the thermal flow above the heat source before it leaves the room via two exhaust openings in the ceiling. Since in this way the entrainment is supported with ventilating air a co-flow situation or a compound jet flow is present.

No ventilation of the room takes place: In this cases the plume flow is the only "motor", and a kind of recirculation flow appears. The flow consists of the uprising plume itself, the induced quasi horizontal flow by the entrainment and a recirculation flow mainly near the walls. An argument for the latter one is due to the continuity equation.

The scope of these investigations in general is to improve the understanding of buoyant jet mechanics. Further, it is the objective to create reliable experimental data, that may form a basis for numerical simulation of the flow either through an integral method or a solution of the governing equations of motion.

Since the pure plume (or the plume above a point heat source) makes out a limiting case, this flow is investigated as regards emergence and characteristic parameter values of the flow. A so-called local approximation of the flow is used to find the temperature and velocity distribution factors, and the length of the intermediate region so as the influence by stratification is determined. It is further tested if a simple formula system based on similarity rules expounded in /chapter 4.2.3/ gives a satisfactory description of the flow.

The vertical temperature distribution is varied to create different temperature gradients, and the influence on the buoyant flow is reported in terms of characterizing plume parameters. Here the influence on the vertical volume flux in the plume is interesting because this value is important in the design of displacement ventilation systems. The question is treated, if it is reasonably to use a simple formula based on the rules expounded in the similarity analysis to calculate the vertical volume flux, without taking the vertical temperature gradient into account.

Finally the influence on the plume flow by the ventilation of the room is analyzed. This is done by a comparison of the results when the room is ventilated and when it is not, consequently a comparison of the two flow situations previously described. In this connection it is important to have the same vertical temperature distribution in the two cases.

The measuring in the buoyant flow have taken place by employing the extrapolation method. This approach is described in /chapter 6.2/ as regards set up, placement of probes, data processing and calculation of the various characterizing plume parameters. The related temperature and velocity measuring is discussed in /chapter 6.5 & 6.6/, respectively. The choice of averaging time 180 seconds is chosen so that reasonable constant plume integral properties can be obtained, see /chapter 6.7/. Further the temperature in the surroundings is measured so as the ventilating air flow rate supplied.

7.1 Measurement Series

As a total 24 measurement series are carried out. Their characterizing parameters as regards type of heat source, heat supplied, air change rate (or ventilating air) and intended vertical temperature gradient appear in fig.7.1-3.

In each of the series E1-21 the measuring have taken place in 11 different heights with a mutual distance 0.25 m starting 1.00 m above the floor or 0.75 m above the source since the top of the source is placed 0.25 m above the floor. In the series E22-24 it is 10 different heights with the mutual distance 0.25 m starting 1.25 m above the floor or 0.25 m above the source, since the source is 1.00 m high.

Extrapolation method		Measurement series in clima chamber F			
Heat source	Heat supplied (W)	Air change rate & ventilating air (h^{-1})	(m^3/s)	Vertical tempgrad. (K/m)	Measure-ment se-ria no.
Tube dia. 50 mm	729	0.0	0	≅ 0	E1
		0.7	155	≅ 0	E2
				> 0	E3
	343	0.0	0	≅ 0	E4
		0.7	155	≅ 0	E5
				> 0	E6
	215	0.0	0	≅ 0	E7
		0.7	155	≅ 0	E8
				> 0	E9
	125	0.0	0	≅ 0	E10
		0.7	155	≅ 0	E11
				> 0	E12

Fig.7.1 The 12 extrapolation measurement series involving the tube diameter 50 mm.

Extrapolation method	Measurement series in clima chamber F			
Heat source	Heat supplied (W)	Air change rate & ventilating air (h^{-1}) (m^3/s)	Vertical tempgrad. (K/m)	Measure-ment se-ria no.
Plate dia. 356 mm	400	0.0 0	≅ 0	E13
		0.7 155	≅ 0	E14
			> 0	E15
	200	0.0 0	≅ 0	E16
		0.7 155	≅ 0	E17
			> 0	E18
	100	0.0 0	≅ 0	E19
		0.7 155	≅ 0	E20
			> 0	E21

Fig.7.2 The nine extrapolation measurement series involving the plate diameter 356.8 mm.

Extrapolation method	Measurement series in clima chamber F			
Heat source	Heat supplied (W)	Air change rate & ventilating air (h^{-1}) (m^3/s)	Vertical tempgrad. (K/m)	Measure-ment se-ria no.
Cylinder dia. 400 mm	100	0.0 0	≅ 0	E22
		0.7 155	≅ 0	E23
			> 0	E24

Fig.7.3 The three extrapolation measurement series involving the cylinder diameter 400 mm.

7.2 Measurement Results

The presentation of measurement results does not consist of every single measured temperature and velocity value. Instead the results of the Gaussian fit, calculated plume integral parameters and the local approximation by a plume above a point heat source as described in /chapter 6.2.2-4/ is chosen. In addition the measured vertical temperature distribution in the surroundings is provided. As a total 24 schemes with results are given in /Appendix C/ - one for each measurement series.

7.3 Verification Of The Method

The large scale flow instability in plumes is the reason for the local unsteadiness of the flow. However, it does not exclude the the steadiness of the plume integral properties such as enthalpy flux, volume flux, momentum flux etc. This is the conclusion of /chapter 5.3.1/ and consistent with Popiolek's analysis, ref. /71,74/. The experimental verification of the extrapolation method may be expressed by the lack of measurement results scatter.

One single experiment with the tube diameter 50 mm, heat supplied 215 W and x = 2.25 m above the source is carried out 15 times. The averaging time is 180 seconds. The extrapolation method may be confirmed by the fact that the calculated enthalpy flux in the cross section of the plume does not differ more than ∓ 2 % from the mean value. Further the measurement result scatter is of the order ∓ 4 % as regards the maximum mean temperature excess and ∓ 7 % as regards the maximum mean velocity in the plume. This low measurement result scatter is possible because of two reasons: The data processing, where the true plume axis position is found, followed by a calculation of the true velocity and temperature distributions. The measuring methods, where the temperature difference measuring has a high resolution and the velocity calibration in vertical flow increases the accuracy.

The further verification of the method is split up two parts: An example of the plume axis wandering is given in chapter 7.3.1. Chapter 7.3.2 shows what would happen if the plume axis wandering were left out of account and the measuring were carried out with the probes placed on one single horizontal line through the symmetry axis to the source instead of a placement in a coordinate system.

7.3.1 Plume Axis Wandering

During the same experiment the position of the plume axis is determined 15 times during 45 minutes, and the averaging time still is 180 seconds. The position of the plume axis changes all the time, see the grafical presentation in fig.7.4. This is consistent with the observations by previous authors as described in /chapter 5.3/. The phenomenon is not completely understood yet, it may result from the unsteady flow in the boundary layers, the forming of the plume or from changes in the outer conditions. The phenomenon cannot be said to be stochastic. The plume axis wandering observed is of the order 25 % of r_T, the same value as Popiolek /71p36/ presents. Every attempt are made to produce a stable flow, and from further observations the author has the impression that in occupied rooms the unstability of real plumes is much greater and that extensive sources produce more unstable flows.

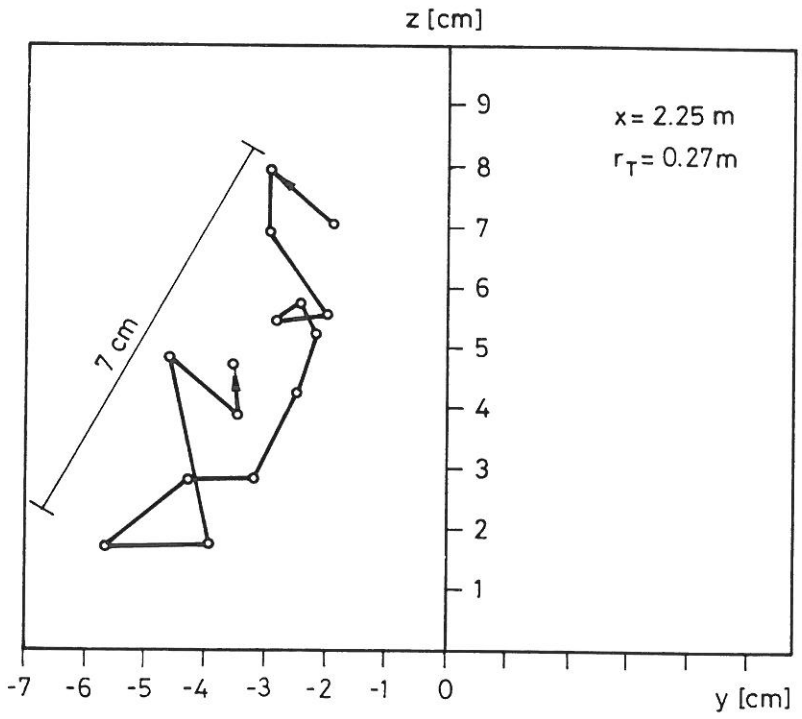

Fig.7.4 Plume axis wandering 2,25 m above the source (*tube diameter 50 mm, Q = 215 W).*

If the plume axis wandering, 25 % of r_T, were not taken into account, e.g. by measuring with the probes placed on just one single line, this would considerable change the measurement results and additional scatter would occur. The measured maximum mean temperature excess ΔT_M would be up to 6 % lower than the real values and the profile width r_T also would be lower. An increase of the averaging time in such a case maybe would increase the width since a kind of averaging out the plume axis wandering would appear. However, the maximum value ΔT_M would remain lower. These arguments also apply for the velocity.

7.3.2 Radial Distributions

One single representative measurement is picked to illustrate: What would happen if the plume axis wandering were left out of account and the measuring were carried out with the probes placed on one single horizontal line through the symmetry axis to the source. The measured mean temperature and mean velocity values are given in fig.7.5 at the given location (x,y,z).

Mesurement results Measurement series E22 Cylinder d=400 mm h=1000 mm Q=100 W									
x (m)	1.50								
y (m)	-0.80	-0.50	-0.30	-0.10	0.00	0.10	0.30	0.50	0.80
u (m/s)	0.01	0.08	0.16	0.20	0.18	0.15	0.08	0.02	0.00
ΔT (K)	0.05	0.13	0.27	0.41	0.39	0.30	0.16	0.07	0.03
z (m)	-0.80	-0.50	-0.30	-0.10	0.00	0.10	0.30	0.50	0.80
u (m/s)	0.00	0.06	0.15	0.20	0.18	0.15	0.04	0.00	0.00
ΔT (K)	0.08	0.12	0.32	0.42	0.39	0.30	0.12	0.03	0.04

Fig.7.5 Measurement results from E22, x = 1.50 m above source.

The measured maximum temperature excess value is ΔT = 0.42 K, while the maximum velocity value is u = 0.20 m/s. It deserves further notice that the maximum values do not appear at the common probe (y,z) = (0,0) in the symmetry axis to the source.

The results by the data processing are given in fig.7.6, they consist of extrapolation method results including the results from two single axis fits. The extrapolation method tells that the true plume axis position is deviated from the origin of the measurement coordinate system (y_0, z_0) = (-0.08,-0.11). In addition the calculated maximum values in the plume axis ΔT_M = 0.43 K and u_M = 0.21 m/s are greater than the maximum values measured.

Plume parameter results after data processing									
Data processing method	Gaussian fit					Integral flux			
	ΔT_M (K)	r_T (m)	y_0 z_0 (m)	u_M (m/s)	r_V (m)	H (W)	$V \cdot 10^3$ $\left(\frac{m^3}{s}\right)$	$M \cdot 10^3$ $\left(\frac{kgm}{s^2}\right)$	$E \cdot 10^3$ (W)
Extrapolation method	.43	.39	-.08 -.11	.21	.38	25.0	95	12	1.7
Single y-axis fit	.39	.40	-.08	.20	.41	24.5	106	10	1.4
Single z-axis fit	.42	.37	-.11	.20	.38	20.5	75	8	1.0

Fig. 7.6 Comparison of plume parameter results when using the extrapolation method and when using a single axis fit. Results from series E22, x = 1.50 m.

The single axis analysis show so as to leave no room for doubt that such an approach results in lower maximum temperature ΔT_M and velocity u_M values than the extrapolation method does. This is caused by the fact that the true plume axis position is deviated from symmetry axis to the source.

In most of the measurement series the plume widths r_T and r_V also have lower values. This is the case in the z-axis fit, and as a result the calculated plume integral fluxes are considerable lower than the values obtained by the extrapolation method.

The attention is drawn to the fact that the plume widths values r_T and r_V on the y-axis fit are slightly greater than the values obtained by the extrapolation method, and lower values were expected. The most simple explanation may be that the plume is not completely axisymmetric. However, the measuring on the y-axis have taken place closer to the border of the plume flow. I.e. lower temperature and velocity values are to be measured. This increases the demands on the measurement equipment.

Finally it must be mentioned once again that the extrapolation method is verified by the low measurement result scatter. This is not the case when measuring with the probes placed on just one single line. In addition measuring by translating one single probe as it is often done by previous authors /26,55,59,82,86/ cannot be considered suitable for plume measurements.

7.4 Pure Plume Flow

The aim of this presentation of measurement results is the experimental verification of the pure plume flow (or the model of a plume above a point heat source). In general the flow in real plumes above pure sources of heat can be divided into 3 zones as shown in fig.7.7, when the plume propagates in environment without stratification. In zone 3 - the zone of complete similarity - the pure plume flow appears. In addition it must be mentioned that fig.2.1 provides a total view over buoyant jets.

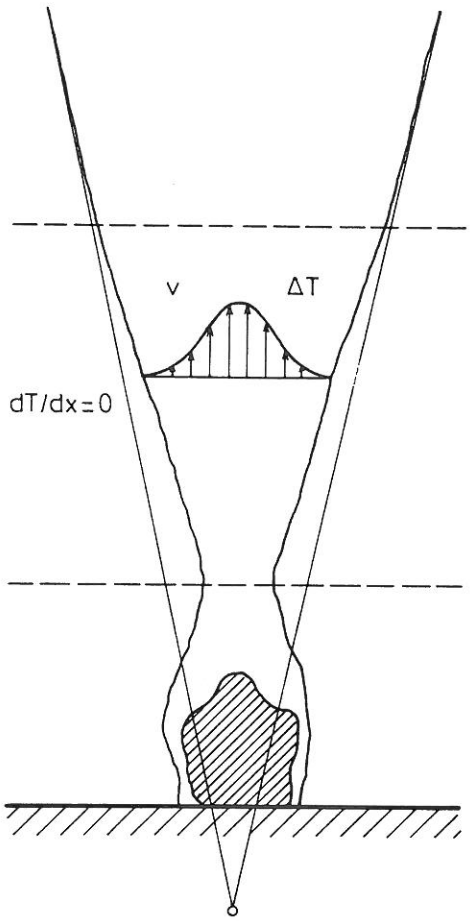

Zone 3, the zone of complete similarity: The flow is fully developed, the plume spreads linearly, the local Archimedes' number Ar and the ratio of temperature and velocity profile widths λ is constant.

$$\lambda = \left(\frac{m}{p} \right)^{1/2} \qquad Ar = \frac{2}{3} \frac{p}{m^{3/2}}$$

Zone 2, the intermediate zone: The plume is turbulent and axisymmetric, the velocity and temperature distribution curves are of Gaussian type, the plume spreads non linearly and the local Archimedes' number Ar and the ratio of temperature and velocity profile widths λ change.

$$\lambda = \frac{r_T}{r_v}$$

Zone 1, the boundary zone: Transition from a boundary layer to a plume form, laminar flow becomes turbulent.

Fig.7.7 Flow regions in a real plume above a pure source of heat when no stratification, S = 0, is presents, ref. /54p4/.

Mierzwinski and Popiolek concludes that one of the necessary conditions of experimental verification of the pure plume flow is to ensure the absolute lack of the environmental stratification /54p13,74/. In rooms where the surface temperatures cannot be controlled environment with zero stratification very seldom occurs. During the measurement series E4 the vertical temperature gradient dT/dx is less than 0.05 K/m in the measuring zone 1.00 to 3.00 m above the floor - the closest to uniform environment that is obtained. Therefore the measurement results from this series is chosen to form the basis for a so-called local approximation of the flow by the model of a plume above a point heat source. The source is concentrated, i.e. the vertical tube diameter 50 mm with heating coils in, and the heat supplied is 343 W.

The pure plume flow is characterized by complete similarity. Measurement series E4 show a tendency, see /Appendix C/: In the area x = 1.75 to 3.25 m above the source a constant ratio between the velocity and temperature excess widths seems to appear, the mean ratio is λ = 0.96. Further the mean enthalpy flux which should equal the convective heat supplied is Q_0 = 221 W. The mean velocity and temperature excess distribution factors in the so-called local approximation are: m = 110 and p = 115.

7.4.1 Axial Distributions

Width

The axial increase of the widths is shown in fig.7.8. The measurements have taken place in two regions: Zone 2, intermediate zone, where the plume spreads non-linearly and the ratio λ of the temperature and velocity profiles changes. Zone 3, the region of complete flow similarity, where the plume spreads linearly and the ratio λ is constant. The experimental temperature width values in zone 3 are reduced to a straight line by means of a least mean square method. Note that the widths do not become zero at the top

of the heat source. In this case the virtual point of plume propagation is situated below the heat source, x_0 = - 0.22 m. The strait line representing the velocity width values is drawn through the virtual point. The excess temperature width spreads with an angle of 7.6 degrees. The spread of the velocity width is greater.

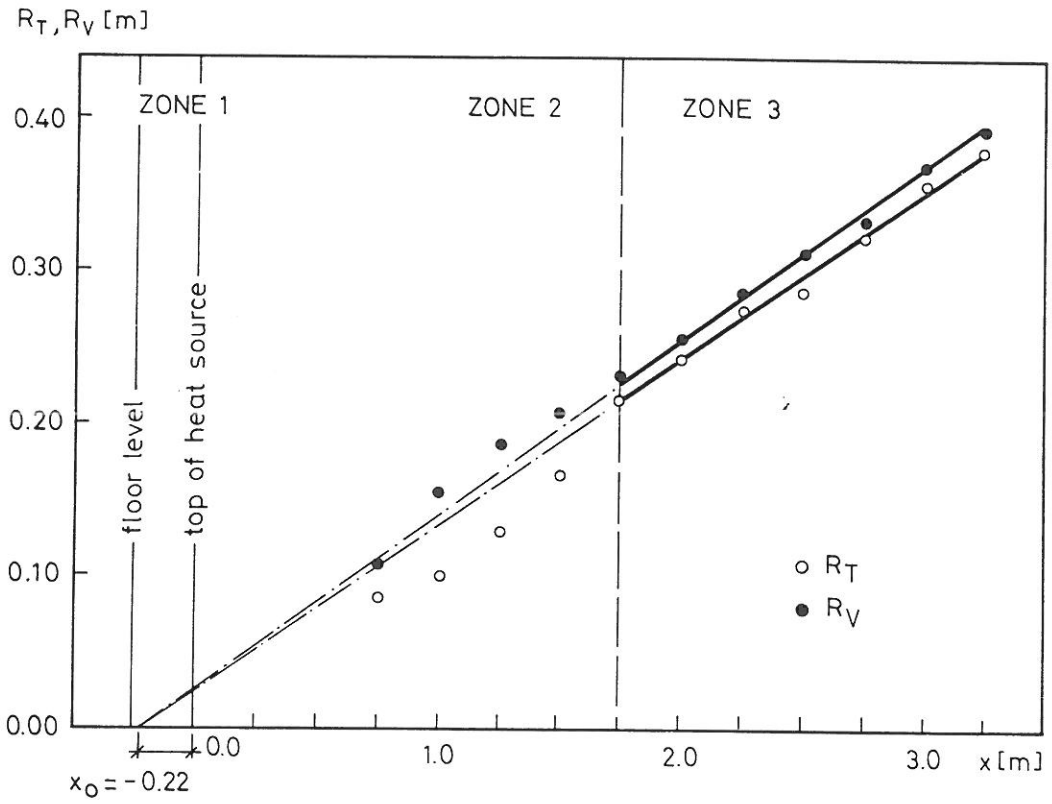

Fig.7.8 Increase of plume widths r_T and r_V.

Velocity

The maximum velocity do also indicate that the flow may be divided in regions as shown in fig.7.9. Zone 2 with acceleration and zone 3 with a velocity decay of the power type:

$$v_M \approx (x-x_0)^k \qquad (7.1)$$

The power k = - 1/3 as indicated in the similarity hypothesis is verified in zone 3. But the velocities are about 7 % lower than the values obtained by equation (4.33). The flow shows no disintegration tendencies. For the practical use it is worth mentioning that the flow up to x = 1.75 m (2.00 m above the floor) still is in the intermediate region, zone 2, where the flow cannot be described by the model of a plume above a point heat source.

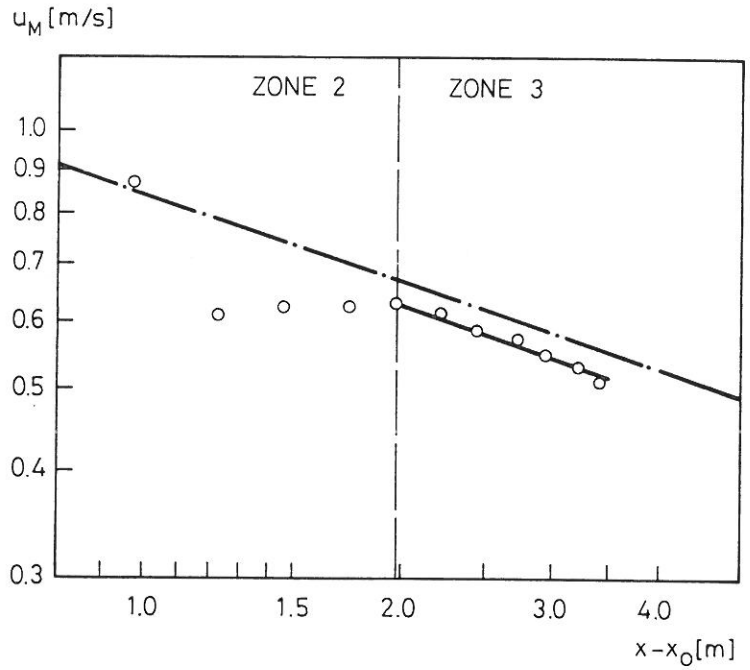

Fig.7.9 Distribution of maximum mean velocity u_M along the axis of the plume. The dash-dotted line represents eq.4.33.

Excess Temperature

The measured mean temperatures are given in fig.7.10. They are below the values given by equation (4.34), and the power is numerically greater than 5/3 as given by the similarity hypothesis. This may indicate the influence by the vertical temperature gradient, though it is very little. This is further indicated by the fall in heat flux H in series 4.

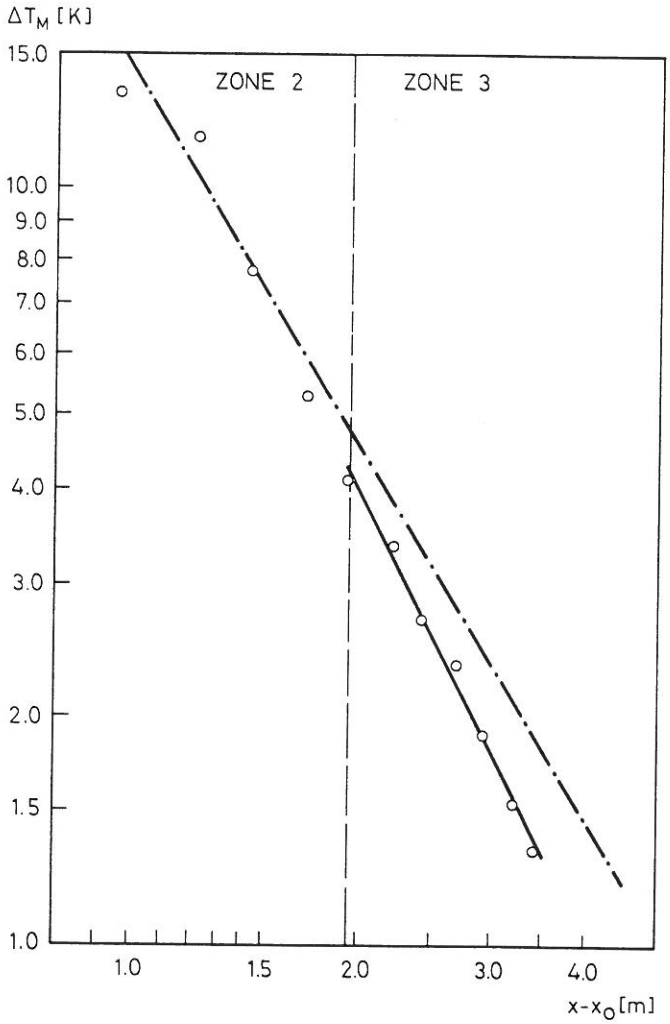

Fig.7.10 Distribution of maximum mean temperature excess ΔT_M along the plume axis. The dash-dotted line represents eq.4.34.

Volume Flux

The vertical volume flux in the plume is found as the volume of the rotation Gaussian distribution function. Substitution of equation (4.33) with the value m = 110 and p = 115 into equation (4.22) followed by integration between the limits give:

$$V = 0.0051\ Q_0^{1/3}\ (x-x_0)^{5/3} \qquad (7.2)$$

Equation (7.2) is similar to the equation (1.3) presented in the /Introduction/.

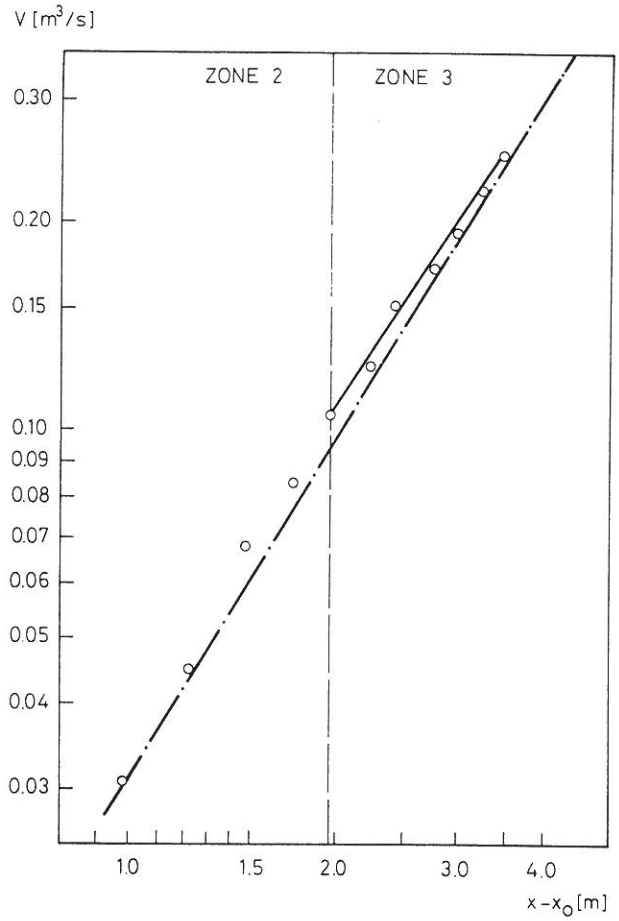

Fig.7.11 Distribution of volume flux $V = \pi\, u_M\, r_V^2$ along the plume axis. The dash-dotted line represents eq.7.2

The measurements show good agreement with equation (7.2). The power 5/3 is observed in both zones, though the flow in zone 2 does not fulfill other elements of the flow in a plume above a point heat source. The explanation is that the width r_V of the velocity profile in zone 2 is greater than indicated by the strait line in fig.7.8, this compensates for the lower velocity u_M in fig.7.9.

Momentum Flux

The equations (4.23, 4.33 & 4.34), m = 110 and p = 115 give the following formula for the momentum flux M

$$M = 0.00043\ Q_0^{2/3}\ (x-x_0)^{4/3} \qquad (7.3)$$

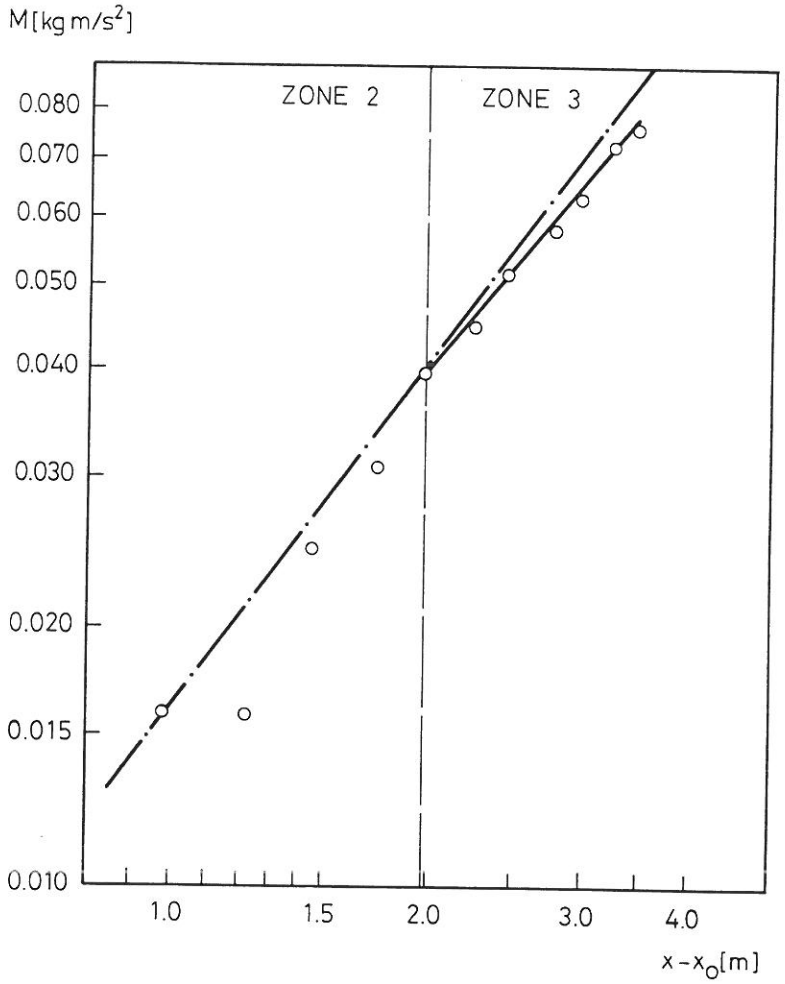

Fig.7.12 Distribution of momentum flux $M = 1/2\ \pi\ \rho\ u_M^2\ r_v^2$ *along the plume axis. The dash-dotted line represents eq.7.3.*

The measurements show good agreement with equation (7.3) in both zones. The explanation is the same as before. The slope in zone 3 is a little smaller than 4/3.

7.4.2 Radial Distributions

Mean velocity and mean temperature excess profiles

The spread of velocity is found greater than that of the temperature $\lambda = r_T/r_v = 0.96 < 1$, and in fig.7.13 the velocity and temperature distribution factors m and p from equation (4.28-29) are compared with the results from previous works.

Velocity and temperature distribution factors and instuments			
m	p	Author	Instrumentation
45?	45	Schmidt 1945 (86)	1 HWA
55	65	George 1977 (26)	1 HWA & 1 RT
65	70	Nakagome 1976 (59)	1 HWA & 1 RT
80		Morton 1956 (55)	1 HWA
96	71	Rouse 1952 (82)	1 VA & 1 TC
110	115	Present work 1990	17 HSA & 17 TC

Abbreviations:
HWA hot wire anemometer
VA vane anemometer
HSA hot sphere anemometer
RT resistance thermometer
TC thermocouple

Fig.7.13 Velocity and temperature distribution factors and instrumentation.

Rouse et al. (82) indicate as the only author that the spread of buoyancy is greater than that of momentum, $p = 71 < m = 96$ and $\lambda = 1.16$. This result may be influenced by the fact that Rouse et al. uses a wane anemometer (3 cm dia.) with a lower limit of 6 cm/s. The accuracy of such an instrument is less than those reported here. In contrast the results of other authors are coincident with the present results. This means that it is more likely that the spread of momentum is at least equal or wider than that of thermal energy, $p > m$ and $\lambda < 1$. The profiles are compared in fig.7.14.

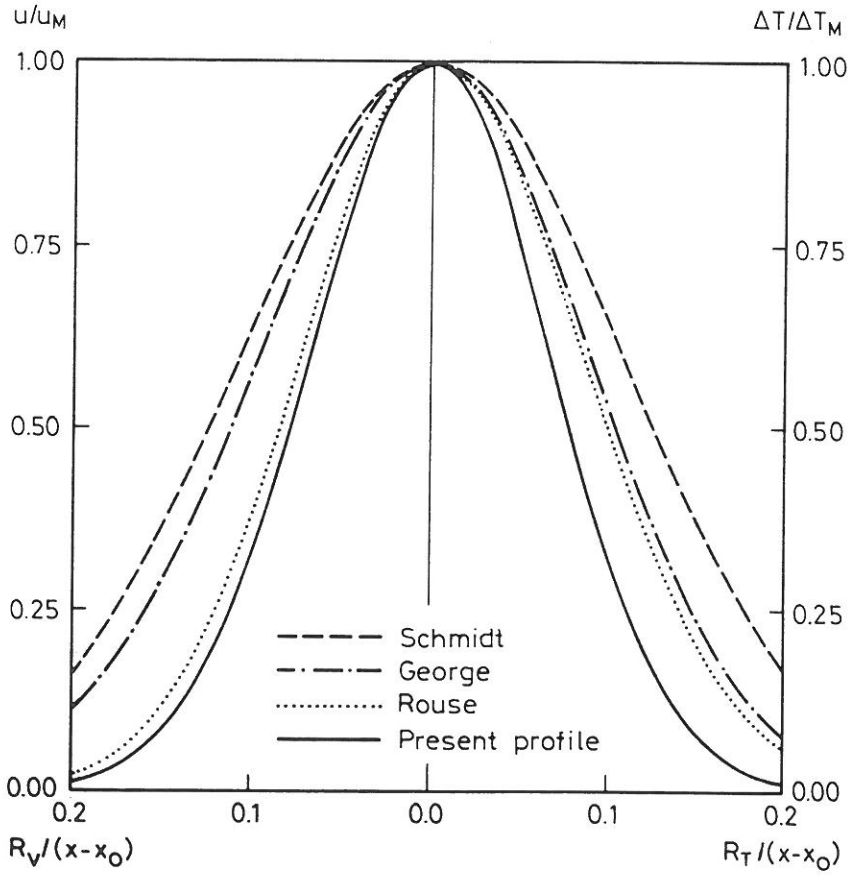

Fig.7.14 Comparison of dimensionless mean velocity u/u_M and mean temperature excess $\Delta T/\Delta T_M$ profiles in a pure plume.

The present work results in more narrow profiles. The explanation may be the following: George et al. (26) mention that their plume maybe has not reached a fully developed state resulting in a larger angle of spread. The same thing could be present in the results of Rouse et al. (82) because they use a gas burner as a source giving a long intermediate region.

7.4.3 Entrainment

In the region of complete similarity the entrainment factor α is constant. Popiolek in his analysis of the flow above a point heat source /71/ presents the following formula:

$$\alpha = \frac{5}{6} m^{-1/2} \qquad (7.4)$$

The entrainment factor α calculated by Morton (55) using data of several authors are consistent with the data shown in fig.7.15. The results are calculated using equation (7.4). The results of the present work shows that the entrainment is smaller than previous assumptions. This is interesting, because the correct formulation of the entrainment is the closure of the integral method of plume calculation. More work has to be carried out in this field.

Entrainment factor $\alpha = \frac{5}{6} m^{-1/2}$						
Author	Schmidt	George	Nakag.	Morton	Rouse	Pr.work
α	0.124	0.112	0.103	0.093	0.085	0.080

Fig.7.15 The entrainment factor α in the model of a plume above a point heat source calculated on the base of results from several authors.

7.4.4 Discussion Of Pure Plume Flow

The pure plume flow or the model of a plume above a point heat source has been verified in terms of showing the power rules expounded in the dimensional analysis. The width of the velocity and temperature excess profiles are found to be more narrowly than that observed by previous authors and therefore the entrainment factor is smaller.

Further the analyses and tests have proved that the pure plume represents a borderline case which only takes place when the flow

rises in surroundings without a vertical temperature gradient, since even very small stratifications influence the flow significantly. This is consistent with the observations by Mierzwinski and Popiolek /54/.

The pure plume modeling may be applied in only three of the 24 measurement series: I.e. in series 1,4 and 7, where the flow is produced by the tube diameter 50 mm and no ventilation of the room have taken place. Even here the complete similarity in terms of constant velocity and temperature distributions factors cannot be said to occur. So the conclusion is that the pure plume or the model of a plume above a point heat source has not been precisely verified in any experimental way yet. However, some information has been given.

The zone of complete similarity may be found above an intermediate region. The length of the intermediate is dependent on the heat source geometry. For the tube diameter 50 mm it is observed longer than the height of a normal office room. For the rest of the sources, i.e. plate diameter 356.8 mm and cylinder dia. 400 mm, the pure plume flow is not observed. In these cases the length of the intermediate region is longer than the region observed or the flow may be extremely sensitive to outside disturbances such as stratifications and room drafts.

7.5 Influence By Stratification

The influence by stratification on the plume flow has already been described as regards the pure plume modeling in /chapter 7.4/, and the measurement results show so as to leave no room for doubt that a vertical temperature gradient strongly influences the flow and this makes the pure plume modeling impossible. The further conclusion is that the exact knowledge of the stratification also is essential for a numerical simulation of the flow, e.g. by means of integral or differential methods such as described in /chapter 4.1 & 4.3.1/, respectively.

In general the flow in a plume above a heat source propagating in stratified surroundings is different from the one without stratification. Fig.7.16 gives a description of the flow.

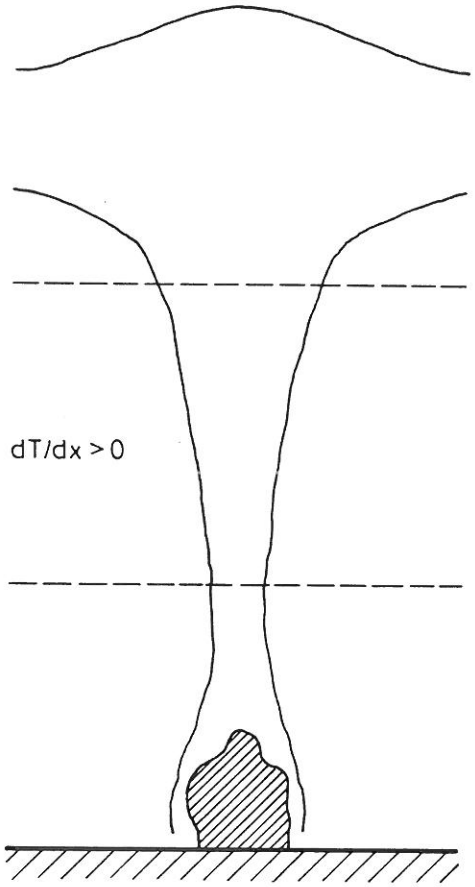

Zone 3, zone of maximum plume rise: The maximum elevation is reached and the air flows out horizontally as a stratified layer

Zone 2, intermediate region: As zone 2 in the case without stratification, but the effect of stratification is significant.

Zone 1, the boundary layer zone: As zone 1 in the case without stratification, however the stratification affects the flow.

Fig.7.16 Flow regions in a real plume above a pure source of heat when stratification, S > 0, is present, ref. /54,p4/. Please compare with fig.7.7 for the case without stratification.

The aim of this presentation of measurement results is to shown some effects on the plume parameters. Again the analysis is carried out by adopting the so-called local approximation of the plume above a point heat source, and the influence by stratification on the plume parameters is determined. For every amount of heat supplied to the source the plume flow has been investigated under the influence of two different temperature gradients, when ventilation of the room takes place. But the vertical temperature distribution is complex, and this makes an exact description of the influence on the plume parameters difficult. However, some general tendencies are provided.

Stratification influences the characterizing parameters in plumes. The measurement results show that the zone of complete similarity does not occur in any of the measurements independent of height. This is caused either by the way of generating the plume or by the environmental conditions. Stratification affects all the plume parameters.

When a vertical temperature gradient is present the velocity and temperature distribution factors m and p are below the values indicated in the model of a plume above a point heat source. An increase of the stratification factor is related with a decrease of the velocity and temperature distribution factor values. This means that the plume has lower velocity and temperature excess values and the entrainment factor is larger. The influence on the maximum temperature excess in the plume is evaluated as the strongest. It follows that the effect on the enthalpy flux also is strong.

It is observed that the plume does not spread linearly and as regards the relation between the temperature and velocity profile widths the ratio λ increases with the height. Sometimes the widths values are smaller sometimes they are greater as a result of increasing stratification, and it cannot be said that they are greater flow downward and smaller in the beginning or vice versa. However, Jaluria and Gebhart's /37/ investigations on stability

and transition of buoyancy induced flows may be to some help: The first effect by stratification on stability is initially to stabilize the flow. However, amplification rates becomes greater than for unstratified media further downstream. Their measurements on transition indicate that stable ambient stratification delays the onset of transition. The description of the present flow and the processes taking place in the measurements is complex, but it could be expected that unstable flow would produce greater width values. Unfortunately it is difficult to evaluate which of the three previously mentioned effects that dominates.

7.5.1 Effect On The Volume Flux

The results from measurement series E22, E23 and E24, see /Appendix C/ form the basis for this presentation. The source is extensive, i.e. the 1 m high black painted cylinder diameter 400 mm and the heat supplied is 100 W. In the two series the room is supplied with the same ventilating air flow rate.

In the case with the vertical temperature gradient dT/dx = 0.30 K/m the effect by stratification is clear, since disintegration tendencies slightly are shown, see series E24: The vertical heat flux H and the temperature excess ΔT_M decrease fast, the velocity and temperature distributions factors m and p approach values below 10 and the entrainment factor α is often more than 2 times greater than the value 0.08. The results from series E23 with the lower gradient dT/dx = 0.09 K/m show the same characteristics. But it is not so clear because the vertical gradient is lower.

Fig.7.17 shows the flow rate in the thermal plume as a function of the distance to the source. The results reported are observed in the rest of the experiments with other heat source geometries. i.e. plate and tube.

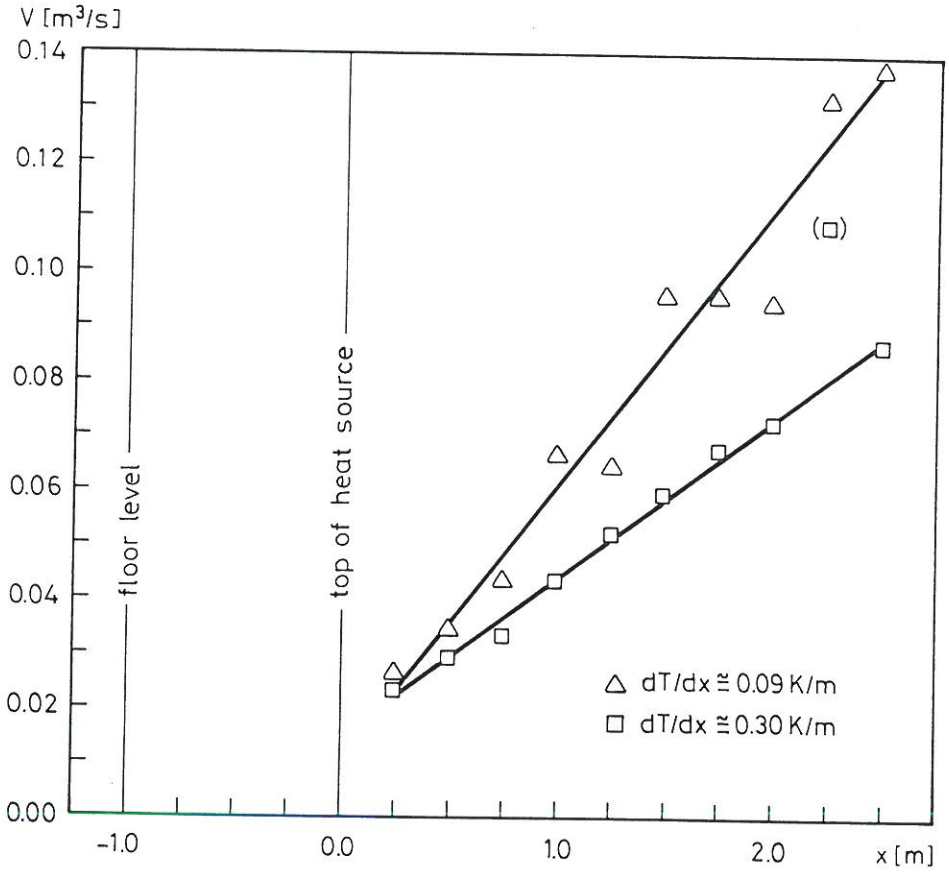

Fig.7.17 Distribution of volume flux $V = \pi\, u_M\, r_V^2$ along the plume axis. The effect of stratification is shown as a reduction of the vertical volume flux.

The vertical volume flux in the thermal plume decreases when the vertical gradient increases.

Finally it must be emphasized that it is important to relate the vertical gradient to the zone where the flow actually takes place, and for the purpose of buoyant plume calculation by means of an integral or differential method the exact knowledge of the vertical temperature distribution is essential.

7.6 Influence By Ventilating The Room

It is pointed out in the beginning of /chapter 7/ that two different flow situations appear when then room is ventilated by the displacement ventilation principle and when it is not ventilated: In the first case a kind of co-flow or compound jet situation is present and in the latter case a kind recirculation appears in the room, since the plume flow is the only "motor".

The aim of this presentation of results is to show the effect on the vertical volume flux by ventilating the room. Again the measurement results from the investigations of the flow above the cylinder dia 400 mm form the basis: i.e. series E22 and E23. Fig.7.18 show the vertical volume flux in the thermal plume as a function of distance to the source.

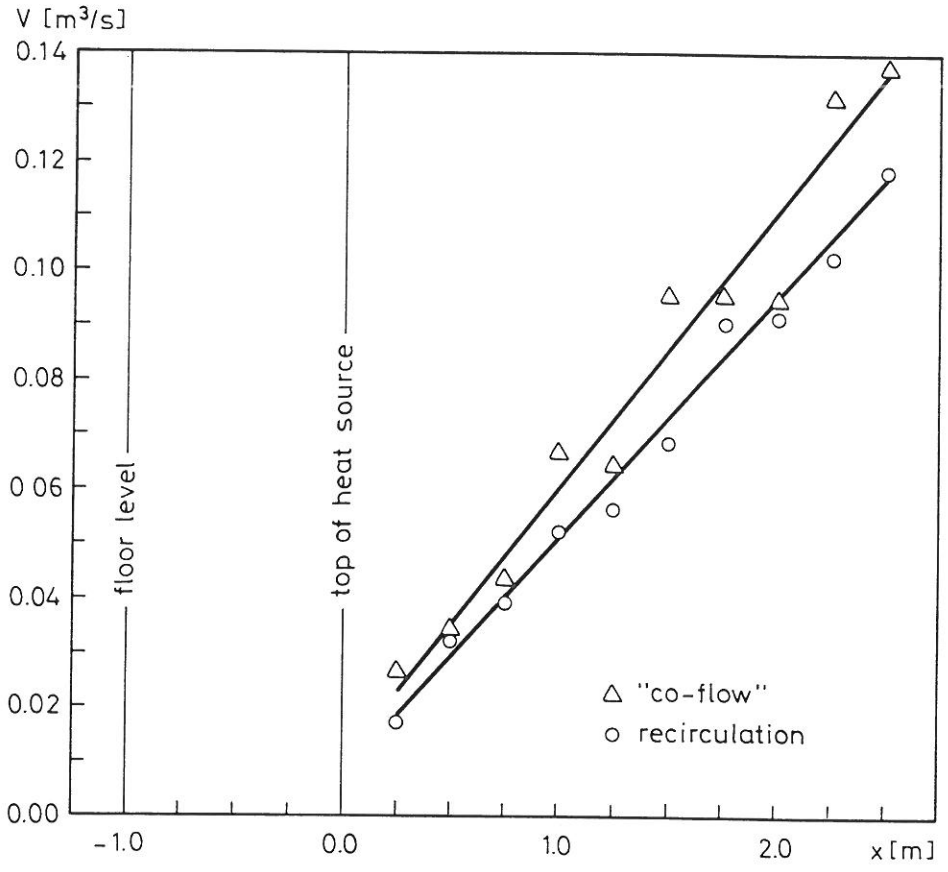

Fig.7.18 Distribution of vertical volume flux $V = \pi\, u_M\, r_V^2$ *along the plume axis. Recirculation flow and co-flow are compared.*

Since the vertical temperature gradient are quite equal in the two cases compared, this factor is left out of further account. In the case with recirculation flow and no ventilation the buoyancy in the flume is the main driving force of the total flow in the room. This is not the case when the entrainment is supported with the ventilating air from the diffusers. As a result the vertical volume flux will increase in co-flow situations.

7.7 Concluding Remarks

The extrapolation method may be regarded as an exemplary one for the investigation of axisymmetrical buoyant jets. The large scale unstability of the flow is treated as a separate phenomenon, which is regarded as a plume axis wandering. This large scale unstability causes measurement result scatter. However, the extrapolation method makes a determination of the plume axis wandering possible. When after each measurement run the real plume axis position is found, the real temperature and velocity distribution can be calculated. This improvement decreases the measurement result scatter significantly, and it is at the same time a verification of the method. The plume axis wandering amounts about 25 % of r_T, and is it evaluated that extensive heat sources produce more unstable flows than intensive heat sources does. Further the measurement result scatter is of the order ∓ 4 % as regards the maximum mean temperature excess and ∓ 7 % as regard the maximum mean velocity in the plume. The enthalpy flux varies ∓ 2 % about the mean value.

According to the analyses carried out the pure plume flow or the model of a plume above a point heat source has been verified in terms of showing the power rules expounded in the similarity analysis. The velocity and temperature excess profiles are found to be more narrowly than that observed by previous authors and therefore the entrainment factor is smaller. However, the complete similarity in terms of constant velocity and temperature distributions factors cannot be said to occur. So the conclusion

is that the pure plume or the model of a plume above a point heat source has not been precisely verified in any experimental way yet.

Consequently the analyses and tests have proved that the pure plume represents a borderline case which only takes place when the flow rises in surroundings without a vertical temperature gradient, since even very small stratifications influence the flow significantly. Stratification leads to smaller maximum mean velocity and maximum mean temperature excess of the flow, and later flow downwards it leads to disintegration or horizontal spread out. It is not possible to give a simple answer to the question, what about the width? but the ratio λ between the temperature and velocity profile widths increased with the height.

Further when investigating buoyant jets from pure sources of heat the length of the intermediate region is fairly long. This together with influence of stratification make the observation of pure plumes rather difficult or impossible. It is the authors impression that the problem of making the plume region fall within the region observed could be overcome by constructing a special plume generator where the ration between buoyancy and momentum can be controlled. Eventually by leading compressed air through a nozzle with heating coils.

When the flow does not spread out horizontally the analyses show a self similarity in terms of Gaussian shaped temperature and velocity distributions in the entire region investigated. This observation is important, since it makes plume calculations by means of an integral method possible. In connection with this it must be emphasized that neither the entrainment factor α nor the ration between the temperature excess and velocity profile λ ought to be assumed constant. This is consistent with Popiolek's observations, ref. /71-74/.

It is important to keep in mind that the measuring have taken place at fairly small vertical temperature gradients and the flow therefore reaches the ceiling. However, there is no reason to believe that this always will be the case. Smoke observations at larger but normal happen temperature gradients confirm this, see the pictures in /Appendix A/.

According to the tests the flow from extensive heat sources of the size of human beings cannot be described by the model of a pure plume in the region observed. This is caused by the generation of the plume. However, when no stratification is present the flow approaches such a model. A simple formula such as equation 1.3 will give some idea about the vertical volume flux in a limited region of the flow. But the stipulation is uncertain since the flow is influence by many factor, where stratification, drafts and co-flow phenomena are some of them.

8. ZERO METHOD MEASUREMENTS

8 ZERO METHOD MEASUREMENTS

These investigations are carried out by placing different heat sources free or near to a single wall, since it is the objective:

> to compare the vertical volume flux in wall jets with that in free jets produced by the same heat source and thereby to determine if symmetry arguments giving a 63 % rule can be verified.
>
> to determine the influence by an increase of the vertical temperature gradient on the entrainment in plumes when it is a wall jet or a free jet

Two different heat sources are employed to create the buoyant flow: i.e. tube diameter 50 mm and cylinder diameter 400 m. Their description is given in /chapter 6.8.1 & 6.8.4/, respectively.

The investigations are carried out in clima chamber F, which is stated in /chapter 6.9.1/. The room is ventilated by the displacement ventilation principle, and the supplied ventilating air creates a floor jet and fills up the lower part of the room. Later the supplied air supports the entrainment by the plume, which rises and is exhausted through an exhaust hood. In this way the flow rate is measured in one single height 2 m above the floor by the use of the zero method, see /chapter 6.3/. Further the vertical temperature gradient out side the flow is measured.

The various measurement series are described in /chapter 8.1/. The results are given in /chapter 8.2/ as volume flux and temperature distribution in the surroundings. Further the zero method measurement results are compared with that from the extrapolation method in /chapter 8.3/ as a kind of verification of the zero method. /Chapter 8.4 and 8.5/ takes up the influence by placement and stratification, respectively.

8.1 Measurement series

As a total nine measurement series are carried out, and their characterizing parameters as regard type of heat source, heat supplied, placement of the source, intended vertical temperature gradient in the room and various volume flow rates exhausted through the hood appear in fig.8.1.

Zero method		Measurement series in clima chamber F Height above floor 2.00 m (x=1.00 m)			
Heat source	Heat supplied (W)	Placement	Vertical tempgrad (K/m)	Air flow exhausted (m^3/h)	Measurement seria no.
Tube dia. 50 mm	343	Free	> 0	200 - 400	Z1
	125	Free plume	≅ 0	200 - 275	Z2
			> 0	175 - 250	Z3
		Wall plume	≅ 0	125 - 200	Z4
			> 0	100 - 225	Z5
Cylinder dia. 400 mm	100	Free plume	≅ 0	175 - 225	Z6
			> 0	125 - 225	Z7
		Wall plume	≅ 0	88 - 175	Z8
			> 0	100 - 175	Z9

Fig.8.1 The nine zero method measurements series and their characterizing parameters.

It is attempted to operate with only two different temperature gradients in the room. In fig.8.1 it is described by a near to zero, $\cong 0$, or a greater than zero, > 0. In this way the influence by one of the two parameters, i.e. placement or vertical temperature gradient, may be determined.

The flow rate exhausted is varied in steps of 25 m^3/h. However, in one single case when the exhausted air flow rate is under 100 m^3/h the size of the step is 12.5 m^3/h. In each measurement series up to eight different exhausted volume flows have been evaluated as regards the estimation of the vertical volume flux in the plume.

8.2 Measurement results

The presentation of the measurement results is divided in the vertical volume fluxes exhausted that estimates the vertical volume flux in the plumes and in the matching vertical temperature distributions in the surroundings.

8.2.1 Vertical Volume Flux

The results, i.e the various air flow rates exhausted that are evaluated to estimate the vertical volume flux in the plumes appear in fig.8.2. If in one measurement series two successive exhausted air flow rates is evaluated too big or too little, respectively, to estimate the volume flux, then the average of the two values is taken as an approximation.

Zero method			Vertical volume flux results Height above floor 2.00 m (x=1.00 m)		
Heat source	Heat supplied (W)	Place-ment	Vertical tempgrad (K/m)	Volume flux (m /h)	Measure-ment se-ria no.
Tube dia. 50 mm	343	Free	1.1	300	Z1
	125	Free plume	0.3	238 >225 <250	Z2
			0.6	200	Z3
		Wall plume	0.3	150	Z4
			0.6	125	Z5
Cylind-er dia. 400 mm	100	Free plume	0.3	200	Z6
			0.5	175	Z7
		Wall plume	0.3	125	Z8
			0.6	112 >100 <125	Z9

Fig.8.2 Flow rates that estimate the vertical volume flux in the investigated vertical buoyant jets.

8.2.2 Vertical Temperature Distribution

The vertical temperature distributions that match the flow rate measurements are given in fig.8.3.

Zero method	Vertical temperature distribution results								
Measure-ment se-ria no.	Height above floor (m) & Temperature (C)								
	0.0	0.1	0.5	1.0	1.5	2.0	2.5	3.0	3.5
Z1	19.6	18.2	18.5	19.3	19.7	20.3	20.6	20.8	20.8
Z2	20.9	20.5	20.7	21.0	21.0	21.1	21.1	21.1	21.1
Z3	21.0	20.3	21.0	21.3	21.4	21.4	21.5	21.6	21.6
Z4	21.6	21.4	21.7	21.8	21.8	21.8	21.8	21.9	21.9
Z5	21.1	20.4	21.0	21.3	21.4	21.5	21.5	21.7	21.7
Z6	21.2	20.9	21.2	21.3	21.4	21.4	21.4	21.5	21.5
Z7	20.9	20.4	20.8	21.1	21.2	21.3	21.3	21.3	21.3
Z8	22.3	22.0	22.4	22.6	22.7	22.6	22.6	22.7	22.7
Z9	20.8	20.1	20.5	20.8	21.0	21.1	21.2	21.3	21.3

Fig.8.3. Vertical temperature distribution measurement results.

Further, for the measurement series Z2 to Z9 fig.8.4-5 provide grafical representations.

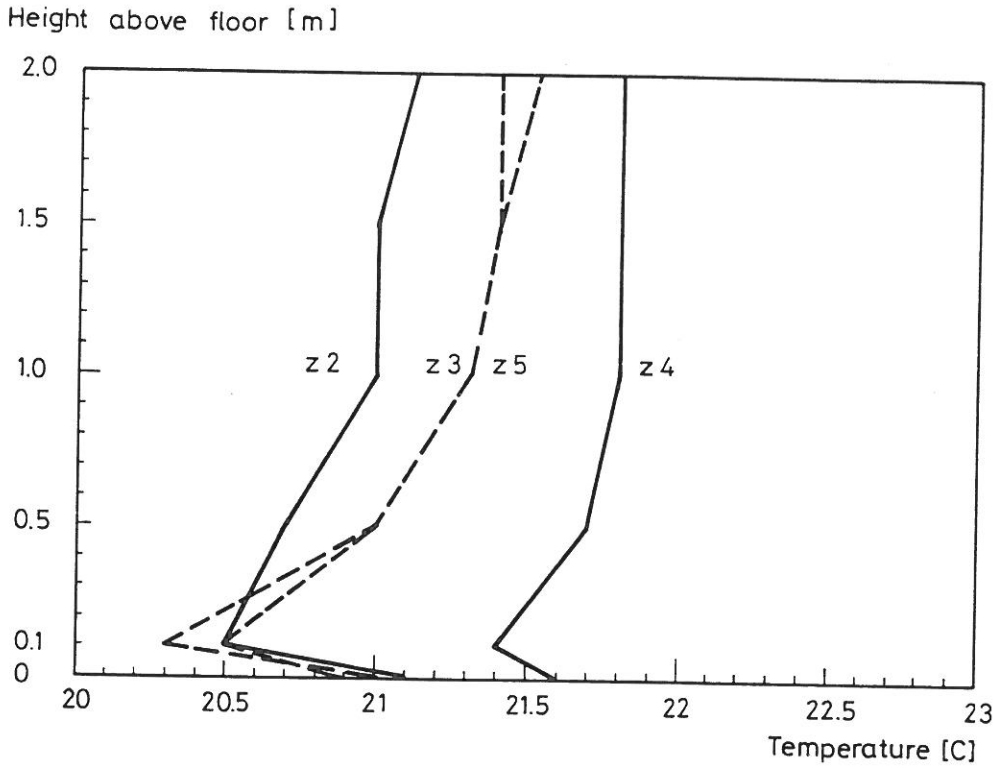

Fig.8.4 Temperature distribution in measurement series Z2-Z5.

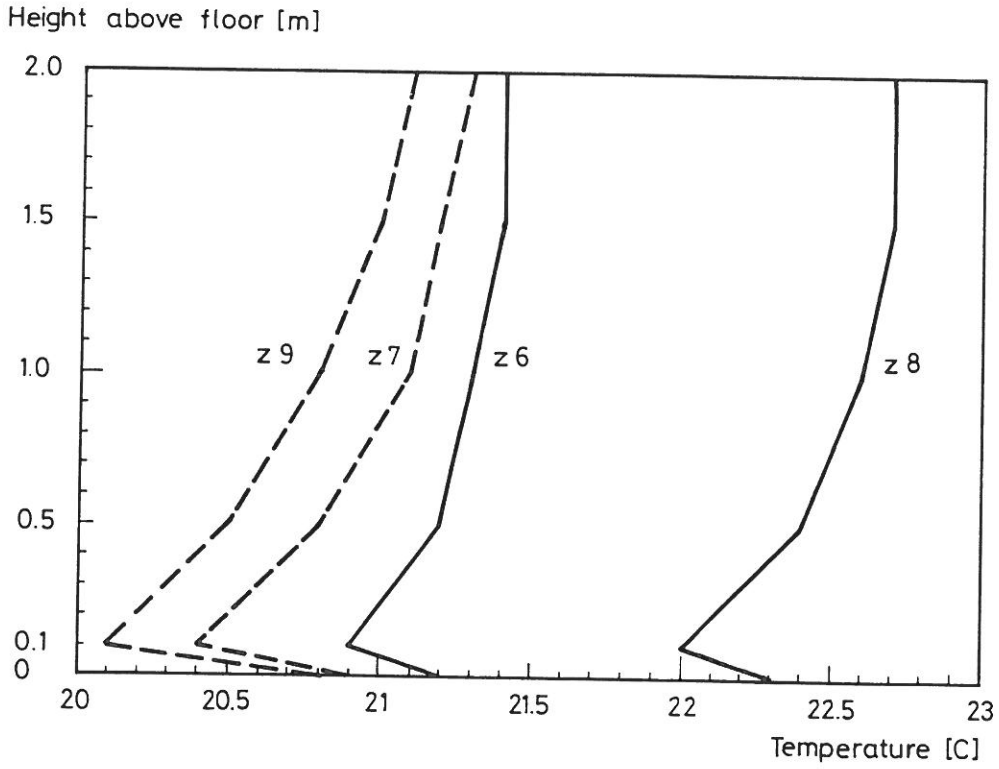

Fig.8.5 Temperature distribution in measurement series Z6-Z9.

8.3 Verification Of The Method

A comparison of measurement results from the extrapolation method forms the verification of the zero method. However, some problems arise since it is not always possible to find corresponding vertical temperature gradients. The comparison is given in fig.8.6 where the vertical temperature gradients from both measurement series are calculated as a value between 0.10 m and 2.00 m above the floor.

Comparison of zero method and extrapolation method measurement results			Fixed height above floor 2.00 m		
Heat source & heat supplied	Zero method		Extrapolat. method		Measurement seies no.
	Vertical tempgrad (K/m)	Volume flux (m^3/h)	Vertical tempgrad (K/m)	Volume flux (m^3/h)	
Tube dia. 50 mm 343 W	1.11	300	0.59 0.89	323 316	-- E6 Z1
Tube dia. 50 mm 125 W	0.32	238	0.25 0.73	240 241	-- Z2 E12
Cylinder dia. 400 mm 100 W	0.26 0.47	200 175	0.14 0.67	237 156	E23 Z6 Z7 E24

Fig.8.6 Comparison of measurement results from the zero method and the extrapolation method.

If the extrapolation method measurement results are regarded as a reference the zero method measurement results seems plausible, since: in measurement series Z1 where the stratification 1.11 K/m is greater the than the values from the extrapolation method 0.59 and 0.89 K/m the estimated volume flux is lower 300 < 316 < 323 m^3/h. This seems likely since the effect of increasing stratification is a reduction of the flow rate. The value of the vertical temperature gradient 0.32 K/m in series Z2 lies between the values 0.25 and 0.73 K/m. In this case the estimated volume flux 238 m^3/h is very near to the 240 and 241 m^3/h of the extrapolation method. The results from measurement series Z6 and Z7 with the vertical cylinder diameter 400 mm provide perhaps the best verification of the method: Here the values 200 and 175 m^3/h lie between the values 237 and 156 m^3/h from the extrapolation method so do the corresponding vertical temperature gradients 0.14 < 0.26 < 0.47 < 0.67 K/m.

The accuracy of the method is difficult to evaluate, but it evaluated that the measured air flow rate estimates the vertical volume flux with an error less than 10 %.

8.4 Influence By Placement

/Chapter 4.4 & 4.4.1/ reflect on flow influenced by enclosing walls, and symmetry considerations lead to the 63 % rule: That the volume flux in a wall plume is 63 % of the volume flux in the corresponding free plume. The necessary calculations are the following, see also /chapter 4.4/:

Free plume:

$$V \approx Q_0^{1/3} \qquad (8.1)$$

Wall plume:

$$V \approx \frac{1}{2} \left(2Q_0 \right)^{1/3} \approx 0.63\ Q_0^{1/3} \qquad (8.2)$$

The measured volume fluxes in the free plumes and the wall plumes have already been presented. In addition fig.8.7 provides a comparison of these two flows.

Zero method		Influence by placement		
Heat source & heat supplied	Vertical tempgrad (K/m)	Vertical volume flux		Measurement seria no. compared
		Free plume (m^3/h)	Wall plume (m^3/h) (% of f.pl)	
Tube dia. 50 mm 125 W	≅ 0.3	238	150 (63 %)	Z2 & Z4
	≅ 0.6	200	125 (63 %)	Z3 & Z5
Cylinder dia. 400 mm 100 W	≅ 0.3	200	125 (63 %)	Z6 & Z8
	≅ 0.6	175	112 (64 %)	Z7 & Z9

Fig.8.7 Comparison of the vertical volume flux in free plumes and wall plumes.

The single wall influences the entrainment in the plume. It looks like, that the volume flux in a wall jet amounts around 63 % of the volume flux in the corresponding free jet. However, for each single wall plume & free plume comparison it is important: That the two vertical temperature distributions are similar, that the two vertical temperature gradients have the same value and

thirdly, that the temperature levels in the room are the same in the two cases. Fig.8.4-5 show the various temperature distributions, which belong together for the comparison.

According to fig.8.4-5 it is evaluated, that the two by two corresponding temperature distributions have the same form. Further the calculation of the vertical temperature gradient is based on the temperature values in 0.10 m and 2.0 m height above the floor. The mutual temperature level in the measurement series Z3 & Z5 and Z7 & Z9 varies less than 0.2 K and therefore are of little influence. However, the mutual temperature differences in the measurement series Z2 & Z4 and Z6 & Z8 are as high as 1.0 K and 1.2 K, respectively. This may cause a change in the source conditions, since a higher temperature level in the room may increase the surface temperature of the source and therefore may change the relation between radiant heat exchange and convection. For the vertical cylinder the change in temperature may have some influence on the flow, since the temperature excess is small and the temperature of the source is around only 35 C.

The set up implies, that the ventilating air flow rate has the same value as the one exhausted, see /chapter 6.3.1/. The ventilating air is entrained in the buoyant jet, thus a compound jet or a co-flow situation is present. When changing the exhausted air flow rate the ventilating air flow rate is also changed. This fact may influence the results, because a new co-flow situation is created. Perhaps it would have been better to keep the same air change rate in the room all the time to eliminate the compound jet problem and just to change the volume flow exhausted to estimate the vertical volume flux in the plume.

The design of a displacement ventilation system involves the choice of a suitable ventilating air volume supplied, since this value determines the height of the occupied zone according to the two zone model. If the wall plume effect is taken into account, this allows lower air change rates: Leaving further discussion out of account it may be concluded that:

The zero method measurement results verify the 63 % rule. I.e. the vertical volume flux in a wall jet amounts around 63 % of the volume flux in the corresponding free jet at the same vertical temperature gradient.

8.5 Influence By Stratification

The influence by a vertical temperature gradient on the flow is discussed in /chapter 5.2.1/ as regards flow rates from extensive sources of heat. The volume flux in a buoyant jet becomes smaller when the vertical temperature gradient increases.

Zero method		Influence by vertical temperature gradient		
Heat source & heat supplied	Plume type	Vertical vol. flux (m^3/h)		Measurement seria no. compared
		Ver.tempgr. ≅ 0.3 (K/m)	Ver.tempgr. ≅ 0.6 (K/m)	
Tube dia. 50 mm 125 W	Free	238	200 (84 %)	Z2 & Z3
	Wall	150	125 (83 %)	Z4 & Z5
Cylinder dia. 400 mm 100 W	Free	200	175 (88 %)	Z6 & Z7
	Wall	125	112 (90 %)	Z8 & Z9

Fig.8.8 Influence by the vertical temperature gradient on the vertical volume flux in free jets and wall jets.

Two different vertical temperature gradients have been present during the investigations, i.e. approximately 0.3 and 0.6 K/m. According to fig.8.8 an increase of the gradient involves a decrease of the volume flux as expected. Immediately it looks like

the influence by the vertical temperature gradient depends on the type of heat source. Immediately it may be concluded that the relative reduction of the flow rate in a free jet and the corresponding wall jet has the same value: For the tube and cylinder a 17 and 11 % reduction, respectively, when the gradient increases from 0.3 to 0.6 K/m.

When making such conclusions it is important to take the mutual vertical temperature gradients into account, they are grafically represented in fig.8.4-5. If the temperature gradient is big the temperature 0.10 m above the floor in the jet flow from the diffusers has a great under temperature. This may cause a greater local cooling of the heat source by forced convection and secondly the radiant heat exchange from the source to the floor may increase due to the lower temperature of the floor. As a result maybe the vertical temperature gradient is not the only factor influencing the plume flow.

8.6 Concluding Remarks

A verification of the zero method is given in terms of measurement results that agree with results from the extrapolation method as regards the vertical volume flux in round plumes.

Several advantages of the method is reported: The method is very easy to use and the results are quickly produced. There is no claim on the velocity distributions, e.g. such as axisymmetrical Gaussian shaped profiles. As a results unstable flows from extensive heat sources and flows influenced by enclosing walls may be investigated, i.e. the buoyant flows that actually takes place in ventilated rooms.

The method has some disadvantages too: It only gives information about the vertical volume flux in the plume and therefore it is not suitable for fluid dynamic investigations. Further the measurement results depend on the operating person who

individually determines the exhausted air flow rate that estimates the vertical volume flux in the plume. However, with some experience reliable results may be produced, and the resolution is evaluated better than ∓ 10 %.

The experiments on wall plumes and corresponding free plumes verify the 63 % rule. I.e. the vertical volume flux in a wall plume amounts around 63 % of the volume flux in the corresponding free plume at the same vertical temperature gradient.

The investigations further implies the statement, that increasing stratification reduces the vertical volume flux in plumes. This observation is consistent with that from the extrapolation method.

The following work is suggested in order to improve the method: A change of the set up can be made by introducing tracer gas into the source zone and by measuring the amount of gas exhausted through the hood. When the air flow rate exhausted estimates the vertical volume flux in the plume a certain percentage of the gas may be found in the exhausted air, one may assume. With this tracer gas measuring a more unequivocal way of measuring than the individual smoke observations is developed.

Further an investigation of buoyant jets in a corner and of the flow when two equal sources are placed close to another are suggested, and if possible to verify the symmetry considerations of /chapter 4.4.1/.

9. STRATIFICATION METHOD MEASUREMENTS

9 STRATIFICATION METHOD MEASUREMENTS

In these investigations the tube diameter 100 mm with a power of 500 W supplied is the only source used to create the buoyant flow, a further description of the source is given in /chapter 6.8.2/. It has been placed in three different positions: free, near to a single wall or in a corner between two walls. Further, the vertical temperature gradient is changed. The scope likely to the one in chapter 8 with the zero method is:

> to compare the vertical volume flux a free plume with that in the corresponding wall plume and plume in a corner between two walls and thereby to determine if a 67 % and a 40 % rule, respectively, can be verified.
>
> to determine the influence by an increase of the vertical temperature gradient on the entrainment in such plumes.

The measurements have taken place in clima chamber F /chapter 6.9.2/. The room is ventilated by the displacement ventilation principle creating two zones: A lower clean zone where supplied ventilating air fills up and is entrained by the buoyant flow. Above this zone a recirculation flow appears. The vertical volume flux is measured by the stratification method which is based on the two zone model: Smoke is induced into the source zone, follows the plume and later it is found in a recirculation zone above the clean zone. In this way the height of stratification is visualized. If no vertical air movement takes place near the walls one may assume that the ventilating air volume flow estimates the vertical volume flux in the buoyant jet in the level of stratification. A further description of the stratification method is given in /chapter 6.4/.

The measurement series are described in /chapter 9.1/ as regards placement of the heat source, vertical temperature gradient in the

room and ventilating air flow rate. The results is reported in /chapter 9.2/ as an observed stratification height. If no down flow were present near the walls the flow in this height would equal the ventilating air flow rate. In /chapter 9.3/ the influence by placement and stratification is taken up.

9.1 Measurement Series

Stratification method		Measurement series in clima chamber L		
Heat source & supply	Placement	Ventilating air (m^3/h)	Vertical temperature gradient (K/m)	Measurement seria no.
Tube dia. 100 mm power 500 W	Free plume	107	- - 2.9 4.1	S1
		215	0.7 3.1 3.6 4.5	S2
		300	0.8 2.2 2.3 3.5	S3
		430	0.5 1.6 2.9 3.0	S4
	Wall plume	107	- - - 3.8	S5
		300	0.5 - 2.2 -	S6
		430	0.4 - 2.4 -	S7
	Plume in a corner	107	- - 3.7 4.1	S8
		215	- - 3.6 -	S9
		430	0.4 - 2.3 -	S10

Fig.9.1 The ten stratification method measurement series.

The vertical temperature gradient is measured, it is determined from temperature values in the lower clean zone from the height 0.10 m above the floor and up to the height x above the heat source. In this way the vertical temperature gradient is only related to the lower area in the room without recirculating flow.

9.2 Measurement Results & Discussion

The height x from the top of the heat source up to the zone with recirculating flow is measured as $x_{ST} = x_{FLOOR} - 0.25$, because the heat source is placed 0.25 m above the floor. The observed stratification heights appear in fig.9.2.

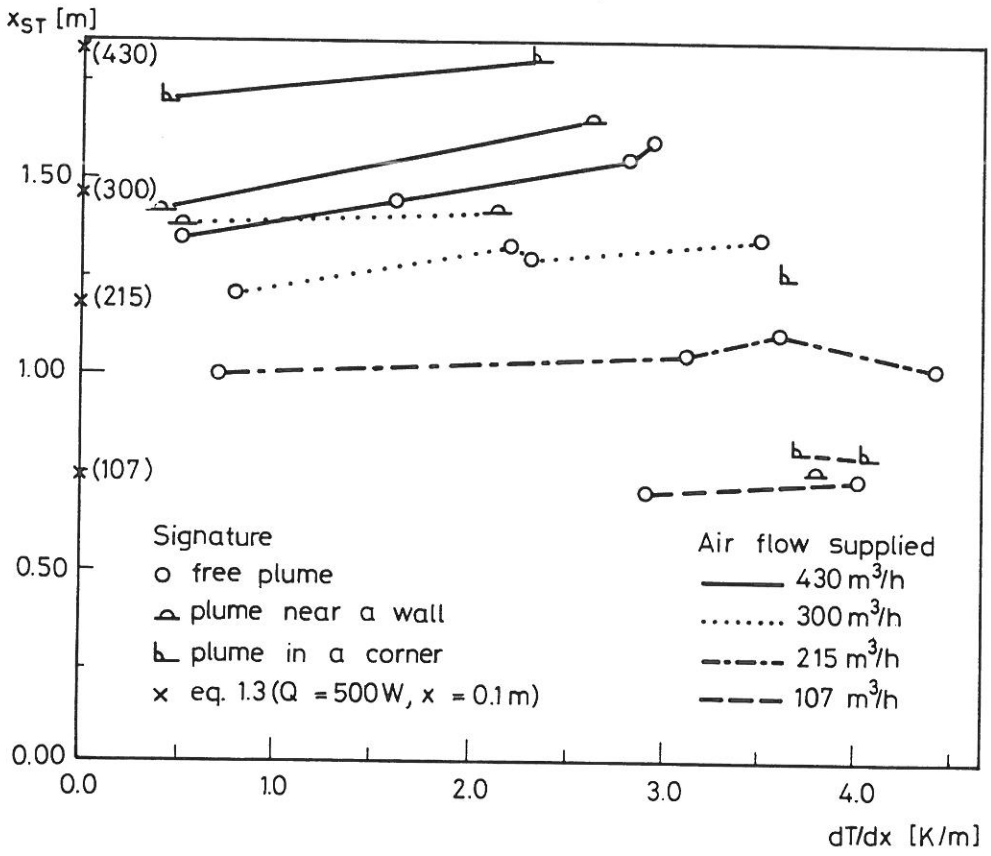

Fig.9.2 The stratification height x_{ST} versus the vertical temperature gradient dT/dx for different heat source locations and ventilating air volume flow supplies.

The height x cannot be regarded as a precise measure of the vertical volume flux in the thermal plume, because there may be cold down draughts near the walls as a result of the higher temperature in the recirculation zone. The cold down draught implies that smoke from the recirculation zone moves along the walls and later on moves horizontally into the lower zone. This makes the measuring difficult and may cause errors. However, the following observations leave no room for doubt:

Fig.9.2 shows that the location of the heat source in relation to surrounding walls has a significant influence on the stratification height. When the plume is in a corner, the height x is at a maximum and the entrainment at a minimum followed by the wall plume and the free plume.

The ventilating air volume flow supplied determines the stratification height x which increases when the air flow supply is increased. This is consistent with principle of the two zone model.

The vertical temperature gradient influence the stratification height x, but not very much. The height of stratification rises with the increase of the vertical temperature gradient.

9.3 Concluding Remarks

A verification of the stratification method in terms of comparing with results from other methods is not possible, since the heat source tube diameter 100 mm is only employed in these experiments.

The method is not so easy to use for vertical volume flux measurements because an exact determination of the stratification height is not possible due to the cold down draughts near the walls. Therefore it is concluded that individual heating and cooling of the walls is necessary to eliminate the disturbing vertical flows and to achieve better accuracy. Further the

ventilating air itself creates a co-flow which supports the entrainment and thereby has an influence. Otherwise the method has the advantage that there is no claims on the velocity distributions. This allows investigations of non symmetrical flows.

The experiments show that the vertical volume flux in the plume is influenced by the location of the source. When the plume rises in a corner between two walls the entrainment is at a minimum followed by the wall plume and the free plume. This is indicated by the growth in stratification height. However, the 40 % and the 63 % rules are not exactly confirmed yet.

The measurement results further imply, that increasing vertical temperature gradients reduce the vertical volume flux, since the stratification height increases.

CONCLUSION

CONCLUSION

Axisymmetric circular buoyant jets are treated both theoretically and experimentally.

From a literature study the author concludes that the state of experimental knowledge is less satisfactory. The source conditions are seldom reported or measured and the influence of these on the establishment of self similarity is unknown. The flow in the intermediate region is characterized be the absolute lack of reported measurements. Further the given mean value data for the plume region are conflicting and of not so good quality, in addition the turbulence data are very limited.

Three different measuring methods, here called the extrapolation method, the zero method and the stratification method, have been established to investigate the thermal plumes from pure sources of heat in ventilated rooms. These methods eliminate the problem of plume axis wandering, a problem which cannot be treated as a normal turbulence phenomena.

The extrapolation method, where velocity and temperature measurements take place in the buoyant flow, may be regarded as an exemplary one for the investigation of axisymmetric circular buoyant jets since it makes the determination of the plume axis wandering possible. This improvement reduces the measurement result scatter. Further the method gives basic knowledge about the mean temperature excess and the mean velocity of the flow. The data processing consists of Gaussian fits and a local approximation of a pure plume model.

The zero method, where the buoyant jet is exhausted through a hood, gives only information about the vertical volume flux in the flow. However, this method is very easy to use and it is possible to investigate non symmetric flows and flows influenced by enclosing walls.

The stratification method implies an observation of the stratification height in a displacement ventilated room and this height is regarded as a measure of the vertical volume flux according to the two-zone model. Some problems of use are reported, but the method gives an idea of what the total flow picture looks like. The method also may be applied for the investigation of buoyant wall jets and buoyant jets in a corner.

According to the analyses carried out the pure plume flow or the model of a plume above a point heat source has been verified in terms of showing the power rules expounded in the similarity analysis. The velocity and temperature excess profiles are found to be more narrowly than the one observed by previous authors and therefore the entrainment factor is smaller. However, the complete similarity in terms of constant velocity and temperature distribution factors cannot be said to occur.

The influence of even very small vertical temperature gradients is reported to be significant. This makes the pure plume modeling impossible and it leads to disintegration tendencies or horizontal spread out of the buoyant flow, larger gradients accelerating the process.

The flows have a fairly long intermediate region and often it exceeds the height of a normal office room. In connection with this extensive heat sources produce long intermediate regions and their flows are more sensible to outside disturbances. Further the ventilating of the room itself is seen to have a significant influence on the flow.

The tests carried out show a significant reduction of the vertical volume flux when the buoyant flow takes place near to enclosing walls - as a wall jet or a jet in a corner. The symmetry considerations are verified as regards the wall jet, i.e. the volume flow rate makes out 63 % of the one in the corresponding free buoyant jet. When the flow takes place in a corner between two walls the percentage is even less.

It is the author's hope that the presented experimental mean data from the extrapolation method may form a basis for some future numerical work.

In this report the problem of calculating the vertical volume flux in buoyant flows is closely related to the design of displacement ventilation. Therefore, it is the author's wish to discuss and to present an input for the design of displacement ventilation systems, especially the stipulation of necessary ventilating air flow rate:

Displacement ventilation has two major advantages compared with traditional mixing systems: - An efficient use of energy because it is possible to remove exhaust air from the room where the temperature is several degrees higher than the one in the occupied zone. - A better air quality for the same air flow rate due to the vertical contaminant distribution which implies that fresh air and polluted air are separated.

The author has the impression that the displacement ventilation principle successfully may be applied in large tall rooms such as public halls and in industrial ventilation since only the occupied zone will be ventilated, giving a higher efficiency. Also in normal office rooms the principle has a meaning. However one should seriously consider the alternative mixing ventilation. The problem with displacement ventilation is the often high air change rates connected with draught risks. Higher heat loads and consequently higher volume flow rates are increasing the draught risk (sometimes 40 W/m^2 is spoken of as an upper limit for displacement ventilation when using wall mounted diffusers). However, it is worth mentioning that solutions with a perforated floor open the possibility of removing large heat loads (greater than 200 W/m^2) and still having a comfortable indoor climate.

The question about the necessary ventilating air remains. There is no reason to believe that the air change rate compared with the one from mixing ventilation may be reduced, on the contrary. E.g.

a chosen stratification height of two meters will in many cases lead to very high and too high ventilating air flow rates. 1 - 1.20 meter seems to be a reasonable choice. The argumentation for the displacement ventilation is still the two previously mentioned reasons but also that the boundary layer around the human body will transport fresh air from below up to the breathing zone, even above the level of stratification.

The vertical volume flux from extensive sources of heat such as human beings, turned on computers, copy machines etc. cannot be described by a simple pure plume model. However, it may give some idea about the size of the volume flow. The flow will most frequently be in an intermediate state or even in the source region, where the knowledge is very limited. Therefore, at the present moment the author draws the conclusion that cataloguing of typical buoyant flows will be a good idea. Further, it seems reasonably to use simple symmetry argumentation to describe the flow near to enclosing walls and when sources are placed close to another, forming only one flow. This will reduce the stipulated necessary ventilating air flow rate. Finally it is worth mentioning, that placing the heat sources as high as possible will raise the stratification height and consequently increase the quality of the air in the occupied zone.

APPENDIXES

APPENDIX A SMOKE PICTURES OF THERMAL FLOWS IN VENTILATED ROOMS

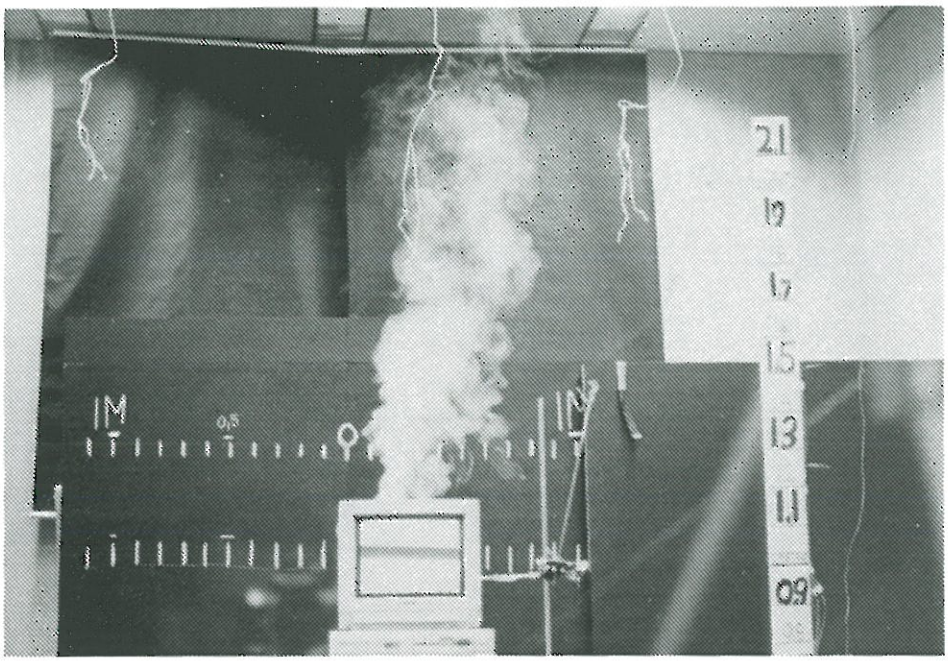

The plume from a turned on computer, with a little vertical gradient in the room, ref. /12/.

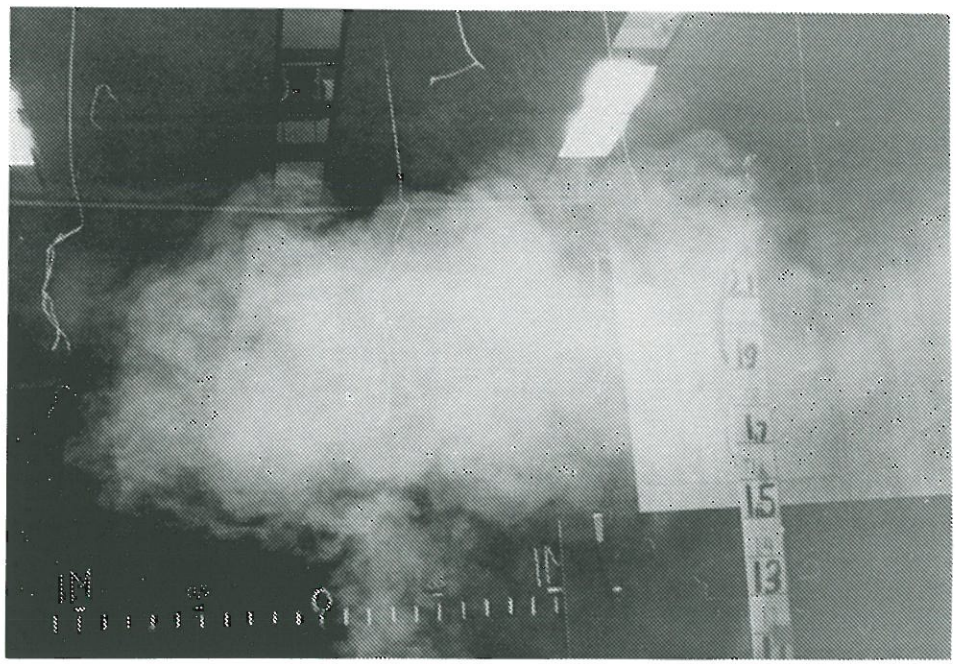

The plume from a turned on computer, with a large vertical gradient in the room, ref. /12/.

APPENDIX B

GOVERNING EQUATIONS OF MOTION FOR VERTICAL ROUND BUOYANT JETS

When the so-called "boundary layer approximations" are used, the governing time averaged equations of motion are:

Conservation of mass, continuity:

$$\frac{\partial(rv)}{\partial r} + \frac{\partial(ru)}{\partial x} = 0$$

Conservation of vertical momentum:

$$\frac{\partial(rvu)}{\partial r} + \frac{\partial(ru^2)}{\partial x} + \frac{\partial}{\partial r}(r\ \mathrm{Cov}\{v'u'\}) - \beta g r \Delta T = 0$$

Conservation of heat:

$$\frac{\partial(rv\Delta T)}{\partial r} + \frac{\partial(ru\Delta T)}{\partial x} + \frac{\partial}{\partial r}(r\ \mathrm{Cov}\{v'\Delta T'\}) = 0$$

APPENDIX C EXTRAPOLATION METHOD MEASUREMENT RESULTS

Measurement series E1	Heat source: Tube d=50 mm h=150 mm Q=729 W Supply air: n=0 h^{-1} G=0 m^3/s											
Plume parameters	Height above source x (m)											
	0.75	1.00	1.25	1.50	1.75	2.00	2.25	2.50	2.75	3.00	3.25	
u_H (m/s)	.781	.612	.674	.700	.701	.692	.688	.649	.616	.597	.571	Gaussian fit by minimizing a sum of squares
r_V (m)	.132	.230	.233	.242	.260	.285	.296	.395	.365	.386	.416	
ΔT (C)	15.1	12.4	8.7	6.3	4.8	3.9	3.4	2.7	2.2	1.9	1.6	
r_T (m)	.104	.120	.150	.190	.221	.251	.264	.304	.336	.380	.427	
H (W)	299	324	352	374	359	367	345	340	317	313	304	Integral plume parameter values
V (m^3/s)	.043	.101	.114	.129	.148	.177	.189	.229	.258	.280	.311	
M (kgm/s^2)	.020	.037	.046	.053	.062	.073	.078	.089	.095	.100	.107	
Ar	.110	.254	.149	.104	.085	.079	.072	.073	.072	.069	.068	
λ	.79	.52	.65	.79	.85	.88	.89	.91	.92	.98	1.03	
m	97	92	116	107	119	120	137	124	121	101	88	Local approximation by a model of a plume above a point source
p	157	338	278	173	164	154	173	151	143	105	84	
α	.085	.087	.077	.081	.077	.076	.071	.075	.076	.083	.089	

Vertical temperature distribution														
x+0.25 (m)	0.00	0.05	0.10	0.50	1.00	1.20	1.50	2.00	2.50	3.00	3.50	4.00	4.62	
Temp. (C)	20.8	20.8	20.8	21.1	21.2	21.3	21.4	21.5	21.6	21.8	21.9	22.0	21.5	

Measurement series E2	Heat source: Tube d=50 mm h=150 mm Q=729 W Supply air: n=0.7 h^{-1} G=0.0042 m^3/s										
Plume parameters	Height above source x (m)										
	0.75	1.00	1.25	1.50	1.75	2.00	2.25	2.50	2.75	3.00	3.25	
u_M (m/s)	.907	.568	.617	.642	.632	.615	.606	.592	.567	.558	.536	Gaussian fit by minimizing a sum of squares
r_V (m)	.114	.223	.237	.256	.287	.314	.337	.374	.393	.422	.452	
ΔT (C)	12.7	10.9	7.5	5.5	4.0	3.3	2.6	2.2	1.8	1.5	1.3	
r_T (m)	.116	.139	.169	.194	.235	.262	.286	.322	.342	.389	.452	
H (W)	288	325	333	319	317	308	289	291	264	262	275	Integral plume parameter values
V (m^3/s)	.037	.088	.109	.132	.163	.191	.216	.260	.275	.312	.344	
M (kgm/s^2)	.020	.030	.040	.051	.062	.070	.078	.092	.094	.105	.111	
Ar	.059	.252	.157	.114	.096	.091	.081	.078	.076	.069	.070	
λ	1.02	.62	.71	.76	.82	.83	.85	.86	.87	.92	1.00	
m	120	46	70	103	106	111	129	133	135	130	91	Local approximation by a model of a plume above a point source
p	117	118	138	180	157	160	179	179	178	153	92	
α	.076	.252	.100	.082	.081	.079	.073	.072	.072	.073	.087	

Vertical temperature distribution													
x+0.25 (m)	0.00	0.05	0.10	0.50	1.00	1.20	1.50	2.00	2.50	3.00	3.50	4.00	4.62
Temp. (C)	20.7	20.6	20.6	20.9	21.3	21.3	21.5	21.6	21.6	21.8	21.9	22.0	21.5

Measurement series E3	Heat source: Tube d=50 mm h=150 mm Q=729 W Supply air: n=0.7 h^{-1} G=0.0042 m^3/s										
Plume parameters	Height above source x (m)										
	0.75	1.00	1.25	1.50	1.75	2.00	2.25	2.50	2.75	3.00	3.25
u_M (m/s)	.947	.590		.618	.618	.614	.591	.557	.539	.507	.524
r_V (m)	.113	.209		.241	.262	.289	.325	.359	.388	.433	.426
ΔT (C)	12.0	10.7		5.1	4.0	3.3	2.5	2.1	1.7	1.4	1.3
r_T (m)	.124	.139		.206	.227	.259	.299	.326	.369	.425	.442
H (W)	301	319		295	277	283	276	258	244	247	243
V (m^3/s)	.038	.081		.113	.133	.161	.195	.226	.255	.298	.298
M (kgm/s^2)	.022	.029		.042	.049	.059	.069	.075	.082	.090	.094
Ar	.051	.214		.109	.092	.084	.079	.081	.075	.079	.068
λ	1.10	.67		.85	.87	.90	.92	.91	.95	.98	1.04
m	120	49		71	92	97	98	99	97	76	83
p	100	111		97	123	121	116	120	108	79	77
α	.076	.119		.099	.087	.084	.086	.084	.084	.095	.091

Gaussian fit by minimizing a sum of squares

Integral plume parameter values

Local approximation by a model of a plume above a point source

Vertical temperature distribution													
x+0.25 (m)	0.00	0.05	0.10	0.50	1.00	1.20	1.50	2.00	2.50	3.00	3.50	4.00	4.62
Temp. (C)	19.7	18.8	18.8	19.8	20.3	20.3	20.5	20.6	20.7	20.9	20.9	21.1	20.6

Measurement series E4	Heat source: Tube d=50 mm h=150 mm Q=343 W Supply air: n=0 h^{-1} G=0 m^3/s											
Plume parameters	Height above source x (m)											
	0.75	1.00	1.25	1.50	1.75	2.00	2.25	2.50	2.75	3.00	3.25	
u_M (m/s)	.874	.607	.625	.624	.631	.615	.587	.572	.557	.535	.517	Gaussian fit by minimizing a sum of squares
r_V (m)	.106	.154	.186	.207	.231	.254	.284	.309	.331	.367	.391	
ΔT (C)	13.3	11.7	7.6	5.3	4.1	3.4	3.0	2.4	1.9	1.5	1.3	
r_T (m)	.085	.099	.129	.164	.214	.241	.273	.284	.319	.354	.376	
H (W)	195	187	206	208	241	240	232	223	210	202	191	Integral plume parameter values
V (m^3/s)	.031	.045	.068	.084	.106	.125	.149	.172	.192	.226	.249	
M (kgm/s^2)	16	16	25	31	40	46	52	59	64	73	77	
Ar	.062	.162	.124	.095	.080	.076	.075	.075	.068	.066	.065	
λ	.80	.64	.69	.79	.93	.95	.96	.92	.96	.96	.96	
n	281	96	125	125	94	95	94	112	112	117	124	Local approximation by a model of a plume above a point source
p	440	223	261	200	110	105	102	134	121	126	134	
α	.050	.085	.074	.075	.086	.086	.086	.078	.078	.077	.075	

Vertical temperature distribution														
x+0.25 (m)	0.00	0.05	0.10	0.50	1.00	1.20	1.50	2.00	2.50	3.00	3.50	4.00	4.62	
Temp. (C)	20.6	20.7	20.7	20.9	21.0	21.0	21.0	21.1	21.0	21.1	21.3	21.4	21.0	

Measurement series E5	Heat source: Tube d=50 mm h=150 mm Q=343 W Supply air: n=0.7 h^{-1} G=0.0042 m^3/h										
Plume parameters	Height above source x (m)										
	0.75	1.00	1.25	1.50	1.75	2.00	2.25	2.50	2.75	3.00	3.25
u_M (m/s)	.	.	.	.	.	.	.	.	.	.	.
r_V (m)	.	.	.	.	.	.	.	.	.	.	.
ΔT (C)											
r_T (m)	.	.	.	.	.	.	.	.	.	.	.
H (W)	187	178	183	181	180	187	180	170	150	140	143
V (m^3/s)	.029	.048	.063	.073	.090	.116	.146	.173	.201	.241	.253
M (kgm/s^2)	.015	.015	.021	.025	.030	.038	.045	.053	.060	.067	.068
Ar	.045	.178	.127	.092	.083	.082	.083	.075	.068	.066	.066
λ	1.06	.72	.79	.89	.97	.93	.93	.91	.90	.92	1.02
n	170	51	71	85	72	87	89	114	145	143	95
p	152	98	114	107	77	101	104	137	177	169	91
α	.064	.116	.099	.090	.098	.089	.088	.078	.069	.070	.086

Gaussian fit by minimizing a sum of squares
Integral plume parameter values
Local approximation by a model of a plume above a point source

Vertical temperature distribution													
x+0.25 (m)	0.00	0.05	0.10	0.50	1.00	1.20	1.50	2.00	2.50	3.00	3.50	4.00	4.62
Temp. (C)	20.0	19.5	19.5	20.0	20.3	20.4	20.5	20.6	20.7	20.9	20.9	21.0	20.7

Measurement series B6	Heat source: Tube d=50 mm h=150 mm Q=343 W Supply air: n=0.7 h^{-1} G=0.0042 m^3/s											
Plume parameters	Height above source x (m)											
	0.75	1.00	1.25	1.50	1.75	2.00	2.25	2.50	2.75	3.00	3.25	
u_M (m/s)		.595	.605	.596			.507	.498	.481	.466	.452	Gaussian fit by minimizing a sum of squares
r_V (m)		.139	.161	.187			.290	.317	.335	.365	.391	
ΔT (C)		10.8	7.3	4.7			2.1	1.8	1.5	1.2	1.1	
r_T (m)		.106	.130	.189			.281	.306	.332	.367	.391	
H (W)		173	170	185			165	162	150	143	138	Integral plume parameter values
V (m^3/s)		.036	.049	.065			.134	.157	.170	.194	.217	
M (kgm/s^2)		.013	.018	.023			.041	.047	.049	.054	.059	
Ar		.142	.107	.082			.080	.076	.072	.068	.068	
λ		.76	.81	1.01			.97	.97	.99	1.01	1.00	
n		66	91	63			79	89	90	93	97	Local approximation by a model of a plume above a point source
p		113	139	61			85	95	91	92	97	
α		.103	.087	.105			.094	.088	.088	.086	.084	

Vertical temperature distribution													
x+0.25 (m)	0.00	0.05	0.10	0.50	1.00	1.20	1.50	2.00	2.50	3.00	3.50	4.00	4.62
Temp. (C)	19.3	18.5	18.6	19.2	19.6	19.7	19.8	20.1	20.1	20.2	20.3	20.4	20.1

Measurement series E7	Heat source: Tube d=50 mm h=150 mm Q=215 W Supply air: n=0 h^{-1} G=0 m^3/s											
Plume parameters	Height above source x (m)											
	0.75	1.00	1.25	1.50	1.75	2.00	2.25	2.50	2.75	3.00	3.25	
u_M (m/s)	.835	.603	.579	.589	.563	.534	.515	.498	.480	.458	.437	Gaussian fit by minimizing a sum of squares
r_V (m)	.089	.125	.156	.172	.203	.238	.273	.299	.324	.354	.382	
ΔT (C)	10.5	10.2	6.3	4.7	3.2	2.6	2.1	1.7	1.4	1.1	.94	
r_T (m)	.085	.097	.128	.154	.202	.234	.264	.292	.324	.361	.396	
H (W)	125	136	136	138	142	147	149	140	132	123	118	Integral plume parameter values
V (m^3/s)	.021	.030	.044	.054	.073	.094	.121	.140	.158	.180	.201	
M (kgm/s^2)	.010	.011	.015	.019	.025	.030	.037	.042	.045	.050	.053	
Ar	.045	.117	.099	.078	.069	.073	.073	.069	.065	.063	.063	
λ	.96	.78	.82	.90	.99	.98	.97	.98	1.00	1.02	1.04	
n	266	89	100	113	95	89	95	104	103	104	97	Local approximation by a model of a plume above a point source
p	291	148	149	140	96	92	102	109	103	100	90	
α	.051	.088	.083	.078	.086	.089	.086	.082	.082	.082	.085	

Vertical temperature distribution														
x+0.25 (m)	0.00	0.05	0.10	0.50	1.00	1.20	1.50	2.00	2.50	3.00	3.50	4.00	4.62	
Temp. (C)	20.2	20.2	20.2	20.3	20.4	20.4	20.5	20.6	20.6	20.8	20.9	20.9	20.7	

Measurement series E8	Heat source: Tube d=50 mm h=150 mm Q=215 W Supply air: n=0.7 h^{-1} G=0.0042 m^3/s											
Plume parameters	Height above source x (m)											
	0.75	1.00	1.25	1.50	1.75	2.00	2.25	2.50	2.75	3.00	3.25	
u_M (m/s)	.541	.507	.526	.517	.498		.441	.424	.400	.420	.404	Gaussian fit by minimizing a sum of squares
r_V (m)	.134	.177	.173	.202	.229		.313	.342	.385	.388	.426	
ΔT (C)	7.8	5.3	5.4	3.9	2.8		1.5	1.3	.97	.88	.76	
r_T (m)	.118	.159	.152	.177	.209		.292	.310	.371	.379	.420	
H (W)	125	143	139	136	126		116	107	105	103	104	Integral plume parameter values
V (m^3/s)	.031	.050	.050	.066	.082		.136	.155	.186	.198	.230	
M (kgm/s^2)	.010	.015	.016	.020	.024		.036	.039	.045	.050	.056	
Ar	.119	.123	.112	.099	.086		.082	.080	.078	.065	.066	
λ	.88	.90	.88	.88	.91		.93	.91	.96	.98	.99	
n	53	46	60	76	85		87	101	84	116	108	Local approximation by a model of a plume above a point source
p	68	57	77	98	102		100	123	90	122	111	
α	.115	.123	.108	.096	.090		.089	.083	.091	.077	.080	

Vertical temperature distribution														
x+0.25 (m)	0.00	0.05	0.10	0.50	1.00	1.20	1.50	2.00	2.50	3.00	3.50	4.00	4.62	
Temp. (C)	20.3	20.4	20.3	20.4	20.5	20.6	20.6	20.8	20.8	20.9	21.0	21.0	20.8	

Measurement series E9	Heat source: Tube d=50 mm h=150 mm Q=215 W Supply air: n=0.7 h^{-1} G=0.0042 m^3/s											
Plume parameters	Height above source x (m)											
	0.75	1.00	1.25	1.50	1.75	2.00	2.25	2.50	2.75	3.00	3.25	
u_M (m/s)	.553	.540	.472	.459	.458	.396	.430	.407	.383	.367	.348	Gaussian fit by minimizing a sum of squares
r_V (m)	.117	.123	.177	.220	.240	.297	.301	.336	.374	.404	.446	
ΔT (C)	10.4	9.0	4.5	3.1	2.4	1.7	1.6	1.3	1.1	.83	.67	
r_T (m)	.093	.101	.163	.211	.242	.296	.292	.334	.344	.440	.485	
H (W)	116	111	117	126	122	111	117	109	99	103	95	Integral plume parameter values
V (m^3/s)	.024	.025	.047	.070	.083	.110	.122	.144	.168	.189	.218	
M (kgm/s^2)	.0079	.0082	.013	.019	.023	.026	.032	.035	.039	.042	.045	
Ar	.134	.127	.121	.109	.092	.107	.089	.086	.091	.084	.083	
λ	.79	.82	.92	.96	1.01	1.00	.97	.99	.92	1.09	1.09	
n	62	60	43	44	50	40	64	61	75	45	47	Local approximation by a model of a plume above a point source
p	99	89	50	48	50	40	68	62	89	38	40	
α	.105	.107	.128	.126	.117	.132	.104	.106	.096	.124	.122	

Vertical temperature distribution														
x+0.25 (m)	0.00	0.05	0.10	0.50	1.00	1.20	1.50	2.00	2.50	3.00	3.50	4.00	4.62	
Temp. (C)	19.7	18.8	18.8	19.4	19.8	19.9	20.0	20.2	20.2	20.4	20.4	20.5	20.3	

Measurement series B10	Heat source: Tube d=50 mm h=150 mm Q=125 W Supply air: n=0 h^{-1} G=0 m^3/s											
Plume parameters	Height above source x (m)											
	0.75	1.00	1.25	1.50	1.75	2.00	2.25	2.50	2.75	3.00	3.25	
u_M (m/s)	.697	.506	.500	.503	.495	.459	.442	.431	.419	.398	.369	Gaussian fit by minimizing a sum of squares
r_V (m)	.086	.121	.142	.169	.185	.225	.253	.282	.304	.340	.383	
ΔT (C)	7.2	7.6	5.3	3.7	2.6	2.0	1.7	1.4	1.17	.85	.79	
r_T (m)	.081	.098	.120	.146	.195	.229	.245	.276	.295	.372	.386	
H (W)	67	85	85	87	89	88	86	87	83	81	72	Integral plume parameter values
V (m^3/s)	.017	.023	.032	.045	.053	.073	.089	.108	.121	.145	.169	
M (kgm/s^2)	.0069	.0071	.0095	.014	.016	.020	.024	.028	.030	.035	.037	
Ar	.043	.121	.101	.083	.067	.071	.072	.069	.068	.061	.066	
λ	.94	.81	.84	.87	1.05	1.02	.97	.98	.97	1.09	1.01	
n	313	71	85	114	81	83	98	101	110	84	99	Local approximation by a model of a plume above a point source
p	356	107	119	152	72	79	104	105	117	70	97	
α	.047	.099	.090	.078	.093	.092	.084	.083	.080	.091	.084	

Vertical temperature distribution														
x+0.25 (m)	0.00	0.05	0.10	0.50	1.00	1.20	1.50	2.00	2.50	3.00	3.50	4.00	4.62	
Temp. (C)	19.9	19.9	19.9	20.0	20.1	20.2	20.2	20.2	20.4	20.5	20.5	20.3	.	

Measurement series E11	Heat source: Tube d=50 mm h=150 mm Q=125 W Supply air: n=0.7 h^{-1} G=0.0042 m^3/s										
Plume parameters	Height above source x (m)										
	0.75	1.00	1.25	1.50	1.75	2.00	2.25	2.50	2.75	3.00	3.25	
u_M (m/s)		.518	.482	.464	.467	.478	.469	.420	.412	.394		Gaussian fit by minimizing a sum of squares
r_V (m)		.106	.135	.191	.213	.254	.262	.285	.304	.350		
ΔT (C)		10.0	6.1	3.6	2.8	2.1	1.8	1.4	1.2	.87		
r_T (m)		.080	.104	.168	.196	.243	.263	.286	.307	.358		
H (W)		84	75	100	103	120	108	92	87	80		Integral plume parameter values
V (m^3/s)		.018	.027	.053	.067	.097	.101	.107	.120	.151		
M (kgm/s^2)		.0057	.0079	.015	.019	.028	.028	.027	.030	.036		
Ar		.138	.118	.107	.091	.080	.070	.077	.72	.065		
λ		.75	.77	.88	.92	.96	1.01	1.00	1.01	1.01		
n		73	90	65	75	83	88	75	83	100		Local approximation by a model of a plume above a point source
p		128	151	85	88	90	87	74	82	99		
α		.098	.088	.103	.096	.092	.089	.096	.092	.083		

Vertical temperature distribution														
x+0.25 (m)	0.00	0.05	0.10	0.50	1.00	1.20	1.50	2.00	2.50	3.00	3.50	4.00	4.62	
Temp. (C)	19.8	19.9	19.9	20.1	20.2	20.3	20.3	20.4	20.3	20.4	20.5	20.5	20.2	

Measurement series E12	Heat source: Tube d=50 mm h=150 mm Q=125 W Supply air: n=0.7 h^{-1} G=0.0042 m^3/s										
Plume parameters	Height above source x (m)										
	0.75	1.00	1.25	1.50	1.75	2.00	2.25	2.50	2.75	3.00	3.25	
u_M (m/s)	.807		.480	.468	.413	.390	.328	.336	.352	.303	.294	Gaussian fit by minimizing a sum of squares
r_V (m)	.075		.141	.169	.227	.264	.317	.319	.321	.401	.417	
ΔT (C)	8.3		5.2	3.2	2.0	1.5	1.0	.94	.83	.60	.54	
r_r (m)	.075		.117	.157	.215	.264	.311	.367	.388	.514	.518	
H (W)	71		76	76	78	77	66	69	68	69	64	Integral plume parameter values
V (m^3/s)	.014		.030	.042	.067	.086	.104	.108	.114	.153	.160	
M (kgm/s^2)	.0069		.0087	.012	.017	.020	.020	.022	.024	.028	.028	
Ar	.032		.106	.084	.091	.087	.099	.089	.072	.088	.088	
λ	1.00		.83	.93	.95	1.00	1.04	1.15	1.21	1.28	1.24	
n	436		84	85	67	59	38	32	40	21	24	Local approximation by a model of a plume above a point source
p	436		123	99	75	60	35	24	28	13	16	
α	.040		.091	.090	.102	.108	.135	.147	.132	.181	.169	

Vertical temperature distribution														
x+0.25 (m)	0.00	0.05	0.10	0.50	1.00	1.20	1.50	2.00	2.50	3.00	3.50	4.00	4.62	
Temp. (C)	19.5	18.6	18.6	19.2	19.6	19.7	19.8	20.0	20.0	20.2	20.2	20.2	20.1	

Measurement series E13	Heat source: Plate d=356 mm Q=400 W Supply air: n=0 h^{-1} G=0 m^3/s											
Plume parameters	Height above source x (m)											
	0.75	1.00	1.25	1.50	1.75	2.00	2.25	2.50	2.75	3.00	3.25	
u_M (m/s)	.817	.694	.664	.656	.620	.614	.591	.565	.540	.512	.493	Gaussian fit by minimizing a sum of squares
r_V (m)	.130	.161	.186	.214	.252	.279	.304	.338	.363	.400	.432	
ΔT (C)	9.9	9.2	6.7	5.1	3.6	3.1	2.5	2.0	1.7	1.3	1.16	
r_T (m)	.124	.129	.162	.197	.247	.265	.296	.330	.358	.426	.454	
H (W)	247	246	253	267	266	270	247	236	224	220	212	Integral plume parameter values
V (m^3/s)	.044	.056	.072	.094	.123	.150	.171	.203	.224	.257	.289	
M (kgm/s^2)	.021	.023	.029	.037	.046	.055	.061	.069	.072	.079	.085	
Ar	.064	.103	.095	.085	.080	.078	.072	.070	.070	.068	.069	
λ	.95	.80	.87	.92	.98	.95	.97	.98	.99	1.06	1.05	
n	130	100	85	86	75	90	96	99	95	74	76	Local approximation by a model of a plume above a point source
p	143	155	112	101	78	100	102	104	97	66	69	
α	.073	.083	.090	.090	.096	.088	.085	.084	.086	.097	.095	

Vertical temperature distribution													
x+0.25 (m)	0.00	0.05	0.10	0.50	1.00	1.20	1.50	2.00	2.50	3.00	3.50	4.00	4.62
Temp. (C)	20.3	20.3	20.3	20.4	20.5	20.6	20.7	20.8	20.9	21.1	21.2	21.3	20.8

Measurement series E14	Heat source: Plate d=356 mm Q=400 W Supply air: n=0.7 h^{-1} G=0.0042 m^3/s											
Plume parameters	Height above source x (m)											
	0.75	1.00	1.25	1.50	1.75	2.00	2.25	2.50	2.75	3.00	3.25	
u_M (m/s)	.782	.625	.608	.598	.607	.571	.560	.526	.518	.489		Gaussian fit by minimizing a sum of squares
r_V (m)	.123	.169	.200	.226	.242	.279	.302	.334	.351	.390		
ΔT (C)	9.9	8.8	5.9	4.6	3.8	2.9	2.4	2.0	1.7	1.3		
r_T (m)	.112	.122	.175	.206	.228	.267	.288	.306	.323	.366		
H (W)	201	203	237	242	244	230	221	201	194	177		Integral plume parameter values
V (m^3/s)	.037	.056	.076	.096	.112	.139	.161	.184	.200	.233		
M (kgm/s^2)	.018	.021	.028	.034	.041	.048	.054	.059	.062	.068		
Ar	.067	.127	.107	.098	.085	.082	.077	.080	.076	.073		
λ	.91	.72	.87	.91	.94	.96	.95	.92	.92	.94		
n	147	101	66	68	79	78	91	98	106	107		Local approximation by a model of a plume above a point source
p	178	194	86	82	90	85	100	117	125	131		
α	.069	.083	.103	.101	.094	.094	.088	.084	.081	.081		

Vertical temperature distribution														
x+0.25 (m)	0.00	0.05	0.10	0.50	1.00	1.20	1.50	2.00	2.50	3.00	3.50	4.00	4.62	
Temp. (C)	20.0	20.1	20.1	20.3	20.4	20.4	20.4	20.5	20.5	20.7	20.7	20.8	20.4	

Measurement series E15	Heat source: Plate d=356 mm Q=400 W Supply air: n=0.7 h^{-1} G=0.0042 m^3/s											
Plume parameters	Height above source x (m)											
	0.75	1.00	1.25	1.50	1.75	2.00	2.25	2.50	2.75	3.00	3.25	
u_M (m/s)	.721	.603	.600	.600	.588	.564	.541	.542	.498	.480	.445	Gaussian fit by minimizing a sum of squares
r_V (m)	.138	.176	.210	.232	.264	.301	.328	.365	.401	.430	.473	
ΔT (C)	10.5	8.0	5.7	4.3	3.3	2.6	2.1	1.8	1.4	.94		
r_T (m)	.118	.144	.192	.219	.248	.283	.299	.335	.364	.410	.471	
H (W)	227	227	260	247	243	233	211	212	190	188	177	Integral plume parameter values
V (m^3/s)	.042	.059	.083	.101	.129	.161	.183	.219	.251	.279	.313	
M (kgm/s^2)	.018	.021	.030	.036	.045	.054	.059	.069	.075	.080	.084	
Ar	.096	.130	.112	.093	.085	.081	.079	.078	.075	.073	.075	
λ	.86	.82	.91	.94	.94	.94	.91	.92	.91	.95	1.00	
n	90	59	51	64	78	86	102	103	115	100	80	Local approximation by a model of a plume above a point source
p	123	88	62	72	88	98	123	122	140	110	81	
α	.088	.109	.116	.104	.094	.090	.082	.082	.078	.083	.093	

Vertical temperature distribution														
x+0.25 (m)	0.00	0.05	0.10	0.50	1.00	1.20	1.50	2.00	2.50	3.00	3.50	4.00	4.62	
Temp. (C)	19.5	18.8	18.8	19.4	19.7	19.8	20.0	20.2	20.2	20.4	20.5	20.5	20.2	

Measurement series E16	Heat source: Plate d=356 mm Q=200 W Supply air: n=0 h^{-1} G=0 m^3/s											
Plume parameters	Height above source x (m)											
	0.75	1.00	1.25	1.50	1.75	2.00	2.25	2.50	2.75	3.00	3.25	
u_M (m/s)	.656	.545	.539	.530	.522	.498	.487	.458	.443	.418	.405	Gaussian fit by minimizing a sum of squares
r_V (m)	.125	.164	.188	.219	.243	.282	.307	.347	.376	.412	.445	
ΔT (C)	6.4	6.0	4.2	3.0	2.4	2.0	1.6	1.3	1.1	.87	.77	
r_T (m)	.122	.132	.167	.211	.238	.257	.292	.345	.370	.405	.454	
H (W)	120	130	134	137	139	137	131	130	125	115	119	Integral plume parameter values
V (m^3/s)	.032	.046	.050	.080	.097	.125	.145	.173	.196	.223	.252	
M (kgm/s^2)	.013	.015	.019	.025	.030	.037	.042	.047	.052	.056	.061	
Ar	.062	.111	.091	.078	.073	.076	.068	.069	.069	.069	.070	
λ	.98	.80	.89	.96	.98	.91	.95	1.00	.98	.98	1.02	
n	126	87	85	85	92	111	116	94	100	101	84	Local approximation by a model of a plume above a point source
p	131	135	108	93	97	134	129	95	103	105	80	
α	.074	.089	.090	.090	.087	.079	.077	.086	.083	.083	.091	

Vertical temperature distribution													
x+0.25 (m)	0.00	0.05	0.10	0.50	1.00	1.20	1.50	2.00	2.50	3.00	3.50	4.00	4.62
Temp. (C)	20.1	20.1	20.1	20.2	20.3	20.3	20.4	20.5	20.5	20.6	20.7	20.7	20.5

Measurement series E17	Heat source: Plate d=356 mm Q=200 W Supply air: n=0.7 h^{-1} G=0.0042 m^3/s											
Plume parameters	Height above source x (m)											
	0.75	1.00	1.25	1.50	1.75	2.00	2.25	2.50	2.75	3.00	3.25	
u_M (m/s)	.640	.527	.518	.506	.493	.481	.467	.443	.430		.395	Gaussian fit by minimizing a sum of squares
r_V (m)	.120	.163	.197	.223	.254	.278	.299	.330	.349		.407	
ΔT (C)	6.9	5.9	4.0	3.0	2.4	2.0	1.5	1.3	1.05		.82	
r_T (m)	.106	.119	.180	.215	.246	.273	.308	.345	.382		.420	
H (W)	105	108	137	138	138	135	124	124	115		104	Integral plume parameter values
V (m^3/s)	.029	.044	.063	.079	.100	.117	.131	.152	.165		.206	
M (kgm/s^2)	.011	.014	.020	.024	.030	.034	.037	.041	.043		.049	
Ar	.067	.115	.098	.088	.083	.079	.070	.073	.067		.013	
λ	.88	.73	.91	.97	.97	.98	1.03	1.04	1.09		1.03	
n	161	118	67	67	74	77	80	71	69		77	Local approximation by a model of a plume above a point source
p	206	222	80	71	79	80	75	65	58		72	
α	.066	.077	.102	.102	.097	.095	.093	.099	.100		.095	

Vertical temperature distribution													
x+0.25 (m)	0.00	0.05	0.10	0.50	1.00	1.20	1.50	2.00	2.50	3.00	3.50	4.00	4.62
Temp. (C)	19.0	20.	20.0	20.2	20.2	20.3	20.3	20.4	20.3	20.5	20.5	20.5	20.3

Measurement series E18	Heat source: Plate d=356 mm Q=200 W Supply air: n=0.7 h^{-1} G=0.0042 m^3/s											
Plume parameters	Height above source x (m)											
	0.75	1.00	1.25	1.50	1.75	2.00	2.25	2.50	2.75	3.00	3.25	
u_M (m/s)	.567	.505	.499	.469	.459	.442	.450	.439	.426	.403	.406	Gaussian fit by minimi-'ing a sum of squares
r_V (m)	.148	.176	.209	.238	.277	.310	.327	.351	.380	.411	.423	
ΔT (C)	6.5	5.0	3.5	2.4	2.0	1.5	1.36	1.14	.96	.80	.68	
r_T (m)	.122	.149	.199	.243	.269	.293	.310	.357	.389	.440	.479	
H (W)	123	123	137	126	128	117	117	119	114	111	106	Integral plume parameter values
V (m^3/s)	.039	.049	.069	.083	.111	.133	.151	.170	.193	.213	.228	
M (kgm/s^2)	.013	.015	.021	.024	.031	.035	.041	.045	.049	.051	.056	
Ar	.100	.115	.098	.089	.087	.082	.074	.070	.067	.068	.059	
λ	.83	.84	.95	1.02	.97	.94	.95	1.02	1.02	1.07	1.13	
n	95	66	57	52	66	82	101	86	89	73	78	Local approximation by a model of a plume above a point source
p	140	93	63	50	70	92	113	83	85	63	61	
α	.085	.102	.111	.115	.102	.092	.083	.090	.088	.098	.094	

Vertical temperature distribution														
x+0.25 (m)	0.00	0.05	0.10	0.50	1.00	1.20	1.50	2.00	2.50	3.00	3.50	4.00	4.62	
Temp. (C)	19.5	18.8	18.8	19.4	19.7	19.8	19.9	20.0	20.1	20.2	20.3	20.3	20.1	

Measurement series E19	Heat source: Plate d=356 mm Q=100 W Supply air: n=0 h^{-1} G=0 m^3/s											
Plume parameters	Height above source x (m)											
	0.75	1.00	1.25	1.50	1.75	2.00	2.25	2.50	2.75	3.00	3.25	
u_M (m/s)	.508	.472	.443	.442	.425	.401		.384	.365	.353		Gaussian fit by minimizing a sum of squares
r_V (m)	.132	.152	.190	.208	.252	.279		.330	.356	.391		
ΔT (C)	5.2	4.0	2.7	2.1	1.6	1.3		.89	.70	.64		
r_T (m)	.108	.128	.178	.209	.237	.274		.329	.380	.382		
H (W)	70	68	76	77	78	73		71	65	63		Integral plume parameter values
V (m^3/s)	.028	.034	.050	.060	.084	.098		.132	.145	.169		
M (kgm/s^2)	.0084	.0098	.013	.016	.022	.024		.030	.031	.036		
Ar	.089	.091	.087	.075	.076	.073		.067	.063	.067		
λ	.82	.84	.94	1.00	.94	.98		1.00	1.07	.98		
n	125	108	76	78	99	89		101	86	109		Local approximation by a model of a plume above a point source
p	186	153	86	77	112	92		101	76	114		
α	.075	.080	.096	.095	.084	.088		.083	.090	.080		

Vertical temperature distribution													
x+0.25 (m)	0.00	0.05	0.10	0.50	1.00	1.20	1.50	2.00	2.50	3.00	3.50	4.00	4.62
Temp. (C)	20.2	20.2	20.2	20.3	20.4	20.4	20.5	20.5	20.5	20.6	20.7	20.7	20.5

Measurement series E20	Heat source: Plate d=356 mm Q=100 W Supply air: n=0.7 h^{-1} G=0.0042 m^3/s										
Plume parameters	Height above source x (m)										
	0.75	1.00	1.25	1.50	1.75	2.00	2.25	2.50	2.75	3.00	3.25	
u_M (m/s)		.447	.441	.429	.415	.406	.388	.376	.364	.365	.353	Gaussian fit by minimizing a sum of squares
r_V (m)		.155	.181	.215	.236	.263	.294	.316	.349	.373	.381	
ΔT (C)		3.9	2.8	2.2	1.6	1.37	1.10	.94	.76	.68	.63	
r_T (m)		.124	.167	.206	.235	.269	.298	.351	.403	.456	.420	
H (W)		61	69	78	72	75	71	74	73	78	67	Integral plume parameter values
V (m^3/s)		.034	.045	.062	.072	.088	.105	.118	.138	.160	.161	
M (kgm/s^2)		.0091	.012	.016	.018	.021	.024	.027	.030	.035	.034	
Ar		.101	.086	.084	.076	.074	.072	.071	.067	.063	.064	
λ		.80	.92	.96	1.00	1.02	1.01	1.11	1.16	1.22	1.10	
n		108	83	74	79	75	81	59	55	50	74	Local approximation by a model of a plume above a point source
p		170	97	81	79	72	79	48	41	33	61	
α		.080	.091	.097	.094	.096	.093	.109	.112	.118	.097	

Vertical temperature distribution														
x+0.25 (m)	0.00	0.05	0.10	0.50	1.00	1.20	1.50	2.00	2.50	3.00	3.50	4.00	4.62	
Temp. (C)	19.9	19.9	20.0	20.1	20.1	20.2	20.2	20.2	20.2	20.3	20.3	20.4	20.2	

Measurement series E21	Heat source: Plate d=356 mm Q=100 W Supply air: n=0.7 h^{-1} G=0.0042 m^3/s											
Plume parameters	Height above source x (m)											
	0.75	1.00	1.25	1.50	1.75	2.00	2.25	2.50	2.75	3.00	3.25	
u_M (m/s)	.454	.411	.396	.388	.367	.353	.348	.344	.319	.303	.279	Gaussian fit by minimizing a sum of squares
r_V (m)	.149	.185	.213	.242	.276	.315	.327	.352	.395	.443	.495	
ΔT (C)	4.4	3.1	2.2	1.64	1.25	.93	.80	.62	.50	.41	.32	
r_T (m)	.118	.164	.198	.228	.263	.341	.334	.380	.452	.515	.652	
H (W)	65	72	68	67	63	66	57	54	54	54	52	Integral plume parameter values
V (m^3/s)	.032	.044	.057	.072	.088	.110	.117	.134	.156	.187	.215	
M (kgm/s^2)	.0026	.0030	.0036	.0043	.0047	.0055	.0057	.0063	.0064	.0069	.0067	
Ar	.107	.113	.098	.088	.086	.078	.072	.062	.065	.067	.068	
λ	.79	.89	.93	.94	.95	1.08	1.02	1.08	1.14	1.16	1.32	
n	99	57	62	72	74	52	79	84	62	55	32	Local approximation by a model of a plume above a point source
p	159	72	72	82	81	45	76	72	47	40	19	
α	.084	.111	.106	.098	.097	.115	.094	.091	.106	.113	.146	

Vertical temperature distribution														
x+0.25 (m)	0.00	0.05	0.10	0.50	1.00	1.20	1.50	2.00	2.50	3.00	3.50	4.00	4.62	
Temp. (C)	19.4	18.8	18.9	19.3	19.6	19.7	19.8	19.9	19.9	20.0	20.1	20.1	19.9	

Measurement series E22	Heat source: Cyl d=400 mm h=1000 mm Q=100 W Supply air: n=0 h^{-1} G=0 m^3/s										
Plume parameters	Height above source	x (m)									
		0.25	0.50	0.75	1.00	1.25	1.50	1.75	2.00	2.25	2.50	
u_M (m/s)		.205	.247	.254	.258	.223	.203	.254	.236	.221	.202	Gaussian fit by minimizing a sum of squares
r_V (m)		.164	.202	.221	.253	.282	.326	.336	.351	.383	.431	
ΔT (C)		2.1	1.4	.95	.71	.50	.43	.36	.29	.25	.18	
r_T (m)		.155	.212	.240	.288	.355	.388	.417	.460	.429	.432	
H (W)		21	27	24	25	21	21	24	20	17	13	Integral plume parameter values
V (m^3/s)		.017	.032	.039	.052	.056	.068	.090	.091	.102	.118	
M (kgm/s^2)		2.1	4.7	6.0	8.0	7.5	8.3	13.8	13.0	13.5	14.3	
Ar		.279	.150	.109	.091	.095	.115	.062	.060	.065	.064	
λ		.95	1.05	1.09	1.14	1.26	1.19	1.24	1.31	1.12	1.00	
n		7	16	27	32	20	17	49	42	66	108	Local approximation by a model of a plume above a point source
p		8	15	23	25	12	12	32	24	53	107	
α		.312	.206	.161	.147	.189	.203	.119	.129	.102	.080	

Vertical temperature distribution														
x+0.25 (m)	0.00	0.05	0.10	0.50	1.00	1.20	1.50	2.00	2.50	3.00	3.50	4.00	4.62	
Temp. (C)	20.0	20.0	20.0	20.1	20.1	20.1	20.2	20.2	20.2	20.3	20.3	20.3	20.2	

Measurement series E23	Heat source: Cyl d=400 mm h=1000 mm Q=100 W Supply air: n=0.7 h^{-1} G=0.0042 m^3/s

Plume parameters	Height above source x (m)										
		0.25	0.50	0.75	1.00	1.25	1.50	1.75	2.00	2.25	2.50	
u_M (m/s)		.180	.254	.203	.238	.233	.210	.208	.174	.187	.168	Gaussian fit by minimizing a sum of squares
r_V (m)		.214	.205	.259	.297	.296	.380	.380	.414	.472	.510	
ΔT (C)		2.0	1.6	.82	.74	.58	.43	.31	.26	.25	.20	
r_T (m)		.198	.196	.305	.298	.336	.385	.564	.713	.781	.612	
H (W)		29	31	25	30	25	25	24	22	29	19	Integral plume parameter values
V (m^3/s)		.026	.034	.043	.066	.064	.095	.095	.094	.131	.137	
M (kgm/s^2)		2.8	5.1	5.2	9.4	9.0	12.0	12.0	9.8	14.8	13.8	
Ar		.446	.174	.172	.130	.106	.124	.090	.120	.115	.121	
λ		.93	.95	1.18	1.00	1.13	1.01	1.48	1.72	1.65	1.20	
n		3	18	8	26	24	27	11	4	5	15	Local approximation by a model of a plume above a point source
p		4	19	6	26	18	27	5	1	2	10	
α		.479	.198	.299	.164	.171	.247	.443	.393	.218	.080	

Vertical temperature distribution													
x+0.25 (m)	0.00	0.05	0.10	0.50	1.00	1.20	1.50	2.00	2.50	3.00	3.50	4.00	4.62
Temp. (C)	20.1	20.2	20.2	20.4	20.4	20.5	20.5	20.5	20.4	20.6	20.6	20.6	20.4

Measurement series E24	Heat source: Cyl d=400 mm h=1000 mm Q=100 W Supply air: n=0.7 h^{-1} G=0.0042 m^3/s

Plume parameters	Height above source x (m)										
		0.25	0.50	0.75	1.00	1.25	1.50	1.75	2.00	2.25	2.50	
u_M (m/s)		.180	.221	.226	.200	.192	.204	.164	.159	.158	.119	Gaussian fit by minimizing a sum of squares
r_V (m)		.203	.206	.215	.263	.292	.303	.360	.381	.363	.478	
ΔT (C)		1.6	1.1	.75	.54	.37	.29	.17	.16	.11	.10	
r_T (m)		.180	.204	.248	.319	.404	.347	.508	.567	.703	.840	
H (W)		20	20	17	17	15	12	9	10	7	8	Integral plume parameter values
V (m^3/s)		.023	.029	.033	.043	.052	.059	.067	.072	.065	.086	
M (kgm/s^2)		2.4	3.8	4.4	5.1	6.0	7.2	6.6	6.9	6.2	6.1	
Ar		.369	.160	.106	.118	.097	.071	.077	.081	.054	.111	
λ		.88	.99	1.15	1.21	1.38	1.15	1.41	1.49	1.94	1.76	
n		5	18	22	15	13	51	19	14	11	4	Local approximation by a model of a plume above a point source
p		7	18	17	10	7	39	9	6	3	1	
α		.361	.197	.177	.218	.232	.116	.193	.224	.252	.430	

Vertical temperature distribution														
x+1.00 (m)	0.00	0.05	0.10	0.50	1.00	1.20	1.50	2.00	2.50	3.00	3.50	4.00	4.62	
Temp. (C)	19.0	18.1	18.1	18.7	19.0	19.1	19.2	19.3	19.3	19.6	19.6	19.6	19.6	

LIST OF FIGURES

LIST OF FIGURES

REFERENCES

REFERENCES

/1/ Abramovich, G.N: The Theory of Turbulent Jets, M.I.T Press, 1963.

/2/ Appelby, P.: Displacement Ventilation: A Design Guide, Building Services, April 1989.

/3/ Bach, H., R. Detz, W. Dittes & R. Mangelsdorf: Einfluss auf den Energieeinsatz bei raumlufttechnischer Anlagen, HLH 32, Nr.7, Juli, 1981.

/4/ Batchelor, G.K.: Heat Convection and Buoyancy Effects in Fluids, Q. Jl. R. Met. Soc., 80, pp.339-358, 1954.

/5/ Baturin, V.V.: Fundamentals of Industrial Ventilation, Pergamon Press, pp.125-127, 1972.

/6/ Beier, R.A. & R.L. Gorton: Thermal Stratification in Factories - Cooling Loads and Temperature Profiles, ASHRAE transactions, vol.84, pt.1, 1978.

/7/ Brügger P. & B. Kegel: Displacement Ventilation for an Office Building with Triple Glazed Windows, 2'nd World Congress on HVAC - Clima2000, Sarajevo, Yugoslavia, 1989.

/8/ Chen, Q.: Indoor Airflow, Air Quality and Energy Consumption of Buildings, Ph.D. thesis, Delft University of Technology, The Netherlands, 1989.

/9/ Chen, Q., van der Kooi: Calculation of Air-conditioning Load in Rooms with Temperature Stratification, 2'nd World Congress on HVAC - Clima2000, Sarajevo, Yugoslavia, 1989.

/10/ Chen, C.J & C.H Chen: On Prediction and Unified Correlation for Decay of Vertical Buoyant Jets, Journal of Heat Transfer, vol.101, pp.532-537, Aug., 1979.

/11/ Chen, C.J.& W. Rodi: Vertical Turbulent Buoyant Jets - A Review of Experimental Data, HMT, vol.4, Pergamon Press, 1980.

/12/ Christensen, B. & J.H. Larsen: Personal communication, University of Aalborg, 1990.

/13/ Davidson, L.: Numerical Simulation of Turbulent Flow in Ventilated Rooms, Ph.D. thesis, Chalmers University of Technology, Sweden, 1989.

/14/ Davis, L.R., M.A. Shirazi & D.L. Siegel: Measurements of Buoyant Jet Entrainment From Single and Multiple Sources, Journal of Heat Transfer, vol.100, pp.442-447, August, 1978.

/15/ Daws, L.F.: Movement of Air Streams Indoors, J I H V E, vol.37, pp.241-253, Feb., 1970.

/16/ Dittes, W. & R. Mangelsdorf: Der Wärmetransport im Raum bei der Luftführung von unten nach oben, HLH 32, Nr.7, Juli, 1981.

/17/ Euser, H., C.J. Hoogendoorn & H. van Ooijen: Airflow in a Room Induced by Natural Convection Streams, ICHMT Congress Heat Transfer in Buildings, Dubrovnik, Aug.22-Sept.2, 1977.

/18/ Fanger, P.O.: Thermal comfort, Analysis and Applications in Environmental Engineering, Originally Presented as the Authors Dr. Techn. thesis at DTH in 1970, McGraw-Hill Book Compagny, 1972. Reprinted Robert E. Krieger, Florida, 1982.

/19/ Fanger, P.O. & N.K. Christensen: Perception of Draught in Ventilated Spaces, Ergonomics, vol.29, no.2, pp.215-235, 1986.

/20/ Fanger, P.O.: Introducing of the olf and the Decipol Units to Quantify Air Pollution Perceived by Humans Indoors and Outdoors, Energy and Buildings, 12 ,pp.1-6, Elsevier Sequoia, 1988.

/21/ Fitzner, K: Luftführung in klimatisierten Sälen, Klimatechnisches Laboratorium Betzdorf, Heinrich NickelGMBH, Klima- und Lufttechnik, 1985.

/22/ Fitzner, K.: Quell-Lüftung, Forschungsbericht Nr. 522, Klimatechnisches Laboratorium Betzdorf, Heinrich NickelGMBH, Klima- und Lufttechnik.

/23/ Fitzner, K.; Impulsarme Luftzufuhr durch Quelllüftung, HLH, Bd.39, Nr.4, April, 1988.

/24/ Fitzner, K.: Förderprofil einer Wärmequelle bei vershiedenen Temperaturgradienten und der Einfluss auf die Raumströmung bei Quelllüftung, Klima-Kälte-Heizung, nr.10, pp.476-481, 1989.

/25/ Fox, D.G.: Forced Plume in a Stratified Fluid, Journ. Geophys. Res., 75, pp.6818-6835, 1970.

/26/ George, W.K, R.L. Alpert & F. Tamini: Turbulence Measurements in an Axisymmetric Plume, Int. J. Heat Mass Transfer, Vol.20, pp.1145-1154, 1977.

/27/ Gottschalk, G.: Downward Air Diffusion for Displacement Ventilation Systems. To be presented.

/28/ Gottschalk, G.: Personal communication, ETH, Zürich, Switzerland, Sept., 1990

/29/ Hatch, T.F & D. Barron-Oronzoo: Air Flow in Free Convection Over Heated Bodies, ASHRAE transactions, vol.63, paper no.1602,pp.275-290, 1957.

/30/ Heiselberg, P.& P.V. Nielsen: Flow Conditions in a Mechanically Ventilated Room with a Convective Heat Source, 9'th AIVC Conference on Effective Ventilation, Gent, Belgium, 1989. Also published in Indoor Environmental Technology, paper no.3, ISSN 0902-7513 R8714, 1988.

/31/ Heiselberg, P. & M. Sandberg: Convection From a Slender Cylinder in a Ventilated Room, RoomVent-90, International Conference, Oslo, Norway, 1990.

/32/ Helander, L., Yen S-M. & R.E. Crank: Maximum Downward Travel of Heated Jets From Standard Long Radius a.s.m.e. Nozzles, ASHRAE transactions, paper no.1475, 1953.

/33/ Homna, H.: The Effect of Free Convection Caused by Occupant's Metabolism on Thermal Environment of a Room, A4-series no.21, Dept. of Heating and Ventilating, Royal Inst. of Technology, Stockholm, Sweden, 1979.

/34/ Homma, H.: Free Convection Caused by Metabolic Heat Around Human Body, RoomVent-87, Stockholm, June 1987.

/35/ Homma, H.: Personal communication, Toyohashi University Of Technology, Japan, marts 1990.

/36/ Jaluria, Y. & B. Gebhart: On Transition Mechanisms in Vertical Natural Convection Flow, Journal Fluid Mech., vol.66, part 2, pp.309-337, 1974.

/37/ Jaluria, Y. & B. Gebhart: Stability and Transition of Buoyancy-induced Flows in a Stratified Fluid, Journal Fluid Mech., vol.66, part 3, pp.593-612, 1974.

/38/ Jaluria, Y. & B. Gebhart: On the Boyancy-induced Flow Arising From a Heated Hemisphere, Int. J. Heat Mass Transfer, vol.18, pp.415-431, Pergamon Press, 1975.

/39/ Kegel, B. & U.W. Schulz: Displacement Ventilation for Office Buildings, 10'th AIVC Conference on Progress and Trends in Air Infiltration and Ventilation Research, Espoo, Findland, Sept.25-28, 1989.

/40/ Kegel, B.: Personal communication, Sulzer Brothers Lmt, Winterthur, Switzerland, 1990.

/41/ Koestel, A.: Computing Temperatures and Velocities in Vertical Jets of Hot and Cold Air, Heating Piping & Air Conditioning, June, 1954.

/42/ Kofoed, P. & P.V. Nielsen: Thermal Plumes in Ventilated Rooms - An Experimental Research Work, 3'rd Seminar on Application of Fluid Mechanics in Environmental Protection, Silesian Technical University, Gliwice, Poland 1988. Also published in Indoor Environmental Technology, paper no.7, ISSN 0902-7513 R8833, 1988.

/43/ Kofoed, P. & P.V. Nielsen: Thermal Plumes in Ventilated Rooms - Measurements in stratified surroundings and analysis by use of an extrapolation method, RoomVent-90, International Conference, Oslo, Norway, 1990.

/44/ Kotsovinos, N.E.: A study of the Entrainment and Turbulence in a Plane Buoyant Jet, Ph.D. thesis, California Inst. of Technology, Pasadena, California, 1975.

/45/ Launder B.E. & D.B. Spalding: Mathematical models of Turbulence, Academic Press, London & New York, 1972.

/46/ List, E.J. & J. Emberger: Turbulent Entrainment in Buoyant Jets and Plumes, Journal of the Hydraulics DIvision, HY9, pp.1461-1474 sept., 1973.

/47/ Madni, K. & R.H. Pletcher: Prediction of Turbulent Forced Plumes Issuing Vertically into Stratified or Uniform Ambients, Journal of Heat Transfer, feb., 1977.

/48/ Malmström, T-G. & J. Oström: Nogåt om lokal ventilationseffektivitet, A4-series No.47. Dir. för Heating and Ventilatong, Royal Inst. Of Technology, Stockholm 1980.

/49/ Malmström, T-G. & A. Algren: Aspects of Efficient Ventilaton en Office Rooms, International Symposium on Indoor Air Pollution, Heat and Eneegy Conservation, Amherst, USA 1981.

/50/ Malmström, T-G. & M. Noguchi: Influence of Leakage When Measuring Air Exchange Efficiencies, RoomVent-87, Stockholm, June 1987.

/51/ Mathisen, H.M.: Analysis and Evaluation of Displacement Ventilation, Dr.ing thesis, Institutt for Varme-Ventilasjon- og sanitærteknikk, Norges Tekniske Højskole, July 1989.

/52/ Melikov, A.K., G. Langkilde: Displacement Ventilaton - Airflow in the Near Zone, RoomVent-90, International Conference, Oslo, Norway, 1990.

/53/ Mierzwinski, S.: Air Motion and Temperature Distribution Above a Human body in Result of Natural Convection, A4-series no.45, Dept. of Heating and Ventilating, Royal Inst. of Technology, Stockholm, Sweden, 1981.

/54/ Mierzwinski, S. & Z. Popiolek: Experimental Verification and Possibilities of Application of a Plume Model Above a Point Heat Source, A4-series no.58, Dept. of Heating and Ventilating, Royal Inst. of Technology, Stockholm, Sweden, 1982.

/55/ Morton, B.R., G.I. Taylor & J.S. Turner: Turbulent Gravitational ConvectIon from Maintained and Instantanous Sources, Proc. Roy. Soc. London, A, 234, pp.1-23, 1956.

/56/ Morton, B.R.: The Choise of Conservation Equations for Plume Models, Journ. of Geophys. Res., vol.76, no.30, pp.7409-7416, Okt.20, 1971.

/57/ Mundt, E.: Convecton Flows Above Common Heat Sources in Rooms with Displacement Ventilation, RoomVent-90, International Conference , Oslo, Norway, 1990.

/58/ Mundt, E.: Personal communication, KTH, Stockholm, 1990.

/59/ Nakagome, H. & M. Hirata: The Structure of Turbulent Diffusion in an Axisymmetric Thermal Plume, ICHMT, vol.1-2, Dubrovnik, 1976.

/60/ Nickel, J.: Air Quality in a Conference Room with Tobacco Smoking Ventilated with Mixed or Displacement Ventilation, RoomVent-90, International Conference, Oslo, Norway, 1990.

/61/ Nielsen, P.V.: Flow in Air Conditioned Rooms, Ph.D. thesis, (english translation of Ph.D. thesis from The Technical University of Denmark 1974), Danfoss A/S, Denmark, 1976.

/62/ Nielsen, P.V. & Å.T.A. Möller: New Developments in Room Air Distribution, chap.12 in Air Conditioning Systems Design for Buildings, McGraw-Hill Book Compagny (UK) Lmt.

/63/ Nielsen, P.V., L. Hoff,L.G. Pedersen: Displacement Ventilation by Different Types of Diffusers, 9'th AIVC Conference on Effective Ventilation, Gent, Belgium, 1989. Also published in Indoor Environmental Technology, paper no.8, ISSN 0902-7513 R8834, 1988.

/64/ Nielsen, P.V.: Displacement Ventilation in a Room with Low-level Diffusors, Kälte-Klima-Tagung 1988, Deutscher Kälte- und Klimatechnicher Verein e.V., Munich 1988. Also published in Indoor Environmental Technology, paper no.10, ISSN 0902-7513 R8836, 1988.

/65/ Nielsen, P.V.: Airflow Simulation Techniques - Progess and Trends, 10'th AIVC Conference on Progress and Trends in Air Infiltration and Ventilation Research, Espoo, Findland, Sept.25-28, 1989. Also published in Indoor Environmental Technology, paper no.11, ISSN 0902-7513 R8926, 1988.

/66/ Nielsen, P.V.: Air Velocity Along the Floor in a Room with Wall Mounted Armature and Displacement Ventilation. Presented at the annual Nordic Ventilation Group meeting, Oslo, Marts 1990. Also published in Indoor Environmental Technology, paper no., ISSN 0902-7513 R9004, 1990.

/67/ Nielsen, P.V.: Personal communication, University Of Aalborg, 1988-1990.

/68/ Overby, H.: Calculation of Vertical Temperature Gradients in Heated Rooms, RoomVent-90, International Conference, Oslo, Norway, 1990.

/69/ Parczewski, K.I. & P.N. Renzi: Scale Model Studies of Temperature Distributions in Internally Heated Enclosures, ASHRAE journal, july 1963.

/70/ Pera, L. & B. Gebhart: Experimental Observations of Wake Formation over Cylindrical Surfaces in Natural Convection Flows, International Journal Heat Mass Transfer, vol.15, pp.175-177, 1972.

/71/ Popiolek, Z.: Problems of Testing and Mathematical Modelling of Plumes Above Human Body and Other Extensive Heat Sources, A4-series no.54, Dept. of Heating and Ventilating, Royal Inst. of Technology, Stockholm, Sweden, 1981.

/72/ Popiolek Z. & P. Knapek: Analysis of the Integral Method of Plume Calculation, A4-series no.59, Dept. of Heating and Ventilating, Royal Inst. of Technology, Stockholm, Sweden, 1982.

/73/ Popiolek, Z. & S. Mierzwinski: Buoyant Plume Calculation by Mean of the Integral Method, A4-series no.89, Dept. of Heating and Ventilating, Royal Inst. of Technology, Stockholm, Sweden, 1984.

/74/ Popiolek, Z.: Personal communication, Silesian Technical University, Gliwice, Poland, April 1988, Marts and June 1989.

/75/ Powe, R.E., J.A. Scarland & T.A. Larson: Flow Studies for Natural Convection in Liquids Between a Sphere and Its Cubical Enclosure, International Journal Heat Mass Transfer, vol.20, pp.159-169, Pergamon Press, 1977.

/76/ Prandtl, L.: Bericht über Untersuchungen zur ausgebildeten Turbulenz, Zeitschr. angw. Math. Mech.,5, pp.136-139, 1925.

/77/ Prandtl, L.: Führer durch die Strömungslehre, Friedr. Vieweg & Sohn, 1965.

/78/ Prochaska, V. & B. Kegel: Control Algorithms for Rooms with Dislacement Ventilation.

/79/ Rajaratnam, N.: Turbulent jets, (Developments in Water Science; 5), Elsevier Scientific Publishing Compagny, 1976.

/80/ Rapp, G.M: Convective Heat Transfer and Convective Coefficients of Nude Man, Cylinders and Spheres at Low Air Velocities, ASHRAE transactions, paper no.2264, pt.1, pp.75-87, 1973.

/81/ Regenscheit, B.: Der Einfluss von Värmequellen auf die Strömung in Reinraum mit turbulenzarmer Verdrängungsströmung, Weihe W.H u.a. (ed.), Reinraum Technik 1., 1973.

/82/ Rouse, H., C.S. Yih & H.W. Humphreys: Gravitational Convection From a Boundary Source, Tellus, 4, pp.201-210, 1952.

/83/ Sandberg, M.: What is Ventilation Efficiency, Building and environmental journal, no.16, 1981.

/84/ Sandberg, M.: Distribution of Ventilation Air and Contaminants in VEntilated Rooms - Theory and Measurements, Dr. thesis, ISSN 0346-2668, The Royal Inst. of Techn., Stockholm, Sweden.

/85/ Sandberg, M. & C. Blomqvist: Displacement Ventilation Systems in Office Rooms, ASHRAE, annual meeting 1989, published in ASHRAE transactions 1989, V.95, pt.2.

/86/ Schmidt, W.: Turbulente Ausbreitung eines Stromes erhitzter Luft, Z. angw. Math. Mech., Bd.21, Nr.5 & 6, Okt. & Dez., 1941.

/87/ Seban, R.A & M.M. Behnia: Turbulent Buoyant Jets in Unstratified Surroundings, International Journal Heat Mass Transfer, vol.19, pp.1197-1204, 1976.

/88/ Seppänen, O.A., W.E. Fisk, J. Eto & D.T. Grimsrud: Comparison of Conventinal Mixing and Displacement Air-Conditioning and Ventilation Systems in U.S. Commercial Buildings, ASHRAE annual meeting 1989, published in ASHRAE transactions 1989, V.95, pt.2.

/89/ Skistad, H.: Fortrengningsventilasjon i komfortanlegg med lavimpuls lufttilførsel i oppholdssonene, Norsk VVS Teknisk Forening, 1989.

/90/ Skåret, E & H.M. Mathisen: Ventilation Efficiency- a guide to efficient ventilation, ASHRAE transactions 1983, vol.89, pl.2A & B, pp.480-489.

/91/ Skåret, E.: Ventilation by Displacement - Characterizing and Design Implications, Ventilation'85 edited by H.D. Goodfellow, Elsevier Science Publishers B.V., Amsterdam, 1986.

/92/ Skåret, E.: Displacement Ventilation, RoomVent-87, Stockholm, June, 1987.

/93/ Sneck, H.J. & D.H Brown: Plume Rise From Large Thermal Sources such as Dry Cooling Towers, Journal of Heat Transfer, May, 1974.

/94/ Socher, H-J.: Verdrängungslüftung zur Energieeinsparung, HLH Bd.39, 1988.

/95/ Sulzer Brothers Limited, Plant and Building Services: Airconditioning Featuring Variable Volume Air Flow and Displacement Ventilation for an Office Building in Winterthur, 1989.

/96/ Sutton, O.G.: The Dispersion of hot Gases in the Atmosphere, Journal of Meteorology, vol.7, pp.307-312, 1950.

/97/ Tamanini, T.: The Effect of Buoyancy on the Turbulence Structure of Vertical Round Jets, Journal of Heat Transfer, vol.100, pp.659-664, Nov., 1978.

/98/ Tapula, M.& K. Koivula: Dimensioning of Supply Air Flow in Displacement Ventilation, 2'nd world Congress on HVAC - Clima2000, Sarajevo, Yugoslavia, 1989.

/99/ Taylor, G.I.: The Transport of Vorticity and Heat Through Fluids in Motion. With an appendix by Fage and Falkner. Proc. Roy. Soc., A, Bd.135, p.685 & p.702, 1932.

/100/ Taylor, G.I.: Dynamics of a Mass of Hot Gas Rising in Air, U.S. Atomic Energy Comm., MDDC, 919, LADC 276, 1945.

/101/ Van der Kooi, J. & C. Quingyan: Termal Performance of a Room with Air Displacement Ventilation Systems, 2'nd World Congress on HVAC - Clima2000, Sarajevo, Yugoslavia, 1989.

DANSK RESUME

DANSK RESUME

Aksesymmetriske cirkulaere opdriftsstroemninger er behandlet baade teoretisk og eksperimentelt.

Med basis i et litteraturstudie konkluderer forfatteren, at den eksperimentelle viden er mindre tilfredsstillende. Kildebetingelserne er sjaeldent rapporteret eller maalt, og deres indflydelse paa etableringen af ligedannethed er ukendt. Flowet i overgangszonen er karakteriseret ved en absolut mangel paa rapporterede maalinger. De givne middelvaerdidata for plumezonen er i konflikt med hinanden og er ofte af ikke saa god kvalitet. Dertil kommer, at turbulensdata er meget sparsomme.

Tre forskellige maalemetoder (i denne rapport kaldet ekstrapolationsmetoden, nulmetoden og lagdelingsmetoden) er blevet optimeret og anvendt for at undersoege de termiske stroemninger fra "rene" varmekilder. Disse metoder eliminerer alle aksevandringsproblemet, som ikke er af stokastisk karakter og saaledes ikke kan behandles som et normalt turbulensfaenomen.

Ekstrapolationsmetoden, hvor hastigheds- og temperaturmaalinger finder sted i opdriftsstroemningen, kan betragtes som eksemplarisk til undersoegelse af aksesymmetriske cirkulaere jets, da den goer registrering af aksevandring mulig. Denne forbedring reducerer maaleresultatspredningen. Desuden giver metoden basiskendskab til middeltemperatur og hastighed i flowet. Databehandlingen bestaar af Gaussfits og en lokal approksimation af en "ren" plume model.

Nulmetoden, hvor den termiske stroemning bliver suget ud gennem en hov, giver kun information om den vertikale volumenstroem. Metoden er meget let at anvende, og det er muligt at undersoege ikke symmetriske flow og flow paavirket af omgivne vaegge.

Lagdelingsmetoden indebaerer en observation af lagdelingshoejden i et med fortraengningsventilation ventileret rum. Denne hoejde

betragtes som et maal for den vertikale volumenstroem i henhold til to-zone modellen. Flere anvendelsesmaessige problemer er rapporteret, men metoden giver en ide om, hvordan det totale stroemningsbillede ser ud. Metoden kan ogsaa anvendes til undersoegelse af vaegstraaler og stroeminger i et hjoerne mellem to vaegge.

I henhold til de udfoerte analyser er "rent" plume flow eller modellen af en plume over en punktkilde blevet verificeret i kraft af potenslove fra ligedannethedsanalyse. Hastigheds- og overtemperaturprofilerne er fundet smallere end de observeret af andre forfattere, og derfor er medrivningsfaktoren mindre. Endelig skal knyttes den kommentar, at komplet ligedannethed i form af konstante hastigheds- og temperaturfordelingsfaktorer ikke kan siges at forekomme.

Indflydelsen af selv meget smaa vertikale temperaturgradienter er rapporteret signifikant. Dette goer den "rene" plume modellering umulig, og gradienten foerer til oploesningstendenser eller horisontal udspredning af den termiske stroemning. Stoerre gradienter accelerer processen.

De undersoegte flow har en temmelig lang overgangszone, og ofte vil den straekke sig hoejere end et normalt kontorlokale. I denne forbindelse giver ekstensive varmekilder lange overgangszoner, og deres flow er mere sensibel overfor forstyrrelse i omgivelserne. Endelig er selve ventileringen af rummet af stor betydning for udviklingen af den termiske stroemning.

De udfoerte tests viser en signifikant reduktion af den vertikale volumenstroem, naar den termiske stroemning finder sted taet paa omgivne vaegge - som en vaegjet eller en jet i et hjoerne. Symmetriovervejelser er verificeret, hvad angaar vaeg jets. Det vil sige, at volumenstroemmen udgoer 63 % af den i den tilsvarende frie termiske stroemning. Naar flowet finder sted i et hjoerne mellem to vaegge er procentdelen endnu mindre.

Det er forfatterens haab, at de praesenterede eksperimentelle middelvaerdidata fra ekstrapolationsmetoden kan danne basis for fremtidige numeriske arbejder.

I denne rapport er problemet med at beregne den vertikale volumenstroem i termiske stroemninger taet knyttet til fortraengningsventilation. Derfor er det forfatterens oenske at diskutere og at praesentere et input til design af fortraengningsventilationssystemer, specielt estimeringen af den noedvendige ventilationsluftmaengde:

Fortraengningsventilation har sammenlignet med traditionel opblandingsventilation to fordele:- En effektiv udnyttelse af energien, fordi det er muligt at fjerne udsugningsluft fra rummet, hvor temperaturen er flere grader hoejere end den i opholdszonen. - En bedre luftkvalitet ved samme luftskifte paa grund af den vertikale forureningsfordeling, som indebaerer, at frisk luft og uren luft separeres.

Forfatteren er af den overbevisning, at fortraengningventilation med succes kan anvendes i store hoeje lokaler som for eksempel forsamlingslokaler og i industriel ventilation, da kun opholdszonen vil blive ventileret. I kontorlokaler vil princippet ligeledes have en mening, men man skal her serioest overveje den alternative opblandingsventilation. Problemet med fortraengningsventilation er det ofte hoeje luftskifte forbundet med traekrisiko. Stoerre termiske belastninger og som en konsekvens heraf hoejere luftveksler oeger traekrisikoen (nogle gange tales om en oevre graense paa 40 W/m^2, naar der benyttes vaegmonterede diffusorer). Det er imidlertid vaerd at naeve, at loesninger med perforede gulve aabner muligheden for at fjerne store varmemaengder (stoerre end 200 W/m^2) og stadigvaek have et komfortabelt termisk indeklima.

Spoergsmaalet om noedvendig ventilationsluft forbliver. Der er ikke nogen grund til at tro, at luftskiftet sammenlignet med det fra opblandingsventilation kan blive reduceret, tvaertimod. For

eksempel vil en valgt lagdelingshoejde paa 2 meter in mange tilfaelde give for store luftmaengder. 1 til 1,2 meter synes at vaere et fornuftigt valg. Argumentet for fortraengningsventilation er stadig de to foernaevnte fordele, men ogsaa at graenselaget omkring det menneskelige legeme transporterer frisk luft fra den nedre rene zone op til aandingszonen, selv over en eventuel lagdelingshoejde.

Den vertikale volumenstroem fra ekstensive varmekilder som mennesker, taendte computere, kopimaskiner etc. kan ikke beskrives ved en simpel plume model af stroemningen over en punktkilde. Den kan dog give en vis ide om stoerrelsen. Den termiske stroemning vil oftest befinde sig i en overgangszone, hvor kendskabet er meget begraenset. Derfor drager forfatteren paa nuvaerende tidspunkt konklusionen, at en katalogisering af typisk forekomne termiske stroemninger vil vaere en god ide. Derudover synes det fornuftigt at anvende simple symmetriargumenter til beskrivelse af flow taet paa omgivne vaegge og, naar to kilder staar taet og former kun eet flow. Dette vil kunne reducere den estimerede noedvendige ventilationsluftsmaengde. Endelig skal det naevnes, at en muligst hoej placering af varmekilderne vil haeve lagdelings-hoejden og som en foelge deraf vil oege luftkvaliteten i opholdszonen.